TAMPEREEN TEKNILLINEN YLIOPISTO
TAMPERE UNIVERSITY OF TECHNOLOGY
Julkaisu 838 • Publication 838

Lila Nikkola

Methods for Controlling Drug Release from Biodegradable Matrix and Development of Multidrug Releasing Materials

Tampere 2009

Tampereen teknillinen yliopisto. Julkaisu 838
Tampere University of Technology. Publication 838

Lila Nikkola

Methods for Controlling Drug Release from Biodegradable Matrix and Development of Multidrug Releasing Materials

Thesis for the degree of Doctor of Technology to be presented with due permission for public examination and criticism in Rakennustalo Building, Auditorium RG202, at Tampere University of Technology, on the 23rd of October 2009, at 12 noon.

Tampereen teknillinen yliopisto - Tampere University of Technology
Tampere 2009

ISBN 978-952-15-2241-3 (printed)
ISBN 978-952-15-2249-9 (PDF)
ISSN 1459-2045

Abstract

Local drug delivery devices are advantageous for use in pharmaceutical therapies to control tissue reaction at implant site. Tissue healing and regeneration is a multistep process, control of which is challenging. The presence of a therapeutic dose of several active agents at suitable time frames during tissue healing and regeneration could lead to optimal outcome of the implant. A scaffold where cells can attach and proliferate can considerably enhance the regeneration of tissue. To obtain the suitable dose and release period of drug, the control of the release rate from biodegradable polymeric devices has been based on the degradation behavior of polymer and the diffusion rate of the drug from the polymer matrix. In addition, most of the drug-releasing materials carry only a single agent lacking the possibility for enhanced therapeutic effect.

The main objective in this thesis was to manufacture biodegradable drug-releasing composites with controlled drug release. To enhance the tissue ingrowth, three studies of drug releasing nanofiber scaffolds for use as a component in composite are also introduced. In polymer composites, the control of the drug release rate was achieved by a combination of components having different release profiles into one piece, i.e. a multicomponent rod. These rods were intended for use in bone fixation. In addition, studies are presented of the development of multidrug-releasing biodegradable polymer composites in the form of multilayered and multiphase composites. The manufacturing methods of components comprise multiple melt and solvent-based polymer processing techniques (electrospinning, melt extrusion, fiber spinning, compression molding, and emulsion evaporation method). The biodegradable polymers that were used in these studies are based on lactic acid and its copolymers. The selection of active agents was based on the control of inflammatory reactions and hence, they comprised the well-known anti-inflammatory agents, diclofenac sodium and dexamethasone. A third agent, bone-forming bisphosphonate was also loaded in the multilayer composite, which was aimed at bone applications as tissue guiding material.

The release kinetics and some explanatory studies on microstructures, thermal properties, and mechanical properties were performed. The results showed that the use of slowly degradable or high molecular weight faster degradable biodegradable polymers in drug-loaded nanofibers can extend the release to almost three months. In addition, with slowly degrading polymer the microstructure was maintained after the drug release. The release from multicomponent rods can be controlled by combining the components with different release profiles. However, the mechanical strength of the

rods was unsatisfactory and only one rod type could be used in low stress applications, such as cranio-maxillofacial fixation. In the drug release studies, it was found that the drug release from multilayer composite was dependent on the processing variables. The manufactured multilayer composite had suitable release profiles for possible use in bone guidance applications. The drug release rates from the multiphase fiber composite could be varied by loading agents in different polymer phases, i.e. components, thus offering the possibility to vary the release of different agents as desired.

Thesis Outline

1. Nikkola L, Seppälä J, Harlin A, Ndreu A, Ashammakhi N. Electrospun diclofenac sodium releasing nanoscaffold. J Nanosci Nanotechnol. Sep-Oct;6(9-10):3290-5 (2006)

2. Piras AM, Nikkola L, Chiellini F, Chiellini E, Ashammakhi N. Development of diclofenac sodium releasing bio-erodible polymeric nanomats. J Nanosci Nanotechnol. Sep-Oct;6 (9-10):3310-20 (2006)

3. Nikkola L, Morton T, Jukola H, Harlin A, van Griensven M, Ashammakhi N. PLGA Nanoscaffold releasing diclofenac sodium, J Tissue Eng Regen Med (Submitted)

4. Nikkola L, Viitanen P, Ashammakhi N. Novel diclofenac sodium releasing PLGA 80/20 rods. J Biomed Mater Res B Appl Biomater 89 (2): 518-526 (2009)

5. Nikkola L, Vapalahti K, Ashammakhi N. Multicomponent implant releasing dexamethasone. AIP Conference Proceedings Vol. 973, 766-771 (2008)

6. Nikkola L, Vapalahti K, Huolman R, Seppälä J, Harlin A, Ashammakhi N, Multilayer Implant with Triple Drug Releasing Properties. J Biomed Nanotechnol 2009 (4), 331-338 (2008)

7. Nikkola L, Jukola H, Ashammakhi N. Multiphase drug releasing fiber. Acta Biomaterialia (Submitted)

Author’s Contribution

The author undertook all the work involved in manufacturing the nanoscaffolds and composites for papers I, III, IV, V, VI, and VII, including planning the experiments, testing and analyzing the data, and writing the manuscript. For paper II the author determined the processing parameters of electrospinning and planned the experiments together with the first author.

Abbreviations

COX-1	Cyclo-oxygenase 1
COX-2	Cyclo-oxygenase 2
DDD	Drug delivery device
DMF	Dimethylformamide
DS	Diclofenac sodium
DSC	Differential scanning calorimetry
DX	Dexamethasone
EDH	Etidronate
GI	Gastrointestinal
GMO	Glycerol monooleate
HPLC	High performance liquid chromatography
HPMC	Hydroxypropyl methyl cellulose
kGy	Kilo Gray, SI unit of absorbed ionizing radiation dose
LCST	Lower Critical Solution Temperature
NSAID	Non-steroidal anti-inflammatory agent
P(DLLA)	Poly(D/L-lactide)
PAH	Polyanhydride
PAM14	Maleic acid based n-butyl hemiester of poly(maleic anhydride-alt-2-methoxyethyl vinyl ether)
PCL	Poly-ε-caprolactone
PDLGA	Poly(D,L-lactide-co-glycolide)
PDLLCL	Poly(D,L-lactide-co- ε-caprolactone)
PEG	Polyethylene glycol
PGA	Poly(glycolic acid)
PHB/V	Poly(hydroxybutyrate/valerate)
PLA	Poly(lactic acid)
PLGA	Poly(lactide-co-glycolide)
PLLA	Poly(L-lactide)
POE	Polyorthoester
PVA	Poly(vinyl alcohol)
SEM	Scanning electron microscopy
T_g	Glass transition temperature
TGA	Thermogravimetric analysis
T_m	Melting temperature
UCST	Upper critical solution temperature

UV	Ultraviolet
w-o-w	Water-in oil-in water
ΔCp	Change of heat capacity
ΔH	Enthalpy change

Definitions

Amorphous

Lack of distinct crystallinity.

Anti-inflammatory agent

Agent that counteracts or suppresses inflammation.

Anti-microbial agent

Capable of destroying or suppressing growth or reproduction of bacteria.

Apoptosis

Form of programmed cell death, characterized by endonuclease digestion of DNA.

Bioabsorbable

Capable of being degraded or dissolved and subsequently metabolized within an organism.

Biodegradation

Gradual breakdown of a material mediated by a biological system.

Bioerodible polymer

Water-insoluble polymer that is converted under physiological conditions into water-soluble materials without regard to the specific mechanism involved in the erosion process.

Bioerosion

Removal of matter from the surface of a biomaterial following regard to the specific mechanism involved.

Blend

A uniform combination of two or more materials.

Citric acid cycle

A series of enzymatic reactions in aerobic organisms involving oxidative metabolism of acetyl units and producing high-energy phosphate compounds, which serve as the main source of cellular energy.

Copolymer

Polymer consisting of molecules characterized by the repetition of two or more different types of monomeric units.

Cranio-maxillofacial

Cranium and upper and lower part of the face.

Cytotoxic agent

Term used for drugs used in the treatment of cancer.

Degree of crystallinity

Total crystalline content of a partially crystalline material.

Dielectric constant

Property of a material which describes the electric flux density produced when the material is excited by an emf source.

Diffusion

Process of becoming diffused, or widely spread.

Enterohepatic cycle

The cycle in which bile salts and other substances excreted by the liver are absorbed by the intestinal mucosa and returned to the liver via the portal circulation.

Glass transition temperature

Temperature at which a polymer transforms from a brittle to a rubbery condition.

Growth factor

Any of the group of polypeptide hormones which regulate the division of cells.

Homopolymer

Polymer that is derived from a single monomer and consists of identical repeating units.

Hydrophilic

Having affinity for water.

Hydrophobic

Not readily absorbing or interacting with water

Hydroxyapatite

1. Hydrated calcium phosphate occurring widely in natural tissues such as enamel, bone, etc.
2. Hydrated calcium phosphate, prepared by any one of several routes and existing in several different forms, that is used as a ceramic biomaterial.

Immunosuppression

Artificial suppression of the immune response by the use of drugs which interfere with lymphocyte growth, by irradiation, or by the use of antibodies against lymphocytes.

Invasive

Involving puncture of the skin or insertion of an instrument or foreign material into the body.

Isotropic

Having the same value of a property, e.g., refractive index, in all direction.

Matrix

More or less continuous matter in which something is embedded.

Intercellular substance of a tissue or the tissue from which a structure develops.

Microstructure

Units of microscopic size (about 1 to 100 μm in diameter) which occur in materials.

Monolithic

Consisting of or constituting a single unit.

Constituting a massive undifferentiated and often rigid whole.

Monomer

Substance comprised of small molecules with high chemical reactivity, each being capable of linking up with others to produce polymer chains.

Nanoparticle

Any particle of a substance with dimensions in the region of one-tenth of a micron.

Oligomer

Polymer formed by the combination of relatively few monomers.

Osteoblast

Bone forming cell.

Osteoclast

Large multinuclear cell associated with absorption and removal of bone.

Osteomyelitis

Inflammation of bone, localized or generalized, due to pyogenic infection.

Osteoporosis

Enlargement of bone marrow and canals, and abnormal porosity of bone.

Phospoholipid

Any lipid that contains phosphorous.

Phospholipase A_2

An enzyme that catalyzes the hydrolysis of a phospholipid.

Plasticizer

Substance incorporated into a material to increase its workability, flexibility, or distensibility.

Racemic

Optically inactive, being composed of equal amounts of dextrorotary isomers.

Rheology

Science of deformation and flow of matter, such as the flow of blood through the heart and blood vessels.

Steroid

Any of a group of polycyclic compounds having 17-carbon atom ring system as a nucleus.

Surfactant

Compound that reduces the surface tension of its solvent.

Sustained release

Regulation of the rate of drug delivery, usually by physic-chemical means, in order to prolong drug action and availability.

Syndiotactic

Pertaining to a type of polymer molecule in which groups of atoms that are not part of the primary backbone structure alternate regularly on opposite sides of the chain.

Tacticity

Regularity or symmetry in the molecular arrangement or structure of a polymer molecule.

Vasodilatation

State of increase caliber of the blood vessels.

van der Waals interaction

A group of relatively weak intermolecular interactions which generally result when a molecule or group of molecules become polarized into a magnetic dipole.

According to Williams Dictionary of Biomaterials (Williams 1999).

Table of Contents

1 INTRODUCTION

The development of drug-releasing materials has been carried out for the last three decades. Their suitability for use in fields such as pharmaceutical therapy (Weinberg *et al.*, 2008, Hatefi and Amsden 2002), tissue engineering (Chung and Park 2007), especially for bone and cartilage tissue engineering (Lee and Shin 2007, Holland and Mikos 2006), and cancer therapy (Mak *et al.*, 1995, Fung and Saltzman 1997) have been well assessed. Drug delivery devices offer several advantages over conventional drug administration methods. The most evident advantages of local drug delivery are the prevention of systemic adverse effects of drugs and speed of clearance through the liver, sustained drug concentration, and convenience for patients. Biodegradable polymers have been studied for several decades for biomedical applications and also for such drug-releasing applications as rods (Viitanen *et al.*, 2006), screws (Veiranto *et al.*, 2002), fillers (Koort *et al.*, 2006), membranes (Ahola *et al.*, 2003), hydrogels (Shantha and Harding 2003), microspheres (Ravi Kumar 2000), micelles (Chen *et al.*, 2007, Hagan *et al.*, 1995), nanofibers (Agarwal *et al.*, 2008), and nanoparticles (Panyam and Labhasetwar 2004, Panyam *et al.*, 2004, Saxena *et al.*, 2004). The selection of delivery matrix polymer has been based mainly on the requirements of the application. The release rate can be adjusted to be rapid, immediate, delayed, pulsed, or very long term. In addition to the shape, size, and processing method of the device, the drug release mechanism is strongly dependent on the type of chemical composition as well as the degradation behavior of the polymer. Recent interest has focused on smart materials from which drug release can be controlled. More targeted and controlled therapies are needed in the future since the trend is to develop tailor-made therapies. Moreover, combination therapies, where multiple drugs can be delivered simultaneously, will provide greater opportunities for individualized care.

This thesis presents new approaches and developments in biodegradable polymeric drug releasing composites with controlled release rates. Since the guidance of tissue growth and regeneration is important at implant site, it is essential that there is a suitable scaffold for cells to attach to, penetrate, and proliferate. The first three publications present the developments of an anti-inflammatory agent, diclofenac sodium, released by biodegradable nanofiber structures for use as a scaffold for tissue growth in a composite. The biodegradable polymer composites were prepared using a combination of components with known release profiles. These composites comprised multicomponent rods loaded with diclofenac sodium or a steroidal anti-inflammatory agent, dexamethasone with controlled release. These are presented in publications IV

and V. Multidrug-releasing composites are introduced in publications VI and VII. These allow simultaneous release of diclofenac sodium, dexamethasone and bisphosphonate, etidronate (in publ. VI only). The drug release kinetics was investigated in addition to other related studies, along with a discussion of the results.

The literature review provides an overview of the basics of drug release, composites, and the factors concerning the drug release kinetics from biodegradable synthetic aliphatic polyester polymers that were used in the studies. It also introduces some synthetic biodegradable polymers and active agents that are related to this thesis. In addition, the literature review briefly describes the biodegradable drug-releasing materials, nanofibers and polymeric composites that have been already reported in the literature.

2 LITERATURE REVIEW

2.1. Concept of drug delivery

The concept of drug delivery can be traced to the 1930s, when the first studies reported delivery of therapeutic agents from implanted compressed estrogen delivery pellets implanted subcutaneously in livestock. In the 1950s hormonal implantation was already in common practice and since then research into implantable drug delivery devices (DDD) has grown rapidly (Dash and Cudworth II 1998). In conventional drug administration, e.g. oral administration, the drug concentration in plasma fluctuates according to the administration rate (Fig. 1).

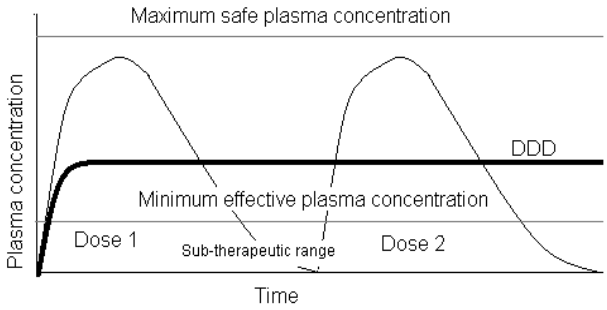

Figure 1. Representation of plasma drug concentration in conventional drug administration and controlled drug release from DDD.

With implantable DDDs it is possible to obtain steady plasma or site concentrations with prolonged drug therapy. The other advantages are better patient compliance since they do not need to remember to take the medicine at set times of the day. Compared to oral administration by using DDDs, the enterohepatic cycle can be avoided and a smaller total amount of drug is needed. However, it should be noted that in conventional administration, some drugs are site-selective and lower dosages are effective enough to achieve the therapeutic effect as well as diminishing the side effects and drug burden to the body (Harrison 2007).

2.1.1. Local drug delivery

A problem can arise when blood supply to the target site is impaired and the drug cannot be delivered effectively. In such cases, local administration of the drug is very beneficial. Local administration can be performed in various ways, such as injection of drug to the target site. However, injection of drug in a liquid dissolves easily and the

drug can escape from the target site relatively fast, thus enabling only short-term therapy. With local drug delivery devices the administration of drug is prolonged and targeted to the specific site. The disadvantage that occurs with local DDDs is the need of invasive methods for placement, from injection to surgical implantation. However, during implantation of the DDD during surgery, such as in the treatment of osteomyelitis where infected tissue is removed, antibiotic drug-releasing filler can be implanted into the residual cavity to treat the remaining infection (Koort *et al.,* 2006, Koort *et al.,* 2005, Gürsel *et al.,* 2001). Some advantages of local drug delivery are presented in Table 1.

Table 1. Advantages of local drug delivery devices (Jain et al., 2005)

Advantages
1. Drugs with low bioavailability can be targeted
2. The patient-to-patient variability in drug pharmacokinetics is reduced, especially important for therapeutic agents with a narrow therapeutic index pharmacokinetics is reduced, especially important for therapeutic agents with a narrow therapeutic index.
3. Localized delivery is beneficial for drugs with dose dependent activity
4. It reduces or obviates the need of premedication in case of drugs which show adverse effects when given systemically
5. Local delivery also makes it easier to overcome dose differential problems seen in extending animal studies to a clinical trial in man
6. In case of anticancer drugs, intratumoral delivery is not limited by poor blood supply caused by radiation therapy or surgery

Local DDDs can also have other functions than drug release and thus give a device multifunctional properties. These other functions include bone fixation (Veiranto *et al.,* 2002, Veiranto *et al.,* 2004b), filling (Koort *et al.,* 2006, Koort *et al.,* 2005), supporting structures for cells (Ashammakhi *et al.,* 2008), or sutures (He *et al.,* 2009). It is reported that bone fixation with PLGA screws has caused osteolysis due to local acidity (Weiler *et al.,* 1996). The release of anti-inflammatory drugs from this fixation device could provoke inflammatory reaction and further osteolysis caused by the acidic degradation products of the polymer. The development of multifunctional DDDs is difficult since the device must also meet the other requirements of the application. For example, drug-loaded bone fixation devices that degrade by bulk erosion lose their strength faster than unloaded devices (Veiranto *et al.,* 2002).

2.1.2. Categorization of drug delivery devices

Drug delivery devices can be categorized as a) diffusion controlled, b) water penetration controlled, c) chemically controlled, and d) regulated devices (Heller 1996). Diffusion controlled devices can be either monolithic, where drug is dispersed in the carrying matrix and released by diffusion, or systems comprising an outer diffusion-controlling membrane and an inner drug-loaded core. Water penetration-controlled systems are also of two types, being either osmotically and swelling controlled. Osmotically controlled systems contain an osmotically active agent within a rigid housing separated from the

therapeutic agent by a movable wall. In an aqueous environment, water is osmotically driven across the semipermeable wall of the housing, increasing pressure in the compartment of the osmotic agent. The pressure forces the wall to move, which then forces the agent out of the device through the delivery orifice. In swelling controlled systems the agent is dispersed in a hydrophilic polymer, which is glassy in the dehydrated state. In an aqueous environment the polymer swells, releasing the agent simultaneously. In chemically controlled systems the therapeutic agent can be attached to a polymer backbone and the disintegration of the backbone by hydrolysis breaks the bond and releases the agent. The drug can also be dispersed in a biodegradable core. The core does not undergo transformation during the drug release period but will later be slowly degraded. The third option comprises biodegradable devices. The agent is dispersed in a biodegradable polymer matrix and the release occurs as a result of the degradation of the polymer. The principal releasing methods are diffusion and polymer degradation by surface erosion or bulk erosion. The regulated drug delivery systems can be externally regulated devices that use, for example, microprocessors or a magnetic field or self-regulating devices. The drug release is altered in response to an external change in the environment, such as pH or temperature. These systems are usually made of stimuli-responsive polymers (Harrison 2007, Heller 1996).

2.2. General basis of drug release

The drug can be dissolved, dispersed, or partially dissolved in the polymer matrix. The release of a drug from stabile polymers is based on diffusion, which can occur as either zero or first order kinetics (Fig. 2) (Jones 2004).

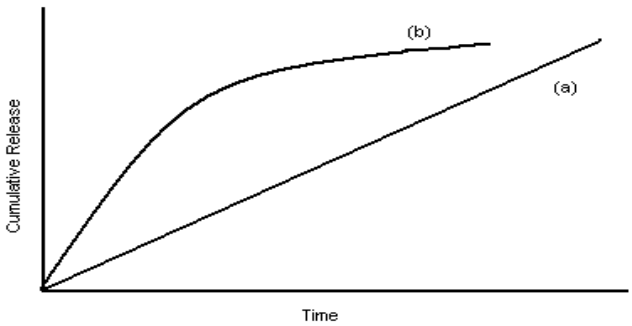

Figure 2. Schematic illustration of release profiles of (a) zero order kinetics and (b) first order kinetics release.

The release of drug from biodegradable polymers is predominantly a consequence of diffusion of the drug molecule and simultaneous degradation of the polymer matrix (Topp 2000). In addition, there are multiple other factors that need to be taken into account when drug releasing devices are being developed.

2.2.1. Diffusion of drug molecules from stabile matrix polymer

The thermodynamic bases of diffusion related to drug release from a polymer matrix is explained by the most fundamental theory of diffusion, Fick's laws. The mathematical equation of one dimensional mass transportation by Fick's first law is

$$J = -D\frac{dC}{dx} \qquad (1)$$

where J is the rate of mass transport per unit area (*flux*), D is the diffusion coefficient, dC/dx is the gradient in concentration C, and x is the direction of mass transport. The law is based on the concentration gradient since the diffusion coefficient has a proportionality relating to the flux to the concentration gradient. The diffusion coefficient is dependent on the properties of the drug, the temperature, and matrix properties (Topp 2000, Crank 1975).

The more applicable equation for drug release is Fick's second law, which is derived from the first law and it is based on mass balance. Fick's second law is

$$\frac{\partial C_A}{\partial t} = D\frac{\partial^2 C_A}{\partial x^2} \qquad (2)$$

where C_A is the concentration of the drug and t is time (Topp 2000, Crank 1975).

Higuchi was the first to derive an equation for drug release from an insoluble matrix (Higuchi 1961). The equation is based on Fickian diffusion, proposing the release to be the square root of a time-dependent process. The Higuchi equation can be expressed with low concentrations

$$M = A\sqrt{DC_s(2C - C_s)t} \qquad (3)$$

and in cases where drug loading is in excess of the solubility of the drug in the polymer matrix

$$M = A\sqrt{2DC_sCt} \qquad (4)$$

where M is the mass of released drug at time t, A is the surface area of the device, C is the initial mass of drug in system, C_s is the saturation solubility of the drug in the polymer matrix, and D is the diffusion coefficient of the drug in the polymer matrix (Jones 2004, Higuchi 1961).

Because of the depletion of the drug from the outer area due to outward diffusion, the release rate changes over time. The following equations have been proposed from slab geometry for early and late time approximations.

Early time approximation:

$$\frac{M_t}{M_0} = 4\sqrt{\frac{Dt}{\pi L^2}} \qquad \text{for } 0 \le \frac{M_t}{M_0} \le 0.6 \tag{5}$$

Late time approximation:

$$\frac{M_t}{M_0} = 1 - \frac{8}{\pi^2}\exp\left(\frac{-\pi^2 Dt}{L^2}\right) \text{ for } 0.4 \le \frac{M_t}{M_0} \le 1.0 \tag{6}$$

where M_t is the mass of the drug released at time t, M_0 is the initial mass of the drug, D is the diffusion coefficient, and L is the thickness of the slab (Jones 2004, Baker 1987).

2.2.2. Diffusion of drug from biodegradable matrix polymer

With biodegradable polymers the mathematical considerations of drug release become more complex, since the degradation of the polymer has to be taken into account. Assuming that the diffusion is less than the rate of polymer degradation, the release for spheres can be calculated from the equation

$$\frac{M_t}{M_\infty} = 1 - \left(1 - \frac{(k_0 t)}{Ca}\right)^3 \tag{7}$$

from cylindrical geometry

$$\frac{M_t}{M_\infty} = 1 - \left(1 - \frac{(k_0 t)}{Ca}\right)^2 \tag{8}$$

and from a slab of thickness 2a

$$\frac{M_t}{M_\infty} = 1 - \left(1 - \frac{(k_0 t)}{Ca}\right)^1 = \frac{(k_0 t)}{(Ca)} \tag{9}$$

where k_0 is the drug release rate, C the initial loading of drug, and a is the initial radius of the delivery system. From equation 9 it can be seen that zero order release can only be observed from slab geometry (Jones 2004).

When the drug diffusion is much greater than the rate of polymer degradation the release rate of the drug may be described using Higuchi's equations. However, the degradation of the matrix needs to be included in the equation and can be expressed by Baker *et al.* (1987)

$$M = A\sqrt{2DC_s e^{kt} Ct} \qquad (10)$$

where e^{kt} is the rate of degradation of the matrix polymer (Jones 2004, Baker 1987).

2.3. General basis of composites

Composite materials are comprised of two or more different components or phases. The scope of composites is wide due to the fact that they are tailored to meet service conditions with enhanced properties (Hull and Clyne 1996). The most common reason for using composite structures is to enhance mechanical properties, for example, by reinforcing the polymer matrix with aligned continuous glass fibers (Jukola *et al.*, 2008). The stiffness of the fiber-reinforced composite can be estimated using the well-known "Rule of Mixtures" equation

$$E_l = (1 - f)E_m + fE_f \qquad (11)$$

where the E_l is the modulus of the composite, f is the volume fraction of fibers, E_m is the modulus of the matrix, and E_f is the modulus of the fibers (Hull and Clyne 1996).

In addition to fiber-reinforced composites, laminate structures are used for enhancing mechanical strength, especially the stiffness of materials. Laminates consists of layers of sheets or plates that are reinforced with fibers. The fibers can be long and oriented, or chopped in the lamina. The strength and stiffness of the laminate can be varied according to the way the laminae are assembled and aligned to each other. In addition, the fibers in a lamina can be woven, knitted, or braided (Hull and Clyne 1996). Prediction of the stiffness of laminates can be complex, depending on assembly (the angle between the orientations of the fibers in the lamina) of the laminate. Further discussion of this topic, however, lies outside the scope of the present study.

One type of composite is particulate reinforced composites, where the reinforcing material is dispersed throughout the matrix material. These composites are isotropic and the reinforcing effect depends on the particle size, shape, and surface chemistry as well as loading (particle to particle interactions). Usually the particles reduce the T_g of the polymer matrix while poorly dispersed particles can form flaws in the structure. Depletion of particles from the surface of a composite material increases with particle

size. The properties of the particle and matrix also exert a major influence on the strengthening effect of particles (Rothon 2002). The effect of homogenous dispersion and particle size becomes evident in small-diameter fibers, where features such as the agglomeration of particles can cause stress concentrations adjacent to the agglomeration, causing early breakage. For particulate reinforced composites the estimation of elastic modulus can be calculated from

$$E = E_m \frac{E_m + (E_d - E_m)V_d^{2/3}}{E_m + / E_d - E_m)V_d^{2/3}(1 - V_d^{1/3})} \quad (12)$$

where E_m is the modulus of matrix, E_d the modulus of the particulate, and V_d is the volume fraction of the particulate (Huang and Ramakrishna 2004).

Monolithic drug delivery materials can be considered as particulate composites, although the drug does not have a reinforcing role. Conversely, the drug particulate can decrease the mechanical properties of composite, which is demonstrated in studies of biodegradable polymer-based materials (Veiranto *et al.*, 2002, Huolman and Ashammakhi 2007).

2.4. Biodegradable polymers in drug delivery devices

Extensive research and development into biodegradable polymers have today led to the emergence of a wide variety of medical applications. These applications include fixation devices for bone, drug delivery devices, and scaffolds for tissue engineering. The polymers can be divided into surface erodible and bulk erodible polymers on the basis of their degradation behavior. Polyorthoesters (POE) and polyanhydrides (PAH) represent groups of surface erodible polymers, of which POEs have been developed specifically for use as drug release matrix materials. The release of active agent can be adjusted to follow zero order kinetics due to the erosion characteristics. One well known and widely applied group of biodegradable polymers is the synthetic polyesters, especially aliphatic α-hydroxy acids such as polylactides (PLAs) and polyglycolides (PGAs) and their copolymers. These polymers degrade by bulk erosion, degrading by hydrolytic chain scission to produce acidic, though non-toxic degradation products, which are eliminated from the human body through natural body functions in the citric acid cycle. Poly-ε-caprolactone (PCL) is also a widely-used polyester, especially in drug releasing applications. However, the monomer chain of PCL has five hydrophobic hydrocarbons in line, which increase the hydrophobicity of the polymer when compared to PLAs and PGAs, changing it to become slowly biodegradable (Kwon and Furgeson 2007, Henton *et al.*, 2005, Kohn and Langer 1996).

Recently, polymers that respond to changes in the environment have been developed. The changes, such as in pH or temperature, can induce conformational changes to the

polymer chain, making them applicable for a variety of medical applications like tissue engineering scaffolds and drug delivery devices (Chan and Mooney 2008, Mano 2008).

2.4.1. Surface erodible polymers

Since the 1970s polyortoesters have been developed especially for drug delivery purposes. There are four different polyortoester generations, POE I-IV. The synthesis of POEs varies according to the type of generation as follows: POE I by transesterification of diols and diethoxytetrahydrofuran (Kwon and Furgeson 2007), POE II by addition of diol to diketene acetal (Heller *et al.,* 2002), POE III by transesterification of trimethyl orthoacetate and 1,2,6, hexanetriol (Merkli *et al.,* 1996), and POE IV by the addition of polyols to dikete acetals (Kwon and Furgeson 2007). The first, POE I (Fig. 3a), has high autocatalytic properties due to acidic degradation products and this is no longer under development. In the second generation, POE II (Fig. 3b), autocatalytic degradation was avoided by changing the initial hydrolysis products to neutral. However, POE II was very hydrophopic and its hydrolytic degradation was very slow. Its remarkable ability to form cross linked structures and still remain biodegradable by hydrolysis is unique to POE II. Since the ester linkages are acid-labile, attempts were made to control and decrease the degradation period by adding acidic additives to the polymer matrix. However, this approach proved only partially successful and so POE II was not developed for commercial use. POE III has very a flexible backbone (Fig. 3c) resulting in a semi-solid character at room temperature. The main advantage of POE III was the ability of mixing therapeutic agents directly to the polymer matrix at room temperature. However, the synthesis of certain molecular weight POE III was difficult and time consuming and the polymer is no longer under development. POE IV (Fig. 3d) is a modification of POE II, but without acidic substances. Control over degradation has been achieved by the addition of acidic monomers, such as fast hydrolysable glycolic or lactic acid, to the diol-forming latent acid diol. The latent acidic diol is copolymerized to the backbone and during erosion the acidic hydrolyzed monomers catalyze the autocatalytic degradation. The amount of latent acid is small, maintaining the hydrophobic nature of the polymer. These acids catalyze orthoester linkages and by varying the ratio of acidic copolymer to the backbone, erosion can be adjusted .

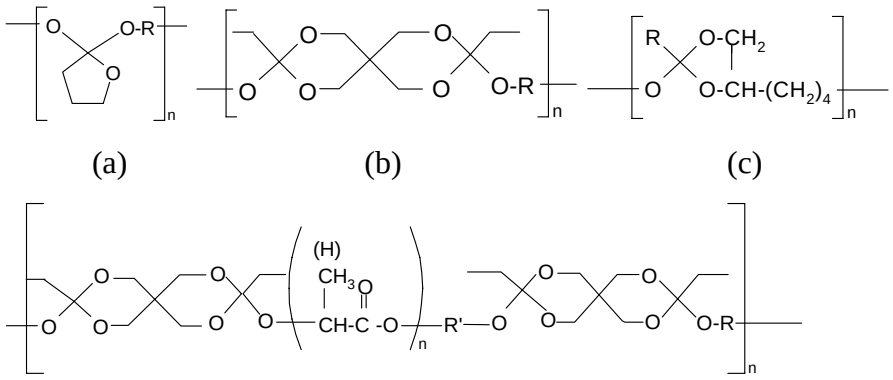

Figure 3. Chemical structure of POE I-IV. a) POE I, b) POE II, c) POE III, and d) POE IV monomer units (Kwon and Furgeson 2007).

POE IV is an attractive choice for a matrix polymer for drug-releasing devices since the release occurs predominantly from the surface of the material, caused only by erosion. An exception is when there are hydrophilic drugs loaded with high concentrations. The increase in hydrophilicity within the matrix enables the latent acid to hydrolyse, which increases the degradation rate. The thermal and mechanical properties of POE IV can be adjusted by changing the R-group of the latent acidic diol, resulting in a wide range of polymers having different T_g and T_m (Heller *et al.*, 2002, Kellomäki *et al.*, 2000). Since POE IV has good thermal stability, it is suitable for melt-based processing techniques. POE IV is soluble in tetrahydrofuran, ethyl acetate, and methylene chloride also enabling solvent-based processing techniques (Kwon and Furgeson 2007, Heller *et al.*, 2002). POE IV has been studied with successful results for applications such as drug delivery in eye treatment (Heller 2005) and post surgical pain management (Barr *et al.*, 2002).

The development of polyanhydrides started in the early 1900s and continued in 1930s and 1950s. It has been targeted at improving the chemical stability of the PAH (Fig. 4) chain by the synthetization of aliphatic and aromatic groups to the polymer backbone. PAHs can be manufactured as aliphatic or aromatic homopolymers or copolymers, cross linked polymers, or branched polymers. The polymerization of PAHs can be performed in many ways, but the most common way to synthesize linear PAH is melt polycondensation.

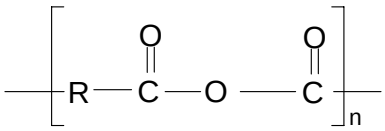

Figure 4. Chemical structure of PAH monomer unit (Kwon and Furgeson 2007).

Dimer erucic acid and sebacic acid copolymer (p(FAD-SA)) is an aliphatic PAH that has been developed for drug delivery purposes. In this copolymer the SA is a highly crystalline and brittle in homopolymer as FAD is liquid and not useful in solid delivery devices, but as copolymers they enhance each other's properties. Aliphatic PAHs hydrolyze faster than aromatic PAHs due to their more hydrophilic character. The erosion rate of aromatic PAHs can be adjusted by copolymerization with aliphatic PAHs. Some of the aromatic PAHs have limitations in their processing methods since their thermal degradation starts at melting point. In addition, the solubility of these PAHs in common solvents is low. Cross linked and branched PAHs offer good mechanical properties and yet still retain good drug release ability. Depending on the type of the PAH and copolymer, PAHs can be amorphous or semicrystalline up to 60 %. As with crystallinity, the melting points of PAHs depend largely on the type and copolymer ratio. PAHs are water insoluble but they degrade into water soluble oligomers before they erode. The drug release from PAHs can occur in three ways: by diffusion, swelling, or erosion (Göpferich 1999). One well-known commercial drug delivery product is Gliadel® for treatment of malignant glioma. It is made of poly1,3-bis-*para*-carboxyphenoxypropane copolymerized with sebaic acid p(CPP-SA) and loaded with the anticancer agent carmustine (Burke *et al.*, 1999).

2.4.2. Bulk erodible polymers

Poly(lactic acid) and copolymers

The raw material for PLAs is derived from renewable resources by a fermentation process. PLAs are polymerized from ring opening polymerization from cyclic lactide dimer or less often by direct condensation from lactic acid (Henton *et al.*, 2005). Lactic acid is a chiral molecule and it has two stereoisomeric forms, D-lactide and L-lactide, which occur in nature (Fig. 5).

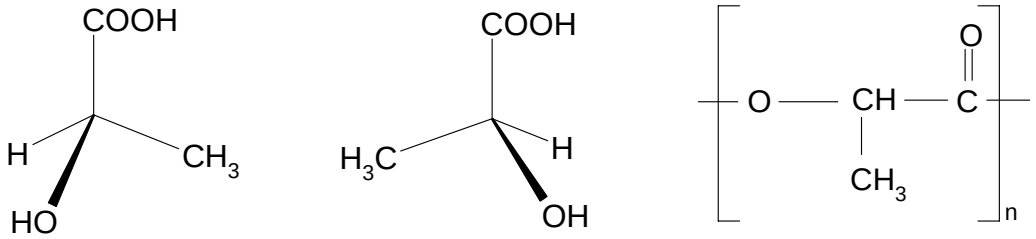

L-lactic acid D-lactic acid PLA monomer unit

Figure 5. Chiral forms of lactic acid and PLA monomer unit (Henton *et al.*, 2005).

The racemic form, syndiotactic P(D/LLA), is amorphous while PLAs can also be semicrystalline depending on the stereochemistry and thermal history. The melting point and glass transition temperatures of PLAs are 130-230 °C and -58 °C, respectively, depending on the structure (Henton *et al.*, 2005). The mechanical strength of PLAs depends on the crystallinity, chemical structure, molecular weight, and

molecular orientation of the polymer. For example, the tensile strength of PLLA varies between 11.4-82.7 MPa (Agrawal 2002). The solubility of PLAs is dependent on the molar mass, crystallinity, and the properties and amount of comonomer in the polymer. PLLA is soluble, e.g. in chloroform and furan, while the racemic form is soluble in xylene, ethyl acetate, acetone etc. (Södergård and Stolt 2002). The hydrolytic degradation depends on the degree of crystallization and the molecular weight of the polymer. By varying the ratio of D- and L-PLA, the degradation period and mechanical properties of the polymer can be modified (Kohn and Langer 1996). Lactides are usually copolymerized with poly(glycolic acid), poly-ε-caprolactone, and aliphatic polycarbonates, such as trimethylene carbonate (Södergård and Stolt 2002, Chu 2003).

Polylactides have quite a long history of clinical use and have been especially successful in self-reinforced poly(L-lactide) (PLLA) pins, screws, wires, and meniscus arrows (Törmälä *et al.,* 1998, Rokkanen *et al.,* 2000). In the field of drug delivery, copolymerization with glycolic acid and ε-caprolactone has widened the use of PLA. For example, several drug-releasing polylactide-co-glycolide (PLGA)-based devices are commercially available, such as Lupron Depot®-releasing leuprolide acetate (Okada 1997, Wischke and Schwendeman 2008) and Zoladex®-releasing goserelin (Schally and Maria Comaru-Schally 1997).

Poly(glycolic acid) and copolymers

Depending of the required molecular weight of PGA (Fig. 6), it is synthesized by polycondensation reaction (< 10,000 g/mol) or by ring opening polymerization of cyclid dimers of glycolic acid (Chu 2003). PGA is a highly crystalline (semicrystalline) aliphatic polyester. It has a high melting point (226-228˚C) and glass transition temperature of 36˚C. Like PLAs, the strength of PGA depends on the molecular weight, crystallinity, and molecular orientation of the polymer. The initial strength of PGA varies between 57-69 MPa (Agrawal 2002). PGA is poorly soluble in organic solvents, but it is soluble in fluorinated solvents, such as hexafluroisopropanol and hexafluroacetone (Schmitt and Bailey 1973). PGA implants tend to rapidly lose their mechanical strength after implantation due to their relatively fast degradation rate (Kohn and Langer 1996). It has been proposed that the degradation of PGA occurs as a two-stage erosion mechanism. First, the amorphous phase is hydrolytically cleaved by diffusion of water in the polymer and then the crystalline phase goes through the same hydrolytic degradation (Kwon and Furgeson 2007). PGA is usually copolymerized with lactic acid, poly-ε-caprolactone, and carbonates (Agrawal 2002, Chu 2003).

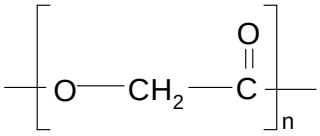

Figure 6. Chemical structure of PGA monomer unit (Kwon and Furgeson 2007).

PGA was already in commercial use as Dexon sutures in the early 1970s (Kwon and Furgeson 2007). Self-reinforced PGA rods have also been used in fixation of displaced ankle fractures, radial head fractures, and fractures in children. Due to their fast degradation rate, PGA devices have been reported to cause adverse tissue responses (mainly local inflammatory reactions) in 2-46.7 % (Bostman and Pihlajamäki 2000), of clinical cases (Törmälä *et al.*, 1998). By copolymeration, glycolide with more hydrophobic lactide reduces the rate of hydrolysis and local acidity caused by too rapid degradation of PGA can be avoided (Kohn and Langer 1996).

Poly(ε-caprolactone) and copolymers

PCL (Fig. 7) can be synthesized from ε-caprolactone monomer in various ways, such as anionic polymerization, cationic polymerization, coordination polymerization, and free radical polymerization (Kwon and Furgeson 2007). PCL is a semicrystalline polymer that has high solubility and a melting point of 59-64 ˚C, depending on the degree of crystallinity. The low T_g (about -60 ˚C) makes it rubbery and flexible at room temperature. It has exceptional ability to form blends with other polyesters and it is normally used in long term drug delivery systems. PCL has low tensile strength (approximately 23 MPa) and very high elongation at break (< 700 %) (Nair and Laurencin 2007). PCL degrades much slower than, for example, PLA due to its relatively long hydrocarbon monomer. Enzymatic activity is usually associated with degradation of PCL in the body environment (Liu *et al.*, 2006). Depending on the molecular weight of the polymer, PCL can sustain a release and degradation period of more than a year (Kohn and Langer 1996).

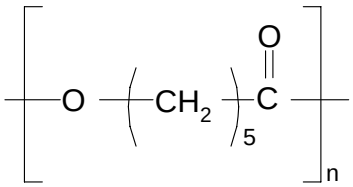

Figure 7. Chemical structure of PCL monomer unit (Kwon and Furgeson 2007).

Due to the long biodegradation time, ε-caprolactone is copolymerized with faster degrading polymer monomers like lactic acid. By copolymerizing it with polyethylene glycol (PEG), it can be used for micelle technology for drug delivery applications. PCL is in commercial use in a contraceptive called Capronor® and a copolymer of PCL, PLA, PGA, and PEG for delivery of small and medium size agents called SynBiosys® (Nair and Laurencin 2007).

2.4.3. Stimuli-responsive polymers

Stimuli-responsive polymers exhibit a marked change in properties when environmental changes occur. The change in a polymer can be any of the following: a conformational change of the polymer chain, a change in solubility, swelling or collapsing,

micellisation, or alteration of the hydrophopic and hydrophilic balance. The changes in environment can be due to temperature, pH, or salt concentration, of which the latter two are the most important (Schmaljohann 2006). These properties make stimuli-responsive polymers very attractive for use in binding to cell surface, disrupting cellular membranes, and in drug delivery applications.

For drug delivery, temperature-responsive polymers that exhibit volume phase transitions are well suited. The phase transitions can be caused by several interactions, such as Wan-der-Waals interaction, hydrophobic interaction, hydrogen bonding with change in ionic interaction, and attractive ionic interaction. Thermo-responsive polymers that become insoluble at a certain temperature have a so-called lower critical solution temperature (LCST). Conversely, if the polymer becomes soluble upon heating, it has an upper critical solution temperature (UCST). One well-known temperature responsive polymer having LCST is Poly(N-isopropylacrylamide), PNIPAAm (Mano 2008, Schmaljohann 2006).

The pH responsive polymers are ionisable polymers having pK_a between 3 and 10 (Schmaljohann 2006). In normal body fluids pH is usually ~7.4 and drug delivery by pH responsive polymer by, for example, micelle deorganization at sites such as the gastrointestinal (GI) tract (pH 2- 8, can be used. The most widely studied monomers are acrylic acid (AAc), methacrylic acid (MAAc), maleic anhydride (MA), and N,N-dimethylaminoethyl methacrylate (DMAEMA). An interesting one is a maleic acid-based *n*-butyl hemiester of poly(maleic anhydride-*alt*-2-methoxyethyl vinyl ether) (PAM 14) developed by Chiellini and Solaro (1995). The polymer is capable of changing from compact coil to open random structure. It is amorphous and bioerodible in water-based liquids (Chiellini *et al.*, 2001, Villiers *et al.*, 1979).

2.5. Pharmaceutical agents for controlling inflammation and osteolysis

There are various active agents on the market that have been studied for implantable drug delivery devices. These include anti-inflammatory and anti-microbial agents, cytostatic agents, hormones, and proteins, such as growth factors (Dash and Cudworth II 1998). Depending on the nature of the disease or health problem, the drug delivery can be local or long term release for systemic therapy. Acute inflammation occurs when tissues are damaged by procedures such as implantation. In addition, the release of monomers or oligomers from biodegradable polymers as a result of hydrolysis can induce an inflammatory reaction. In bone, biodegradation can induce adverse effects such as inflammation and resorption (Bös̈tman and Pihlajamäki 2000, Böstman 1991). These conditions can be treated with anti-inflammatories and agents that inhibit bone resorption, like bisphosphonates.

2.5.1. Anti-inflammatory agents

Inflammation is a normal body response to tissue damage or other stimulating agents such as invasion of infective agents or foreign proteins, which cause an immunological response. Cellular damage stimulates the synthesis and release of inflammatory mediators from the cells. These mediators include histamine, prostaglandins, and leucotrienes. These induce the cardinal signs of inflammation; redness, swelling, heat, and pain. The most important mediators in inflammation are eicosanoids, of which prostaglandins are the best known. They are synthesized from arachidonic acid, which is released in cell injury or following the actions of inflammatory cells on the basis of a signal from phospholipids in the cell membrane (Gard 2000). The synthetization occurs due to the activity of an enzyme called cyclo-oxygenase (COX). Usually, the COX enzymes are categorized according to two types; COX-1 and COX-2. COX-1 is present in mast cells, while COX-2 is more related to inflammatory responses. Prostaglandins are responsible for vasodilatation, increase in vascular permeability and stimulation of local sensory pain receptors during inflammatory reactions. They also have a role in producing fever in infection (Gard 2000).

Anti-inflammatory agents are usually divided into steroidal and non-steroidal anti-inflammatory drugs (NSAIDs). Steroids are related to the adrenal glucocorticoid cortisol by their structure, having four rings (Fig. 8). They also have immunosuppressive properties. Steroids have several adverse effects, especially in long term use. Steroids inhibit phospholipase A_2, which further inhibits synthesis of prostaglandins. In addition to other anti-inflammatory effects, glucocorticoids decrease expression of COX-2 (Gard 2000). One well-known steroid is dexamethasone that has been used in the treatment of inflammation.

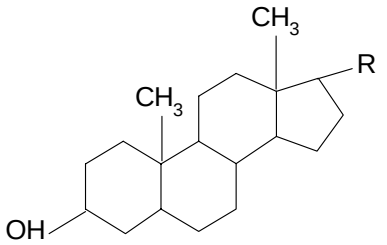

Figure 8. Chemical structure of steroid (Gard 2000).

The well known anti-inflammatory drugs aspirin (acetylsalicylic acid), paracetamol, and ibuprofen fall into the group of NSAIDs, which inhibit COX enzymes and further synthesis of prostaglandins. Different NSAIDs can exhibit selectivity to COX-1 and COX-2 and, for example, ibuprofen is selective to COX-1. The adverse effects of NSAIDS are mostly related to the GI tract because in stomach, prostaglandins are involved in the protection of the gastric mucosa against gastric acid. However, it has been suggested that the protective effect is only related to COX-1 and hence, COX-2

selective NSAIDs could cause less gastric irritation (Gard 2000). The chemical structure of the well-known NSAID diclofenac sodium is presented in Figure 9.

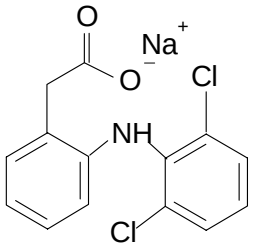

Figure 9. Chemical structure of NSAID diclofenac sodium (Todd and Sorkin 1988).

2.5.2. Bisphosphonates

In normal bone formation and remodeling there is a homeostasis caused by balanced resorption of bone by osteoclasts and bone formation by osteoblasts. Reduced bone formation occurs when the homeostasis of the bone remodeling cycle changes as result of aging or disease, like osteoporosis. Osteoporotic condition is caused by the diminution of osteogenic precursors and usually there is a decrease in the number and activity of osteoblasts as well as a decrease in signaling molecules, like estrogen. Osteoporosis is thus, closely related to postmenopausal women due to the physiological reduction in estrogen production. The activity of osteoblasts decreases considerably, contributing to lower osteogenic activity that leads to problems such as bone healing (Hollinger 2005).

Bisphosphonates are the most commonly used drugs in osteoporosis pharmacotherapy. The basic structure of bisphosphonates includes two phosphates that are bound to the same carbon (P-C-P) (Fig. 10).

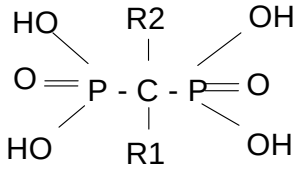

Figure 10. Chemical structure of bisphosphonate (Papapoulos 2008).

The first and well known bisphosphonate is etidronate, from which other bisphosphonates have been derived by changing one of the lateral side chain R2 (Fig. 10) or esterification of the phosphates. They inhibit bone resorption by inhibiting the activity of bone destroying cells, osteoclasts. The P-C-P binds to hydroxyapatite and the side chain R2 determines the antiresorptive efficacy. The proposed modes of bisphosphonate action in bone resorption are direct inhibition of function of mature osteoclasts, induction of osteoclast apoptosis, osteoblast mediated inhibition of osteoclast recruitment, and inhibition of osteoclast differentiation (Singer and Minoofar 2000). The intestinal absorption of bisphosphonates is 1-10 % and after oral or

intravenous administration, 20-80 % is bound to bone while the excess is secreted unchanged into the urine (Singer and Minoofar 2000). Thus, one of the problems of bisphosphonates is their poor bioavailability, especially in oral administration.

2.6. Drug release from biodegradable aliphatic polyesters

The release of drug from biodegradable aliphatic polyester matrices have predominantly two or three phase release patterns depending on the polymer composition. The first high release peak is caused by the release of drug from the surface of the device followed by low release rate, when drug release occurs mostly by diffusion while at the same time the inner part degrades by hydrolysis. Depending on the degradation characteristics, the rest of the drug can be released in one or two larger phases. The second release peak can be caused by the degradation of the faster degrading co-polymer, leaving pores in the matrix. This enhances the final disruption, collapse of the device and dissolution of the residual oligomers, monomers, and drug to the surroundings (Viitanen *et al.*, 2006, Veiranto *et al.*, 2002, Koort *et al.*, 2006, Ravivaparu 2006). In addition, there are various factors contributing to these release mechanisms. These factors include (Ravivaparu 2006, Alexis 2005)

1. degradation of the polymer matrix,
2. crystallinity,
3. molecular weight of polymer and drug,
4. hydrophilicity/hydrophobicity of polymer and drug,
5. loading of drug in the system,
6. morphology of delivery system such as size, shape, and porosity,
7. properties of additives in the system (acidic, basic, monomers, drugs) solubility of the drug in surrounding medium, including aqueous and polymer solubility,
8. method of fabrication,
9. external stimulus, environment (pH, ionic strength, and thermal and enzymatic action), and
10. sterilization.

1. Degradation

Chemical structures and compositions of polymer and drug are fundamental to an understanding of drug release. In ester-based biodegradable polymer materials the degradation is based on the hydrolytic scission of the ester bonds of the polymer back-bone. The rate of cleavage is dependent on the hydrophobicity of the polymer. For example, the monomers of lactic acid and glycolic acid differ only by the hydrophobic methyl group of LA, making the PLA more hydrophobic, thus more slowly degradable than PGA. The hydrophilicity of the monomer depends on the presence of ionisable groups, such as hydroxyl, carboxyl, and amine groups (Harrison 2007). Enzymes also

play a role in the degradation of polyesters having a long hydrocarbon chain, such as PCL (see point 9.).

2. Crystallinity

The degree of crystallinity also has an effect on the degradation rate, mainly because water penetrates more easily to the amorphous phase than the dense and packed crystalline phase. Crystallinity can, however, increase the release rate when the drug is excluded from crystals. Exclusion generates superasaturation of drug to the amorphous phase and thus crystallization of drug particles. When the aqueous media reach the drug crystals, they dissolve and leave large cavities and thus a greater surface area for hydrolysis (Hurrell and Cameron 2002). In the homopolymer of PLA, the tacticity of the arrangements of the D- and L-lactide in the polymer chain has a major effect on the degradation of the polymer. This contributes to the crystallinity of the polymer (Henton *et al.*, 2005). The racemic form of PDLLA is syndiotactic turning the racemic form totally amorphous (Kohn and Langer 1996). Li *et al.*, (1990) reported that the presence of D- and L-lactide in the copolymer of GA (PDLLA) decreased the degradation rate of the polymer compared to L-lactide copolymer (PLGA). This was explained by the faster degradation of the GA component, causing the L-lactide-rich fragments to crystallize. In addition to the degree of crystallinity, glass transition temperature (T_g) plays a role in drug diffusion when the polymer has low T_g, such as PCL (T_g -60 °C). The diffusion coefficient of a drug is low below T_g, while above T_g the polymer undergo changes and becomes flexible and more permeable, allowing the drugs to diffuse more readily (Harrison 2007).

3. Molecular weight

Degradation is also dependent on the molecular weight of the polymer. When the molecular weight increases, the entanglements of the polymer chains also increase. The entanglements can prevent water penetration to the matrix, thus decreasing the degradation rate. In addition, for high molecular weight polymers the hydrolytic chain scission takes more time to reach the critical value where oligomers are able to diffuse out of the matrix and produce more pores than low molecular weight polymers. In this context, when the M_w of the polymer is low (e.g. 4000 g/mol) the drug is released almost immediately due to the immediate water absorption of the system (Harrison 2007).

4. Hydrophobicity/hydrophilicity of polymer and drug

Polymer hydrophobicity affects the type of degradation, which in turn affects the release. Polymer materials that degrade by surface *erosion* offer zero order kinetics release since the drug is mostly released by the degradation of the polymer material on the surface. Zero order kinetics is usually more desirable in drug delivery devices since they have a steady release rate. More hydrophilic polymers enable the permeation of water into the matrix and the material degrades simultaneously throughout the material,

i.e. by *bulk erosion*. The drug dissolves in the penetrating water and is flushed out through the cavities that result from polymer degradation. The release patterns of these materials are more complex than polymers that degrade by surface erosion. Poly-α-hydroxyesters degrade by bulk degradation while, for example, polyorthoesters degrade by surface erosion (Ravivaparu 2006).

The effect of hydrophilic drug dispersed in hydrophobic polymer matrix causes water uptake and thus a rise in osmotic pressure when there is an increase in the difference between hydrophilicity and hydrophobicity (Ravivaparu 2006) and ionic salt concentrations between media and matrix (Lemmouchi and Schacht 1997). This naturally increases the release rate of the drug (Sung *et al.*, 1998).

5. Drug loading

The amount of drug in the polymer matrix has an effect on the release rate. Higher loading causes higher release rates. This is due to the presence of more drug particles close to the surface having a shorter distance to diffuse. For example, the osmotic pressure that a hydrophilic drug induces in a hydrophobic polymer matrix is higher when there are more drugs present (Ravivaparu 2006). The released drug leaves empty cavities in the polymer matrix. These increase the surface area of the material and with high drug loading, cavity formation is naturally increased. Hence, the release rate increases the faster the matrix degrades. Lemmouchi *et al.*, (1998) have demonstrated the osmotic pressure caused by the drug to the system. This seems to accelerate water penetration into the matrix and therefore increase the release rate.

6. Morphology

The size of the system plays a significant role in the drug release rate, especially in diffusion-controlled release. Size also naturally contributes to polymer degradation since hydrolysis is dependent on water penetration into the polymer, which degrades by bulk erosion. In surface erodible polymers, a larger device inevitably takes more time to degrade. Li *et al.*, reported that in massive PLA devices the inner part degrades faster than the surface. In fact, a slower degrading layer is formed on the surface of the system and only oligomers can diffuse through it. In terms of drug release, the rate increases dramatically at the end of degradation of the matrix. Lemmouchi and Schacht, (1997) studied drug-loaded rods having different diameters and demonstrated that in the diffusion controlled release, the size of the implant has a major influence on the release rate, i.e. the thicker the rod, the slower release rate.

Highly porous structures and nano- and micro-carriers, such as particles and fibrous structures, have a high surface area compared to their volume. These structures release the agents relatively fast due to the short diffusion distance from the surface and a large area for hydrolytic degradation (Berkland *et al.*, 2002).

7. Properties of additives in the system

There are conflicting reports on the role of chemically active compounds, i.e. drugs in drug release. Li *et al.,* (1996) observed that a low loading amount of a basic compound (caffeine) accelerated release by catalyzing the degradation of the carrying matrix PDLLA. Frank *et al.,* (2005) have also reported that the basic form of lidocaine accelerated release from PDLGA more than the salt form of the drug. This catalytic effect of basic drug was characterized by Giunchedi *et al.,* (1998) who studied the release of lactic acid and glycolic acid monomers with high performance liquid chromatography (HPLC) from the basic drug, diazepam carrying PLGA matrix. Other studies have reported complexation of the basic drug with carboxylic end groups neutralizing the autocatalytic hydrolysis of acidic end groups, which actually leads to a slower release rate of the drug (Ravivaparu 2006, Miyajima *et al.*, 1998, Miyajima *et al.*, 1999). Adding monomers to the matrix can accelerate the degradation of polymer matrix and thus drug release (Yoo *et al.*, 2007). Solubility of the drug in a polymer has a considerable effect on the release rate. Panyam *et al.,* (2004) studied the encapsulation and release of hydrophobic drugs from PLGA/PLA nanoparticles and found that hydrophobic dexamethasone dissolved more easily in pure PLA than in the more hydrophilic copolymer, PLGA. However, the release from more solubilized formulations was shown to have an inverse correlation to the cumulative percentage of released drug.

8. Method of fabrication

The thermal history of the polymer matrix has an effect on degradation. The effect of different melt-based manufacturing methods, such as melt extrusion and injection molding on drug release were studied by Rothen-Weinbold *et al.,* (1999). They manufactured loaded vapreotide (somatostatin analogue) PLLA rods by using both methods. The release rate was higher with the extruded rods. This was explained by the use of a higher processing temperature together with high pressure injection molding, which resulted in a decrease in $M_{w.}$ This enabled molecular reassembly and also an increase in the degree of crystallization and thus morphology. The high pressure also resulted in higher density of the material compared to the extruded rod, whose microstructure became more porous during *in vitro* tests.

Patel *et al.,* (2008) studied doxycycline-loaded PLGA microspheres manufactured by double emulsion water-in-oil-in-water (w-o-w) methods and spray drying. The microspheres manufactured by double emulsion released the drug faster than the spray dried microspheres. The faster release was assumed to be related to the migration of hydrophilic drug to the aqueous layer of surfactant during the process, having a shorter diffusion distance to the medium.

In addition to manufacturing method, the parameters of the manufacturing process can have a significant effect on the release rate. Tsuji *et al.,* (2007) reported the effect of

melt processing parameters (shear rate, time, and strain) on proteinase K and lipase-catalyzed enzymatic degradation of PLLA and PCL blends. They varied the shear rate and time in extrusion and also examined the polymer degradation rates. They obtained blends with different properties, such as polydispersity and crystallinity, which contribute to the drug release rate.

9. External stimulus and environment

There are many reports on the effect of the pH of the medium on the release rate. For example, Li *et al.,* (2008) studied the effect of the pH of the medium on the degradation of PLGA-PEG microspheres. At pH of 1.2, degradation was fastest while at pH of 10.08 it was slowest. With pH responsive polymers, the changes in pH of the environment are a natural driving force in controlling the release rate (Mano 2008, Schmaljohann 2006). Ko *et al.,* (2007) studied the effect of the surrounding pH on the drug release from pH responsive microparticles. They observed that the release rate was higher at pH 6.4 than at 7.4. Thus, the release was retarded in a normal body environment. In addition, the ionic strength of the medium can affect the release rate when ionizing drugs are combined with the polymer by changing the osmotic pressure inside the polymer matrix (Lemmouchi and Schacht 1997).

The presence of enzymes, which are capable of cleavage of polymer chains, naturally increases the release rate of drugs. For example, certain studies have reported that lipase of *P. Cepacia* (Kulkarni *et al.,* 2007), *Rhizopus arrhizus* (Tsuji *et al.,* 2006), and *Pseudomonas* (Kulkarni *et al.,* 2008) catalyzed the degradation of PCL and PCL diols. They also compared the enzymatic degradation to hydrolytic degradation. The degradation was enhanced by the presence of lipase and an increase in temperature and enzyme concentration (Kulkarni *et al.* 2007). Hoshino and Isono, (2002) studied the degradation of five different polyesters (PCL, PLA, polybutylene succinate (PBS), polybutylene succinate-co-adipate (PBSA), and poly(hydroxybutyrate valerate) (PHBV) with 18 different lipases. They found that only PLA and PHBV were not degraded by any of the lipases.

10. Sterilization - radiation

Biodegradable polymers are sterilized with γ-radiation, ethylene oxide (EtO) or other less-known techniques (Middleton and Tipton 2000). The disadvantage of γ-radiation is that it causes changes in polymer properties, such as scission of the polymer chain (Loo *et al.,* 2005, Chia *et al.,* 2008, Loo *et al.,* 2006). The accelerating effect of γ-sterilization was reported by Soriano *et al.,* (2006). With a dosage of 25 kGy, they increased the release of fluconazole from PLDLA and PLLA matrix. Similar results were obtained by other researchers with microspheres (Kryczka *et al.,* 2003, Lee *et al.,* 2002), thus indicating that sterilization with γ-radiation increases the release rate of the drug by accelerating the degradation of the matrix polymer.

2.7. Biodegradable drug releasing nanofibers

Nanofibers offer major advantages for delivering the drug because of the tailorable morphology, porosity, and composition of the nanofibrous structure (Kim *et al.,* 2004, Cui *et al.,* 2006). Several biodegradable nanofiber-based drug-releasing structures have been developed such as those from synthetic poly(lactic acid) (PLA) (Kenawy *et al.,* 2002, Zeng *et al.,* 2005, Zeng *et al.,* 2003), blends with PEVAc (Kenawy *et al.,* 2002), poly(glycolic acid) (PLGA) (Kim *et al.,* 2004, Katti *et al.,* 2004, Luu *et al.,* 2003, Zong *et al.,* 2004, Xie and Wang 2006, Hong *et al.,* 2008), poly(ethylene glycolide) (PLA-PEG) (Luu *et al.,* 2003, Kim *et al.,* 2003), copolymer of caprolactone P(DLCLA) (Jiang *et al.,* 2004, Huang *et al.,* 2006, Luong-Van *et al.,* 2006), and PVA (Kenawy *et al.,* 2007). Drug releasing nanoscaffolds are comprehensively reviewed by Agarwal *et al.* (2008), Martins *et al.* (2008), and Ashammakhi *et al.,* (2008).

Most of the drug-releasing nanofibers are manufactured by electrostatic spinning due to ease, simplicity, and reasonable cost. The electrospinning process is well described by Reneker and Chun, (1996) and several studies present the fundamentals of forces (Hohman *et al.,* 2001, Reneker and Yarin 2008) related to fiber formation. Briefly, the electrospinning set up comprises a needle or spinneret connected to a vial for the polymer solution, a collector, and a voltage generator. A pump for the polymer solution feed can also be applied. In the process, an electric field is generated between the needle tip and collector, forcing the charged polymer solution to be drawn from the needle towards the nearest point having opposite polarity, i.e. collector. The process starts when the force of the electric field overcomes the surface tension of the polymer solution and a hyperbolic cone forms. This is also called the Taylor cone according to the developer of the fundamentals of jet formation. The polymer fibers in the jet the sprouts and the fibers elongate to eventually form fibers of nano size. This process is caused by electrically driven instabilities that cause bending, winding, spiraling, and looping path in three dimensions. During the process, the solvent evaporates to allow solidification of the fibers (Reneker and Chun 1996). In addition to solvent-based electrospinning, melt-based electrospinning has also been studied (Dalton *et al.,* 2006), where the polymer is formed into a viscous melt and spun into fibers.

There are numerous variables that have an effect on the nanofiber morphology and size. The entanglements of the polymer chains are essential for fiber formation and this is basically related to the molecular weight of the polymer (Mit-Uppatham *et al.,* 2004, Shenoy *et al.,* 2005). Besides molecular weight, the concentration of the polymer solution plays an essential role in forming the viscous solution. Several studies show that an increase in the concentration of the polymer solution leads to an increase in fiber diameter and reduced bead formation (Ashammakhi *et al.,* 2007). The conductivity of the polymer solution is important. Adding salt or solvent that has a high dielectric constant such as N, N.dimethyl formamide (DMF), increases the conductivity of the

polymer solution. This enhances the process and results in smoother and beadless fibers (Ndreu *et al.,* 2008). In addition, high volatility of the solvent leads to thicker fibers by faster evaporation and earlier fiber solidification (Megelski *et al.,* 2002). Other parameters that are related to the apparatus are the strength of the applied electric field, the distance between needle tip and collector (Deitzel *et al.,* 2001), and flowrate (Zong *et al.,* 2002). These also have a major effect on the process and the resulting nanofibers. Thinner fibers are formed by increasing the force of the electric field, the distance between needle tip and collector, or decreasing the polymer feed (Zong *et al.,* 2002). By applying a suitable combination of parameters, the morphology, shape, and the diameter can be adjusted.

Drug release depends on the encapsulation efficiency of the drug in the matrix. Most of the electrospun drug loadings in nanofibers are performed by adding the drug directly to the polymer solution (Zeng *et al.,* 2005, Zong *et al.,* 2004, Luong-Van *et al.,* 2006), where the solubility of drug to the solvent plays an important role in the encapsulation efficiency and thus, the release pattern (Table 2). A similar degree of hydrophobicity of both drug and polymer enhances encapsulation efficiency. However, increased polymer concentration (Cui *et al.,* 2006) or high evaporation velocity of the solvent can, for example, cause accumulation of drug on the fiber surface (He *et al.,* 2009, Kim *et al.,* 2004, Kenawy *et al.,* 2002). Some studies have proposed adding the drug afterwards to the hydrophobic nanofibrous structure by, for example, pipetting the drug solution on the scaffold. This is reported to result in very fast release (<24 h) (Bölgen *et al.,* 2007) because the drug is not located inside the polymer fiber. Most of the reported release periods are quite short, lasting only a couple of days (Kim *et al.,* 2004, Cui *et al.,* 2006, Kenawy *et al.,* 2007). However, other studies on extended release periods have also been reported (Xie *et al.,* 2008), I, II). Drug-loaded nanofibers are presented in Table 2.

Table 2.Biodegradable or water soluble nanofibers loaded with pharmaceutical agent and their solubility in aqueous phase

Matrix polymer	Solubility to water	Agent	Solubility to water	Reference
PCL	insoluble	ornidazole	slightly soluble	Bölgen *et al.* (2007)
PCL	insoluble	heparin	soluble	Luong-Van *et al* . (2006)
Core/shell: PCL	insoluble	Resveratrol	slightly soluble	Huang *et al.* (2006)
Core/shell: PCL	insoluble	Gentamycin Sulfate	soluble	Huang *et al.* (2006)
PDLCLA5/95	insoluble	diclofenac sodium	soluble (pH 5-8)	I
PLA	insoluble	tetracycline hydrocloride	soluble	Kenavy *et al.* (2002)
PLLA	insoluble	Mefoxin	soluble	Zong *et al.* (2004)
PLLA	insoluble	rifampin, paclitaxel	low	Zeng *et al.* (2003)
PLLA	insoluble	Paclitaxel	slightly soluble	Zeng et al. (2005)
PLLA	insoluble	Doxorubicin HCl and base	soluble	Zeng et al. (2005)
PLLA	insoluble	Cisplatin	slightly soluble	Xie *et al.* (2008)
PLDLA	insoluble	Mefoxin	soluble	Zong *et al.* (2004)
PLDLA	insoluble	paracetamol	poorly soluble	Cui *et al.* (2006)
PLGA	insoluble	cefoxin sodium	highly soluble	Zong *et al.* (2004)
PLGA 50/50	insoluble	Cefozolin	highly soluble	Katti *et al.* (2004)
PLGA50/50	insoluble	paclitaxel	slightly soluble	Xie *et al.* (2006)
PLGA	insoluble	Mefoxin	soluble	Kim *et al.* (2004)
PLGA	insoluble	tetracycline hydrocloride	soluble	Hong *et al.* (2008)
Blend PLA/PEVA[(1)]	insoluble	tetracycline hydrocloride	soluble	Kenavy *et al.* (2002)
PEVA[(2)]	insoluble	tetracycline hydrocloride	soluble	Kenavy *et al.* (2002)
PLA-PEG/Chi[(3)]	partly soluble	ibuprofen	slightly soluble	Jiang *et al.* (2004)
PEG-PLA	partly soluble	Mefoxin	soluble	Kim et al. (2003)
HPMC[(4)]	soluble	itraconatsole	poor	Verreck et al. (2003)
PAM14[(5)]	soluble	diclofenac sodium	soluble (pH 5-8)	III
PVA[(6)]	soluble	Ketoprofen	insoluble	Kenavy et al. (2007)

[1] poly(lactide)/poly8ethylene vinyl acetate)

[2] poly(ethylene vinyl acetate)

[3] poly(lactide)-poly(ethylene glycol)/chitosan

[4] hydroxypropylmethylcellulose

[5] maleic acid based n-butyl hemiester of poly(maleic anhydride-alt-2-methoxyethyl vinyl ether)

[6] poly(vinyl alcohol)

Electrospun nanoscaffolds in particular have evoked interest in tissue engineering since the nano fiber size mimics the diameters of natural fibers in an extracellular matrix (ECM). Several authors have loaded the fibers with growth factors such as epidermal growth factors (Choi *et al.*, 2008), bone morphogenetic proteins (Moroni *et al.*, 2006), nerve growth factors (Chew *et al.*, 2005), and platelet derived growth factors (Liao *et al.*, 2006). The suitability of nanoscaffolds loaded with growth factors has been demonstrated by many authors.

Several attempts have been made to control drug release from nanofibers. Drug-loaded nanoscaffolds tend to have a strong burst release during the first few hours. The degree of similarity in hydrophilicity between drug and polymer plays a major role in drug encapsulation into electrospun fibers. When the solubility of polymer and drug to the solvent is different, the drug tends to locate nearer to the surface of the fiber, resulting in a fast release rate (Zeng *et al.*, 2005). As first reported by Sun *et al.*, (2003), co-axial electrospinning makes it possible to manufacture composite nanofibers having a core-shell structure. The problem of large burst release from the nanofibers can be avoided

with such a structure (Zhang *et al.*, 2006) since it is possible to vary the release rate of the drug from the core polymer (Huang *et al.*, 2006). Core-shell structures can also be obtained by emulsion electrospinning without the two spinneret system employed in co-axial electrospinning. The properties of water-in-oil (w/o) emulsion formed of amphiphilic polymer, such as PLA-PEG and added surfactant, defines the core-shell structure. For example, if a hydrophilic drug is added directly to PLA-PEG in a chloroform solution, the drug is squeezed to the surface because of the rapid evaporation of chloroform and fiber stretching during the electrospinning process. However, when the drug is first dissolved in water prior to w/o emulsion, it is located on the inner part of the formed core-shell nanofibers (Xu *et al.*, 2005, Xu *et al.*, 2008).

In order to obtain extended release from nanofibers, Kim *et al.*, (2004) and Luu *et al.*, (2003) studied the effect on the drug release rate of changing the ratio between hydrophilic PEG-PLA copolymer and PLGA. They observed that a larger proportion of PLGA increased the thickness of the fibers and resulted in a slower drug release. Cui *et al.*, (2006) also observed the straightforward relationship between fiber size, drug loading and release rate with paracetamol-loaded P(DLLA) nanofibers. Another approach was to manufacture composite nanofibers by adding nano-sized HAp particles to nanofiber structures (Nie and Wang 2007, Fu *et al.*, 2008, Erisken *et al.*, 2008). For example, Nie and Wang (2007) manufactured HAp and DNA-loaded PLGA nanofibers by loading in three different ways. DNA was loaded either by dipping the Hap-loaded scaffold in a naked DNA solution, first encapsulating the DNA into chitosan nanoparticles and then dipping the scaffolds in a nanoparticle solution, and adding DNA-loaded nanoparticles to the spinning solution. As a result, HAp increased the release rate of DNA and the cells grew better in the scaffold into which DNA was first loaded in chitosan nanoparticles.

Other applications for which drug-releasing nanofibers have been suggested are the prevention of abdominal adhesions (Zong *et al.*, 2004, Bölgen *et al.*, 2007), sutures (He *et al.*, 2009), and coatings of neural electrodes (Abidian *et al.*, 2006).

2.8. Polymeric drug releasing biodegradable composites

Developed in 1970s for treatment of osteomyelitis, one of the first local drug-releasing applications was the antibiotic agent, gentamicin, which released poly(methyl methacrylate) (PMMA) beads (Walenkamp 2001). The inappropriate release of gentamicin at sub-therapeutic levels led to the development of bacterial resistance to gentamicin and failure of the implant (Neut *et al.*, 2003). Thus, adequate release rates and concentrations in target tissue are essential for achieving the necessary therapeutic effects, i.e. the control of tissue reactions by means of a drug-releasing device. As mentioned in Chapter 2.6, the control of drug release from ester-based materials has been based mainly on matrix hydrolysis, followed by a change in textural and

rheological behavior, matrix erosion, and/or drug dissolution and diffusion, with significant dependence on drug solubility and concentration (Lemmouchi *et al.,* 1998, Babazadeh 2006, Jain 2000). Besides the development of matrix polymers and combinations of drug and polymer, one approach is to manufacture biodegradable polymer/drug composite structures to control the release rate from the system. Each component has its unique properties, contributing to the characteristics of the resulting composite.

Another relatively new approach to controlling tissue reactions is the use of drug delivery devices to deliver many drugs simultaneously in one device. This can be advantageous in the treatment of various pathologies such as resistant infections, inflammation, and cancers. By combination therapy it is possible to control and support ongoing tissue reactions at certain intervals while also treating the problem from different angles.

2.8.1. Composite structures for controlling the release

Chia *et al.,* (2008) controlled the drug release by developing layer films from PLGA and plasticized PLGA. The layered film degraded more by erosion than by bulk degradation. The more hydrophobic inner layer made of plasticized PLGA degraded more slowly than the hydrophilic PLGA. They also controlled the release by electron beam radiation, thus changing the onset of polymer layer mass loss. Another layered structure, a composite comprising an outer layer with micro-orifices, a thin diffusion middle layer, and a tetracycline-loaded inner layer was introduced by Ryu *et al.,* (2007). The outer and inner layers were made of PLGA85/15 and the diffusion layer was PLGA50/50. The variation in the dimensions and the locations of the micro-orifices and the thickness of the diffusion layer changed the release pattern of the drug and osmotic pressure. Zalfen *et al.,* (2008) studied the release of levonorgestrel (LNG) from PCL microparticles, which were loaded in a 2-hydroxyethyl methacrylate (pHEMA) hydrogel. The LNG was released much faster from hydrogel than from the microparticles in hydrogel. However, the release from LNG-loaded microparticles was slower than that from microparticles in hydrogel. This was explained by the different experimental conditions and the better solubility of poorly water soluble LNG to pHEMA than aqueous media, which was used in the release test. A similar approach was introduced by Kempen *et al.,* (2005). They loaded poly(propylene fumarate) (PPF) or PLGA microparticles with the model drug Texas Red Dextran and these microspheres were loaded in an injectable and porous PPF scaffold. The microspheres were prepared using a w-o-w solvent evaporation technique. The scaffolds loaded with microspheres were prepared by a foaming technique using N-vinylpyrrolidone (NVP) as a crosslinker, benzoyl peroxide (BP) as an initiator, and N,N dimethyl-p-toluidine (DMT) as an accelerator. PPF, microspheres and other substances were mixed and after initiation of foaming, the polymer paste was extruded through a syringe with a needle into Teflon® molds. The scaffolds that formed were left to polymerize overnight and

then lyophilized. Five different scaffold types were studied: 1) high or 2) low microsphere concentration, 3) PPF or 4) PLGA microspheres, and 5) drug loaded directly in the scaffold polymer without encapsulation in microspheres. The PPF scaffold loaded with PLGA microspheres released the drug faster than the scaffold with PPF microspheres and also, surprisingly, the scaffold that had been directly loaded with plain drug. When they increased the concentration of drug-loaded microspheres in scaffolds, the differences in the release from the PLGA or PPF microsphere scaffold decreased. The burst release of microspheres loaded in composites was significantly lower than from microspheres directly. The release rate from both PLGA and PPF microsphere-loaded scaffolds had a biphasic release profile.

The high burst release of drug can be a problem in monolithic materials. Ahmed *et al.*, (2008) reported a reduction in burst release of phosphorothioate oligonucleotide drug from microparticles, which were incorporated to glycerol monooleate (GMO) formulations. Molten pure GMO or preformed cubic phase based on GMO considerably reduced the release from microparticles. GMO swells in aqueous media and the release from microparticles was considered to occur through water channels in the GMO matrix. They also developed an *in situ* forming GMO phase by adding cosolvents (ethanol, propylene glycol, polyethylene glycol 300). This formulation reduced the release, though to a lesser extent than pure GMO and preformed GMO. Naraharisetti *et al.*, (2005) studied composite discs that were manufactured by compression molding of gentamicin-loaded microspheres with PEG. Microparticles were prepared by w-o-w technique. The presence of PEG in the composite discs seemed to act as a porogen, since it dissolved rapidly in the buffer solution. The low amount of PEG did not have a great effect on the gentamicin release but by adding 10 % PEG to the composite, the release was enhanced.

One patent for a polymer composite structure with controlled release has been issued. The patent covers a structure, in which active agents are loaded in biodegradable (PLGA) tablets that are arranged either in line or in a sandwich-like structure. There are three types of tablets manufactured from variable copolymer ratios, which contribute to the release and degradation of the implant. The active agent can be a natural or synthetic hormone (Deasy 1989).

2.8.2. Multidrug releasing polymer composites

There are several reports of micelles that are loaded with two active agents. Lee *et al.*, (2008) encapsulated indomethasin and basic fibroblast growth factor into Tetronic®–PCL–heparin composite micelles. Indomethasin was loaded in the micelles by single emulsion and solvent evaporation into the core of the micelle. After that the fibroblast growth factor was attached to the heparin on the micelle surface. The loading of both agents made the release of indomethasin more sustained than when it was loaded alone in the micelle. However, double loading did not affect the release of basic fibroblast

growth factor from the surface. Wei *et al.,* (2009) reported contrasting results concerning the discrete release characteristics with poly(L-glutamic acid)-b-poly(propylene oxide)-b-poly (L-glutamic acid) (GPG) micelles carrying doxorubicin that were loaded in aspirin-loaded poly(vinyl alcohol) (PVA) or PVA/chitosan hydrogels. The micelles were manufactured by dialysis of the polymer solution against distilled water. In hydrogel manufacture, the PVA and aspirin were dissolved in water and doxorubicin-loaded micelles were added to the solution. The resulting drug/polymer/micelle solution was freeze-thawed in a special mold. It was found that doxorubicin-loaded micelles were temperature- and pH-sensitive and the release from hydrogel was controlled by the carrier micelle. The release of aspirin was fast and seemed to have no temperature or pH sensitivity in PVA hydrogel, but changed to become pH sensitive by adjusting the chitosan ratio in the hydrogel. A similar approach was reported by Holland *et al.,* (2005). They loaded low cross-linked gelatin microparticles with insulin-like growth factor-1 (IGF-1) and transforming growth factor-β1 (TGF- β1), into oligo(poly(ethylene glycol) fumarate) (OPF) hydrogel. In addition, they loaded TGF- β1 directly to the hydrogel. The release of TGF β1 differed according to whether it was loaded in the microparticles or in the hydrogel. From hydrogel, the release of TGF- β1 had high burst release followed by a steady release rate by diffusion. The TGF- β1 release from the microparticles in hydrogel had lower burst release and a steadier release rate caused by the collagenase digestive activity in the hydrogel. Eventually, both types of scaffold released the TGF- β1 over the same period but at different release rates. IGF-1 was released at similar rates from both of the scaffolds.

Ye *et al.,* (1996) dispersed levonorgestrel and estradiol-17β into a copolymer with different ratios of lactide and caprolactone and prepared disks and laminate cylinders with and without coating. The discs were manufactured by compression molding and solvent casting by dipping a liner into the drug/polymer solution. To manufacture the cylinders, the polymer and the drugs were mixed and melt extruded into the form of rods. The cylinders were formed from the rods. The cylinders were coated with levonorgestrel and a polymer solution by dipping. By increasing the ratio of caprolactone in the copolymer, the release of both agents accelerated. The release of both levonorgestrel and estradiol-17β could be controlled by changing the thickness of the coating and loadings.

Nelson *et al.,* (2003) patented a biodegradable fabric, which can release many agents. The agents are loaded in a solution of spun fibers and the fibers are then woven, non woven, knitted or combinations of these to form a fabric. This fabric can be used as a scaffold in a single plane or in multilayered form. The drug release can be controlled by the coaxial layered structure of the fiber.

3 AIMS OF THE STUDY

The aims of the current study were to investigate following issues:

1. The development and characterization of drug-releasing biodegradable polymer composites with controlled release characteristics (I-VII).

2. The development and characterization of nanofiber structures for use as scaffolds for tissue ingrowth (I, II, III).

3. The development and characterization of biodegradable polymeric composites with controlled release from components with known release characteristics. (IV, V).

4. The development and characterization of multidrug-loaded composites with controlled release from components with known release characteristics (VI. VII).

4 MATERIALS AND METHODS

4.1. Materials

Most of the polymer materials were purchased from suppliers as were all drugs, solvents, and other materials. The hydrolysis media were prepared in the laboratory at TUT.

Polymers:

1. Poly(D,L-lactide-co- ε-caprolactone) 5/95 (P(DLLCL) 5/95) was prepared at Helsinki University of Technology, Helsinki, Finland. Polymerization was carried out in bulk under an argon atmosphere. The catalyst used was 0.1mmol/mol monomer stannous(II)octanoate, and glycerol served as the co-initiator. The polymer was re-precipitated. The average molecular weight number of the polymer measured with gel permeation chromatography (GPC) was 81 400 g/mol. (I, VI)
2. PAM14 was prepared at the University of Pisa (Pisa, Italy) and upscaled by Polymer Laboratories (UK). (II)
3. Poly(D,L-lactide-co-glycolide) 80/20 (P(DLLGA) 80/20), (PURAC Biochem B.V., Gorinchem, Netherlands). (III, IV, V, VI)
4. Poly(D,L-lactide-co-ε-caprolactone)80/20 (P(DLLCL) 80/20), (Durect Corporation, Lactel Absorbable Products, USA). (VII)
5. Poly(D,L-lactide-co-glycolide) 50/50 (P(DLLGA) 50/50), (Durect Corporation, Lactel Absorbable Products, USA). (VII)
6. Poly(vinyl alcohol) (PVA), (Sigma-Aldrich, USA). (VII)

Drugs:

1. Diclofenac sodium, (Sigma-Aldrich, Espoo, Finland) (I-VII)
2. Dexamethasone, (Sigma-Aldrich, Espoo, Finland) (V-VII)
3. Etidronate, (Sigma-Aldhrich, Espoo, Finland) (VI)

Solvents:

1. Acetic acid, (Mallinckrodt Baker B.V., Netherlands).
2. Acetone, (Baker B.V., Netherlands).
3. Dimethylformamide (DMF), (Labscan, Poland)
4. Dichloromethane (DCM), (J.T. Baker B.V., Deventer, Netherlands).
5. Ethanol, (Oriola Oy, Espoo, Finland).

4.2. Methods

The processing methods used in the preparation of the drug-releasing materials were electrostatic spinning (I, II, III, and VI); melt extrusion (IV); fiber spinning (V, VI, and VII); heat pressing (IV and V); solid state deformation, i.e. self-reinforcement (IV); solvent casting (VI); and water-in-oil-in-water technique (VII). The drug-releasing materials and processing methods used in their manufacture are presented in Table 3.

Table 3. Processing methods and materials used for preparation of drug releasing materials

Definition of material	Structure	Processing Method	Polymer	Agent
Drug loaded nanoscaffolds	porous scaffold	electrostatic spinning	P(DLLCL) 5/95 PAM14 P(DLLGA) 80/20	diclofenac sodium
Multicomponent rod A	rod	melt extrusion+heat pressing	P(DLLGA) 80/20	diclofenac sodium
Multicomponent rod B	rod	melt extrusion+heat pressing	P(DLLGA) 80/20	dexamethasone
Multidrug composite	fiber	melt spinning	P(DLLGA) 80/20	dexamethasone
	sheet	solvent casting	P(DLLCL) 5/95	etidronate
	nanofiber	electrostatic spinning	P(DLLCL) 5/95	diclofenac sodium
Multidrug fiber	fiber	melt spinning	P(DLLCL)80/20	diclofenac sodium
	fiber	melt spinning	P(DLLCL)80/20	dexamethasone
	microparticle	W-O-W	P(DLLGA)50/50+PVA	dexamethasone
	microparticle	W-O-W	P(DLLGA)50/50+PVA	diclofenac sodium

4.2.1. Preparation of nanoscaffolds by electrostatic spinning (I, II, III)

An electrostatic spinning system usually comprises a container for the polymer solution, an electrode for charging the solution, a metallic collector to collect the nanofibers, and a voltage supplier. Several parameters have an effect on the process, such as the distance between needle tip and collector, voltage, and viscosity of the polymer solution. In the electrospinning process an electric field is generated between the polymer solution and the collector using a voltage generator. The actual nanofiber formation is based on several physical instabilities occurring during the electrostatic spinning process. At the needle tip, the forces of the electric field pull the charged polymer solution from the tip towards the collector while the surface tension of the solution acts in the opposite direction. As the voltage is increased, the droplet at the tip elongates and eventually forms a jet in the form of hyperbolic cone, which is also called a Taylor cone (Reneker and Chun 1996). After initiation, the jet travels in a straight line, after which electrically driven instability is triggered by the perturbations of the lateral position and lateral velocity of the jet, causing bending, winding, spiraling and looping path in three dimensions. During the process, the solvent evaporates and allows the polymer to solidify in the form of thin fibers. The most typical defect in fiber formation is the so-called Rayleigh instability, which results in the formation of beads distributed along the fiber length (Hohman *et al.,* 2001). The critical parameters for a successful

process and fiber formation are the molecular weight of the polymer, the volatility of the solvent, electric conductivity of the polymer solution, the distance between needle tip and collector, and the applied voltage (Ashammakhi *et al.,* 2007).

In this thesis, three different types of diclofenac sodium-loaded and unloaded (Publications I, II and III, unloaded P(DLLCL) 5/95 unpublished) nanoscaffolds were manufactured by electrostatic spinning. The polymers studied were P(DLLCL) 5/95, P(DLLGA) 80/20, and PAM14. The parameters used in the electrospinning processes to manufacture the nanoscaffolds being studied are presented in Table 4.

Table 4. Processing parameters and materials used for electrospinning of nanofibers

Polymer	M_w [g/mol]	Solvent	Solution wt-%	Drug wt-%	Distance* x [cm]	Voltage [kV]	Pub
P(DLLCL) 5/95	81400	glacial acetic acid	20	2	10	20	I
P(DLLCL) 5/95	81400	glacial acetic acid	17,3	1,8	15	20	VI
P(DLLGA) 80/20	4.8 dl/g**	acetone	6	20	10	20	III
P(DLLGA) 80/20	4.8 dl/g**	acetone/DMF	6	0	10	20	III
PAM14	18kD	glacial acetic acid and ethanol	5,8,10	2	20-26	20-30	II

*distance between needle tip and collector

** inherent viscosity, no M_w available

The electrospinning system comprised a voltage generator (Simco Chargemaster BP 50), a glass syringe with a metallic needle tip for the polymer solution, and a copper plate as a collector. The copper plate was covered with aluminum foil for collecting the nanofibers. The polymer solution was charged via a metallic needle tip, which acted as an electrode. The collector was grounded to zero potential. The system was placed in a fume chamber. After the electrostatic spinning process, residual solvent was removed by placing the aluminum foil into the fume chamber for 24 hours.

4.2.2. Preparation of multicomponent rods (IV, V)

Extrusion

The components of the multicomponent rods were manufactured by melt extrusion. An extruder consists of 1) a hopper as a raw material feeder, 2) a screw, which propels the polymer forward 3) a heated barrel, 4) a shape-forming nozzle, and a 5) motor drive. The most important part, the screw, is characterized by its length-diameter ratio (L/D ratio). Screws have different zones for feeding, compression, and metering, which have different flight, lead, and outside and root diameters. The feeding zone conveys the polymer granules into the barrel, after which the decrease in the flight depth of the screw causes volume compression of the melting granules, forcing the encapsulated air to move back to the feeding zone. During compression, the polymer melt is subjected to frictional forces, which generate heat and also increase the fluidity of the melt. This increases the mixing and homogenous heat distribution in the melt. The polymer is thoroughly melted when it enters the metering zone, which forces the melt through the

nozzle (Chanda and Roy 2008). The transportation of the polymer in a single screw extruder is based on the friction between the polymer and walls of the channel. In a twin screw extruder the transportation is less dependent on the material properties than in single screw extruders, enabling the materials to be compounded with additives and heat sensitive materials. There are several types of twin screw extruder: a) non-intermeshing, mixing or transport mode; b) intermeshing, counter-rotating or co-rotating; c) conical counter-rotating; and d) self-wiping, co-rotating (Janssen 2005).

In this thesis, a co-rotating and intermeshing twin screw extruder (Mini ZE 20 x 11.5 D, Neste Oy, Koelaitepalvelut, Porvoo, Finland) was used to form 8 wt-% diclofenac sodium-loaded billets (IV) and 2 wt-% and 8 wt-% dexamethasone-loaded fibers with fiber spinning equipment. The polymer (P(DLLGA)80/20) and the drugs were mechanically mixed using an electric blender (Retsch Grindomix GM200, Retsch GmbH and Co. KG, Haan, Germany). The polymer and drugs were dried in a vacuum oven (Binder VD 115, WTB Binder, Germany) before and after mixing. The feeding of the polymer/drug mixture was performed under nitrogen atmosphere. The diameter of the nozzle was 3 mm for the rods and 1mm for the fibers. The extruded diclofenac sodium-loaded billet was channeled through a cooling system (pressurized air and water-cooled plate) to a manually controlled drawing belt to optimize the diameter of the rod and the surface properties. The extruded dexamethasone-loaded fibers were drawn from the nozzle and spun onto the reel with a spinning line consisting of three straps and three ovens. Extrusion parameters were adjusted during the extrusion processes.

Self-reinforcement

Some of the diclofenac sodium billets were self-reinforced to change the drug release rate of the billet. The process is solid state deformation, in which the polymer billet is heated to a few degrees above T_g and below T_m. The billet is drawn through an orifice having a smaller diameter than the billet, forcing the polymer chains to be oriented parallel to the drawing force (Törmälä 1992). The rods were drawn vertically through a die 1.4 mm in diameter. The drawing speed was 16 mm/min and the temperature in both the cylinder and the die was 87 ºC. The self-reinforced billets were 1.16–1.27 mm in diameter, resulting in a draw ratio of about 4.

Gamma irritation

Some of the self-reinforced billets and dexamethasone fibers were sterilized by γ-irradiation with a dosage of 25 kGy (Willy Rüsch Ltd., Kernen-Rommelshausen, Germany). In addition, some of the multicomponent rods were sterilized after manufacture with the same radiation dose.

Compression molding

Multicomponent rods were manufactured by compression molding (NIKE Hydraulics Ab, Eskilstuna, Sweden) from the components to form a single piece. The construction of the multicomponent rods and the parameters are presented is Table 5. The applied pressure for all rods was 20 MPa and the temperature was 120 ˚C. The two different types of molds (slit diameters 1 mm and 3 mm) were made of stainless steel. After turning off the heat, the mold was cooled to room temperature with a circulating cold water cooling system.

Table 5. Compositions and dimensions of multicomponent rods

MC type	Abbrev.	Construction	D/L1*	Mould [ø/ end caps]	Notes	D/L2**	Publ.
Diclofenac rod type 1	MC-1	1 x compounded billet 1 x self-reinforced billet 1 x self-reinforced and sterilized billet	1.0-1.27/25 1.0-1.27/25 1.0-1.27/25	1.5mm/no	heat turned off after reaching target temperature	1.5/30	IV
Diclofenac rod type 2	MC-2	1x compounded billet 3 x self reinforced billets 2 x sterilized self-reinforced billets	2.3/25 1.2/25 1.2/25	3mm/yes	end caps in the mould, heat turned off after reaching target temperature	3/30	IV
Diclofenac rod type 3	MC-3	1x compounded billet 3 x self reinforced billets 2 x sterilized self-reinforced billets	2.3/25 1.2/25 1.2/25	3mm/yes	end caps in the mould, heat turned off after reaching target temperature, γ-	3/30	IV
Dexamethasone rod type 1	MC-DX 1	3 x 2% dexamethasone fibers 3 x 2% sterilized dexamethasone fibers 3 x 8% dexamethasone fibers 3 x 8% sterilized dexamethasone fibers	0.36-0.42/40 0.36-0.42/40 0.36-0.42/40 0.36-0.42/40	1.5mm/no	heated for 5 min	1.5/30	V
Dexamethasone rod type 2	MC-DX 2	3 x 2% dexamethasone fibers 3 x 2% sterilized dexamethasone fibers 3 x 8% dexamethasone fibers 3 x 8% sterilized dexamethasone fibers	0.36-0.42/40 0.36-0.42/40 0.36-0.42/40 0.36-0.42/40	1.5mm/no	heated for 5 min, γ-sterilized	1.5/30	V

*Diameter/lenght of components [mm]

**Diameter/lenght of multicomponent rod [mm]

4.2.3. Preparation of multidrug-loaded composites (VI, VII)

Multilayer composite (VI)

Several processing methods were used in the preparation of the multilayer composite. The composite was constructed of three different components: sheet, nano-size fibers and submicron-size fibers. Each was loaded with a different agent.

Layer 1: Dexamethasone carrying P(DLLGA)80/20 microfiber grid

Dexamethasone-loaded 8 wt-% fibers were manufactured by melt spinning as described in section 4.2.2. The dexamethasone-loaded fiber grid was manufactured by a metallic spinning aid. The resulting fiber grid had an approximate pore size of 10 mm. The grid was heat pressed with a charge compressor (NIKE Hydraulics Ab, Eskilstuna, Sweden) to retain its original form after detachment from the spinning aid. During heat pressing, the applied heat and pressure were 114 ºC and 6 MPa, respectively. After heat pressing, the grid was cut to a size of 40 x 60 mm.

Layer 2: Etidronate carrying P(DLLCL) 5/95 membrane

Layer 2 was manufactured by solvent casting. One milliliter of etidronate (17 wt-% in ethanol) was added to 10 ml of P(DLLCL) 5/95 solution (22 wt-% in glacial acetic acid) and mixed with a magnetic stirrer. Five milliliters of polymer/drug solution was poured into a Teflon mold measuring 50 mm x 70 mm. Layer 1, a dexamethasone-carrying grid, was placed into the mold to ensure it was the correct size and evenly covered with P(DLLCL) 5/95 polymer/drug solution. The mold was placed in a fume chamber overnight to evaporate the solvent, after which it was placed in a vacuum chamber for one day to remove the residual solvent.

Layer 3: Diclofenac sodium carrying P(DLLCL) 5/95 nanofibers

The nanofibrous layer was manufactured by electrostatic spinning. About 4 ml of P(DLLCL) 5/95 diclofenac sodium solution (20 wt-% of polymer and 2 wt-% of drug) was electrospun onto the dual layer (layer 1 and 2) as described above. The distance between needle tip and sample collector was about 15 cm and the applied voltage was 20 kV.

Three different multilayer composites were manufactured: multilayer implant 1 (ML1), which comprised all three layers; multilayer implant 2 (ML2), which comprised etidronate-loaded sheet and diclofenac sodium-loaded nanofibers; multilayer implant 3 (ML3), which comprised unloaded sheet and diclofenac sodium-loaded nanofibers; and multilayer implant 4 (ML4), which comprised dexamethasone fibers and unloaded sheet. The components and processing methods of ML1 are presented in Table 6.

Table 6. Composition of multilayer implant 1

Layer no	Component type	Polymer	Drug	Processing method
1	Submicron fiber	P(DLLGLA) 80/20	Dexamethasone	Melt spinning, knitting
2	Sheet	P(DLLCL)5/95	Etidronate	Solvent casting
3	Nanofibers	P(DLLCL)5/95	Diclofenac sodium	Electrostatic spinning

Multiphase fibers (VII)

The multiphase fibers comprised unloaded or diclofenac sodium- or dexamethasone-loaded microparticles dispersed into unloaded fibers or fibers carrying a drug. Overall, 8 different combinations of fibers were prepared and these are presented in Table 7.

Table 7. Combinations of multiphase fibers

Fiber types	Diclofenac sodium	Dexamethasone	Plain particles	Diclofenac sodium loaded particles	Dexamethasone loaded particles	Drug amount [w-%]	Particle amount [w-%]
DSDXpart fiber				X	X		4,0
DXpartDS fiber	X				X	1,9	2,0
DSpartDX fiber		X		X		2,0	2,0
PlainpartDS fiber	X		X			1,9	1,9
PlainpartDX fiber		X	X			1,9	4,0
NopartDX fiber		X				4,1	
NopartDS fiber	X					3,9	

The microparticles were manufactured using the water-in-oil-in-water (w-o-w) microencapsulation technique described by various researchers. In w-o-w the particle formation is based on solvent extraction/evaporation. In the first step of the process, water-in-oil, a hydrophobic oil polymer solution is added with vigorous mixing to an aqueous solution of surfactant to form the first solution. Depending of the dispersal capability of the mixing procedure, different sizes of particles are formed in the solution. To ensure the physical stability of the particles in the water solution, in the next step the particle solution is added to the aqueous solution with a small amount of surfactant. Finally, the hydrophobic solvent from the polymer solution is removed (Kempen *et al.,* 2006, Freitas *et al.,* 2005, Siepmann and Siepmann 2006).

In the present work, P(DLLGA)50/50 was dissolved in DCM to form 20 w-% polymer solution and 0.5 ml of diclofenac sodium in ethanol (10 wt-%) or dexamethasone in ethanol (10 wt-%) was added to the polymer solution and mixed vigorously with a homogenisator (DI 25 basic, IKA-WERKE GMBH&Co, Germany). PVA (1 wt-%) in water solution was added to the P(DLLGA)50/50 polymer/drug solution and mixed with the homogenisator. The resulting water-in-oil solution was added to a low concentration PVA (0.1 wt- %) water solution and mixed with a magnetic stirrer. The solution was placed in a fume chamber in the magnetic stirrer for four hours for evaporation of DCM. The solution was centrifuged and the pellet that formed was dispersed in 4 ml of distilled water. The samples were allowed to freeze (-20 °C) overnight. The frozen microparticles were lyophilized (Heto DRYWINNER, Jouan Nordic A/S, Allerød, Denmark) and the dried particles were kept in an exsiccator. One batch of microparticles was prepared without any drug, using the same method as described above.

The multiphase fibers were manufactured by batch melt extrusion of P(DLLCL) 20/80. P(DLLCL)20/80 granules, drug, and particles were first mixed and then placed in a glass syringe. The syringe was heated by heating elements up to a temperature of 80-90 °C and the fibers were extruded through the nozzle of the syringe. The fibers that formed were wound onto a collector reel.

4.3. Characterization methods

4.3.1. Characterization of microstructure

The microstructure of the samples was analyzed by scanning electron microscopy (SEM). The samples were cut into appropriate sizes and coated with gold using an Edwards S150 sputter coater. SEM imaging was then carried out using JEOL T100 (JEOL Ltd. Tokyo, Japan) microscope. The fiber diameters of the nanoscaffolds were measured from the SEM images at magnification of 5000. One randomly selected field per specimen was taken and each of these selected fields was divided into four squares, each of which was used for taking 10-15 measurements. Fiber diameters and bead sizes (length and diameter) were determined by means of Image J 1.33u (Wayne Rasband National Institute of Health, USA). Standard deviation and the average of fiber and bead diameters were calculated.

4.3.2. Characterization of drug release

Drug release rates were studied for all drug-loaded nanofibers, multicomponent rods, and multidrug-loaded composites. The measurements were performed by using UV/Vis-spectrophotometer (UNICAM UV 540 UV/VIS spectrophotometer, Thermo Spectronic, Cambridge, UK). Samples were precisely weighed and placed into vials containing buffer solution (KH_2PO_4 + NaOH, pH 7.4 ± 0.02 or Na-PBS, pH 7.4± 0.02) in a ratio of 100 mg of sample in 10 ml of buffer. With the nanofibers, the volume of buffer solution was higher (x 3) due to the expected large burst peak at the beginning of the test and avoidance of drug saturation in solution. The parameters of the samples in drug release tests *in vitro* are presented in Table 8.

Table 8. Parameters of drug release studies of nanofibers, multicomponent rods, and multidrug composites

Sample group	Sample type	Weight [mg]	Buffer [ml]	No of parallels	Interval of measurements [hours]*
Nanoscaffold	P(DLLCL) 5/95 + DS	30	10	5	1, 3, 6, 24
	P(DLLGA) 80/20	50	5	5	6, 24
	PAM14	60	40	3	0.5, 1, 1.5, 2, 2.5, 3.5, 4.5, 5.5, 6.5, 7.5
Multicomponent	MC-1	100	10	3	6, 24
	MC-2	100	10	5	6, 24
	MC-3	100	10	5	6, 24
	MC DX-1, MC DX-2	100	10	5	6, 18, 24
Multidrug composites	ML-1, ML-2, ML-3	100	10	5	6, 24
	Multiphase fibers	100	10	5	6, 24

*during the first 24 hours

The sample vials were kept in a rotating (100 rpm) incubator (Multitron AJ 118g, Infors, Bottmingen, Switzerland) at 37 ºC. At each drug release, measurement absorbancies of five parallel samples (except with MC-1, which had three parallel samples) were detected from buffer solutions that were removed from the vials. The absorbancies of drugs in buffer solution were measured by using UV/Vis. The maximum measured absorbancies of diclofenac sodium, dexamethasone, and etidronate

were at the wavelengths of 276 nm, 242 nm, and 247 nm, respectively. After removal of the buffer solution from the sample vials, they were refilled with fresh buffer solution. The pH of the buffer solutions that had been removed were detected using Mettler Toledo MP 225 pH meter (Mettler-Toledo GmbH, Schwerzebbach, Switzerland). The intervals between the measurements were intentionally varied to avoid saturation of the drug in the buffer. The intervals were based on the type of the sample (surface area versus volume and the degradation behavior of the polymer). During the first week, the measurements were taken daily and later on, two or three times a week. The daily released concentrations were determined by dividing the amount of released drug by the number of days in immersion since the previous measurement.

In the single drug-loaded materials, the values of the diclofenac sodium and dexamethasone absorbancies were calculated using standard curves with linear regression. The formula for calculation of diclofenac sodium was $y = 0.0317x + 0.0091$ with a concentration range 0.5-100 µg/ml and reliability of 0.9999. For dexamethasone it was $y = 0.0377x – 0.0132$ with a concentration range 0.64-80 µg/ml and reliability of 0.9989. Etidronate is not sensitive in the UV/Vis range and therefore a method using chromophore Cu^{2+} complex had to be applied. The method was modified from the method presented by Ostovic *et al.*, (1993). The formula for the calculation of etidronate/Cu^{2+} complex was $y = 0.0043x – 0.1485$ with a concentration range 15-300 µg/ml and reliability of 0.9848.

The maximum absorbance wavelengths of diclofenac sodium and dexamethasone are fairly close, 276 nm and 242 nm respectively. When absorbancies of these drugs are measured simultaneously, some overlapping of absorbance curves might occur. Thus, in multidrug composites, the absorbancies of diclofenac sodium and dexamethasone were measured using multicomponent analysis (MCA) of UNICAM spectrophotometer. The MCA was performed using Visio Pro (Thermo Spectronic, Cambridge, UK) software, which calculates the concentrations of released agents using the Kalman filter and statistical error estimation. The calibration concentration matrix of diclofenac sodium and dexamethasone ranged from 0 µg/ml to 100 µg/ml and from 0 µg/ml to 80 µg/ml, respectively, with different concentration set-ups.

4.3.3. Correlation of drug release rate

Pearson product-moment correlation coefficient analysis was applied to study the correlation between drug release from the different types of diclofenac sodium-loaded rods, multilayer composites, and multiphase fibers. In multicomponent rods, the correlation between components and MC-1 was calculated using values of average daily concentrations, due to the different number of parallel samples. The correlation of drug release between components and other multicomponent rods, multilayer composites, and multiphase fibers was analyzed for all five parallel samples.

4.3.4. Drug localization

Drug localization of the nanofiber scaffolds was studied for diclofenac sodium-loaded P(DLLGA) 80/20 and PAM14 (8 wt-%). The localization was done by means of energy dispersive X-ray microscopy in low vacuum conditions (about 13 Pa) performed with JEOL LSM5600LV. Samples were dried under vacuum, removed from the aluminum foil and analyzed, avoiding further treatments. The detection of chlorine as a chemical element was correlated to the presence of diclofenac sodium (chemical formula $C_{14}H_{10}Cl_2NO_2Na$).

4.3.5. Mechanical tests

The shear strength of multicomponents MC-1, MC DX-1, and MC DX-2 was studied with an Instron 4411 material tester (Instron Ltd., High Wycombe, England). Shear strength tests were carried out using a modified method based on standard ASTM B 769-94. The shear strength (τ) was calculated by:

$$\tau = F / 2A \qquad (13)$$

where F is the force at fracture and A is the area of the cross-section of the sample. The three point method that was utilized cuts the sample at two points, causing a multiplication of cross-sectional area by two. The crosshead speed was 10 mm/min, initial clamp distance 5 cm, and load cell 0.5 kN.

The mechanical properties *in vitro* of the MC-1 rods were tested after 0, 3, 7, and 14 days in immersion at +37 ˚C (KH_2PO_4+NaOH buffer). The mechanical properties *in vitro* of MC DX-1 were tested after 0, 3, 7, 14, and 28 days immersion at +37 ˚C (KH_2PO_4+NaOH buffer). Five parallel samples were used for every measurement.

4.3.6. Thermal properties

Differential scanning calorimetry (DSC) (TA instruments Q1000, TA Instruments Ltd., New Castle, DE, USA) was used for determination of melting temperature (T_m), heat of fusion (ΔH), and glass transition temperature (T_g) from P(DLLCL) 5/95 raw material, electrospun P(DLLCL) 5/95 (unpublished), multicomponent rods (MC-DX, unpublished), and components of MC-1 (A, B, and C) after 0, 3, 7, and 14 days *in vitro*. Samples were weighed using Mettler AT621 precision scale (Mettler Instrumente AG, Grefenzee, Germany) in aluminum pans. As a purge gas, nitrogen was used. The heating cycle applied for P(DLLCL) 5/95 was from -100 ºC to 100 ºC and cooling to -20 ºC at a rate of 20 ºC/ min. The heating cycle for multicomponents was from 10 ºC to 200 ºC and cooling to 10 ºC at a rate of 20 ºC/ min. In both runs indium was used as a calibration standard. The heating program was run twice with every sample. Melting point (T_m) and heat of fusion (ΔH) were determined from the first heating cycle. The

glass transition temperature (T_g) and heat capacity (ΔC_p) were determined from the second heating cycle.

Thermogravimetric analysis (TGA) of multiphase fibers and P(DLLCL) 80/20 polymer was studied using TGA Q 500 thermogravimetric analyzer (TA Instruments, Delaware, USA) to determine the average amounts of different polymer materials and drug in the fiber. The heating rate was 50.00 C°/min and the temperature range 21-600 C°. The mass change and residual material amount after heating were analyzed. From the derivative weight (%/C°) curve, peak maximums and some other minor peaks were explored and the remaining mass percent at peaks was analyzed to estimate the amount of lost mass and material type.

5 RESULTS

5.1. Nanoscaffolds (I, II, III)

5.1.1. Structural properties

The structure of the nanofiber scaffolds was examined by SEM, which revealed a high porosity of the nanoscaffolds. Diclofenac sodium-loaded P(DLLCL) 5/95 formed lamellae structures and at low magnifications the lamellae seemed to be constructed of spheres (Fig. 11a). At higher magnifications the nanofibers were visible, showing an interconnected net with beads (Fig. 11b).

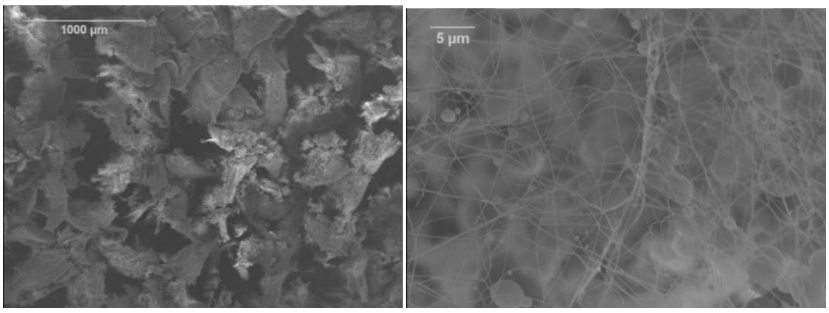

(a) (b)

Figure 11. SEM pictures of diclofenac sodium-loaded P(DLLCL)5/95 nanoscaffold with a) low and b) high magnification (I).

The average diameter of diclofenac the sodium-loaded P(DLLCL) 5/95 nanofibers was 128±36 nm and bead diameter 3.29 ± 1.49 µm. The thickness of the diclofenac sodium-loaded P(DLLCL) 5/95 nanoscaffolds was approximately 2 mm.

Low magnifications of diclofenac sodium-loaded P(DLLGA) 80/20 nanoscaffold showed a highly porous structure. High magnifications showed that the structure contained beads of different shapes (Fig. 12a). The average diameters of the diclofenac sodium-loaded P(DLLGA) 80/20 nanofibers and beads were 500 ± 949 nm and 176 ± 27 µm, respectively. The thickness of the scaffold was approximately 1 mm. Fiber diameter of the unloaded P(DLLGA) 80/20 scaffold was approximately 1.00 ± 0.25 µm and no beads were observed (Fig. 12b). The fiber diameter of the diclofenac sodium-loaded PAM14 nanoscaffolds was 105 - 1050 nm.

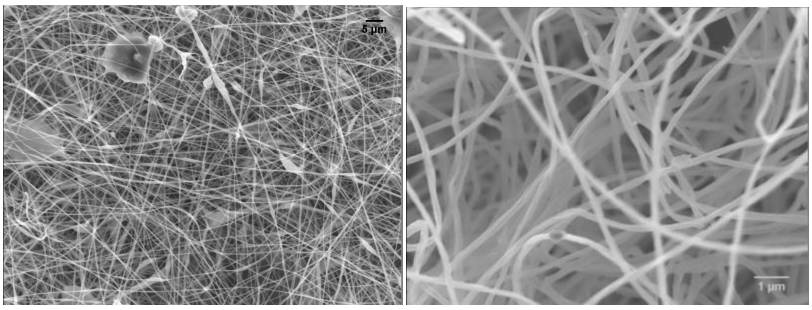

(a) (b)

Figure 12. SEM micrographs of (a) diclofenac sodium-loaded P(DLLGA) 80/20 nanoscaffold and b) unloaded PLGA 80/20 nanoscaffold with high magnification.

5.1.2. Drug release

During the first day in immersion about 45 % of diclofenac sodium was released from the P(DLLCL) 5/95 nanoscaffold (Fig. 13 a). After the burst peak, the release rate decreased from 0.4 µg/ml/day to 0.1 µg/ml/day during the first 30 days and increased up to 0.28 µg/ml/day at day 48. Then the release rate decreased to zero after 90 days in immersion. The drug release test of the non-UV-treated P(DLLGA)80/20 scaffold showed that after a high initial peak during the first day, the drug release rate decreased from a level of 20 µg/m/day to a level of 2 µg/ml/day during the following 11 days (Fig. 13 b). The release period lasted for about 60 days and the material vanished completely in 3.5 months. The drug release test of the UV-treated P(DLLGA) 80/20 scaffold showed that after a high release peak during the first day, drug release rate fell from a level of 5 µg/m/day to a level of 1 µg/ml/day. The entire release period lasted about 25 days. Cumulative calculations showed that only 40 % of loaded drug was released from the UV-treated nanoscaffold while almost all drug was released from the non-treated nanoscaffold.

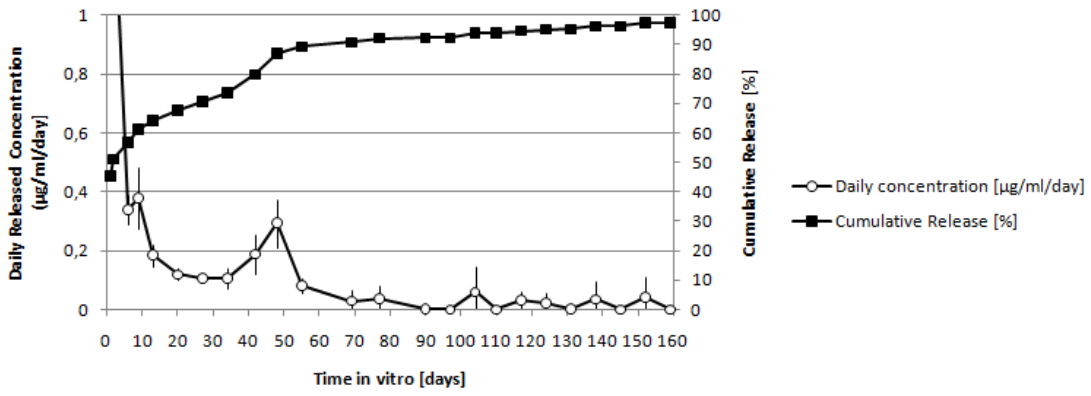

(a)

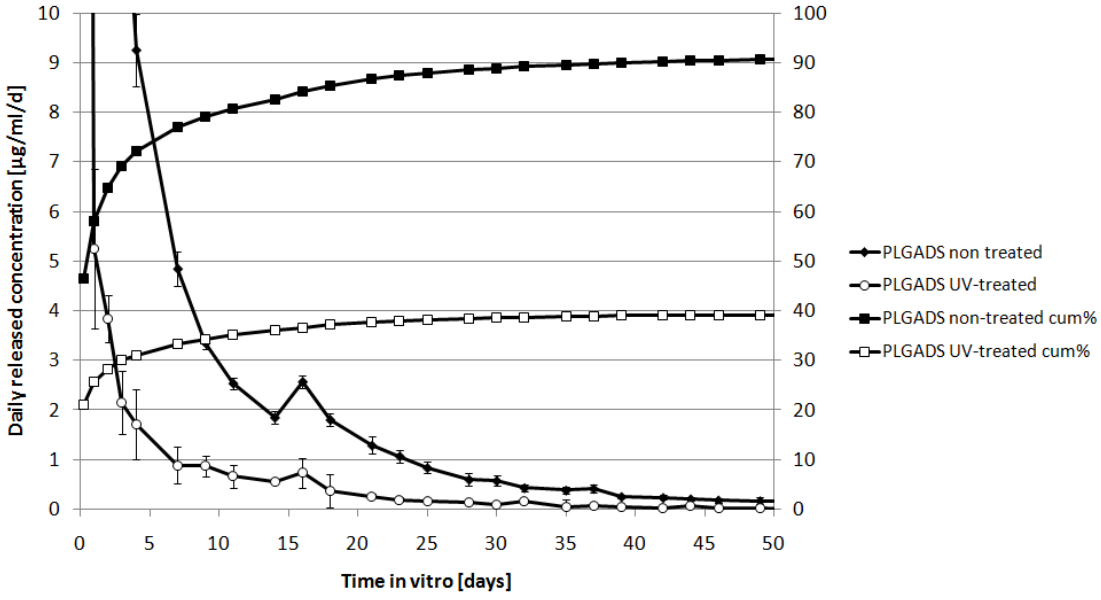

(b)

Figure 13. Cumulative release (%) and daily released drug concentrations from a) P(DLLCL) 5/95 and b) UV-treated and non-UV-treated P(DLLGA) 80/20 nanoscaffolds. (I, III)

Table 9 presents the time points when 50 % and of loaded drug and the rest of the drug was released from the scaffolds. Diclofenac sodium was released from the PAM14 (8 wt-%) nanoscaffolds in less than 30 minutes.

Table 9. Time points (days), when 50 % of loaded drug and the rest of the drug was released from nanoscaffolds

Sample ID	Drug	50 %	End of release	Pub. No
P(DLLCL) 5/95	diclofenac sodium	2 days	97 days	I
P(DLLGLA) 80/20		1 day	60 days	III
P(DLLGLA) 80/20 -UV		1 day	25 days	III
PAM14		<15 min	<30 min	II

5.1.3. Drug localization

Drug localization analysis was performed for diclofenac sodium-loaded P(DLLGA) 80/20 and PAM14 (8 wt-%). In the P(DLLGA) 80/20 nanoscaffolds more chlorine of diclofenac sodium was detected inside the beads than in the fibers while in the PAM14 nanoscaffolds there was little difference in the chlorine distribution between beads and fibers.

5.1.4. Thermal properties

TGA analysis of P(DLLCL) 5/95 revealed two degradation temperatures. The first temperature occurred at 300 °C and the second at 390 °C. DSC analysis of P(DLLCL) 5/95 showed that T_m decreased from 58 °C to 53 °C after adding the drug and electrospinning process (Fig. 14a). However, the T_g did not change and remained close to -63 °C (Fig. 14b).

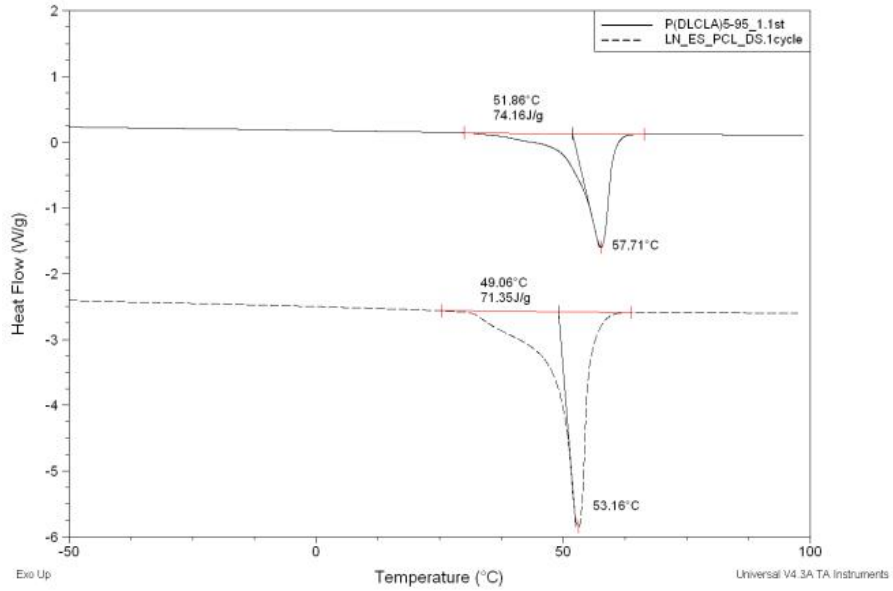

(a)

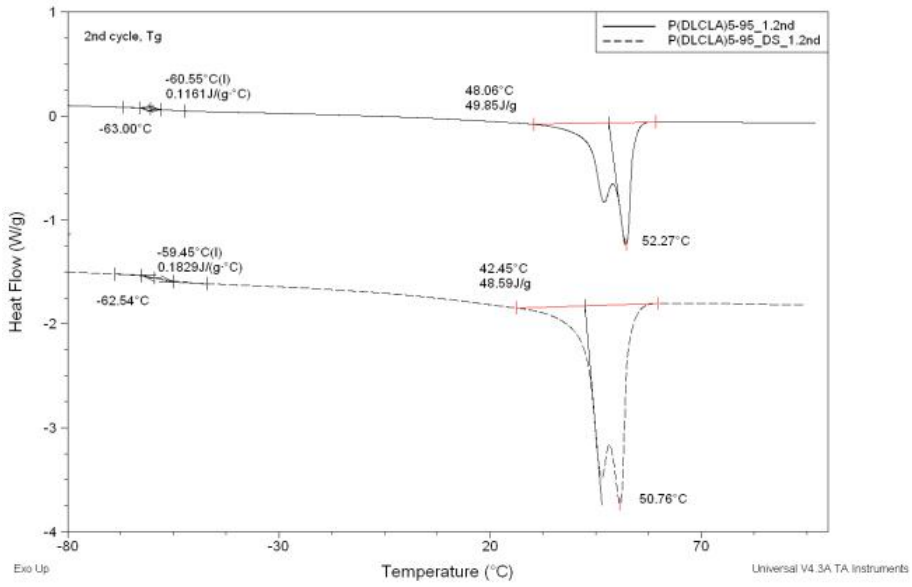

(b)

Figure 14. DCS curves of unloaded P(DLLCL) 5/95 and diclofenac sodium-loaded P(DLLCL) 5/95 nanoscaffolds. a) The first heating cycle with melting temperatures and b) second heating cycle with glass transition temperatures (unpublished).

TGA analysis of PAM14 had three main steps and the first degradation temperature was close to 170 °C. In DSC analysis no melting temperature was observed. The T_g of the electrospun unloaded materials in ethanol solutions was about 52.4 °C and the unprocessed PAM14 was 49.5 °C. The T_g of the drug-loaded nanoscaffolds was slightly higher than the analogous drug-free nanofibers.

5.2. Multicomponent materials (IV, V)

5.2.1. Structural properties

The microstructure of MC-1 was studied by SEM for only two weeks *in vitro* due to the disintegration of components after two weeks. Before hydrolysis and after one week *in vitro*, integration of components seemed to be continuous in the cross section of the rod (Fig. 15a) and no clear boundaries between different components could be observed. However, on the surface of MC-1, small cuts and flakes were observed in the boundaries of different components (Fig. 15b). Some drug particles and arrow tip-like crystals were seen on the cut surface. Disintegration of dexamethasone-loaded multicomponents occurred after four weeks in hydrolysis.

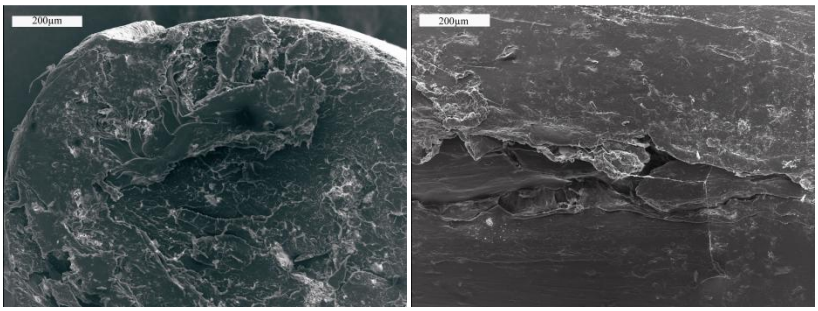

(a) (b)

Figure 15. SEM micrographs of multicomponent rod 1: a) cross-section and b) surface of MC-1 after one week in hydrolysis (IV).

5.2.2. Drug release

The release curves of diclofenac sodium and dexamethasone-loaded components and rods are presented in Figures 16 and 17, respectively. Basically, all components and rods exhibited a start peak during the first day *in vitro*. The components and the multicomponent rods had two peaks in the daily concentration release curves.

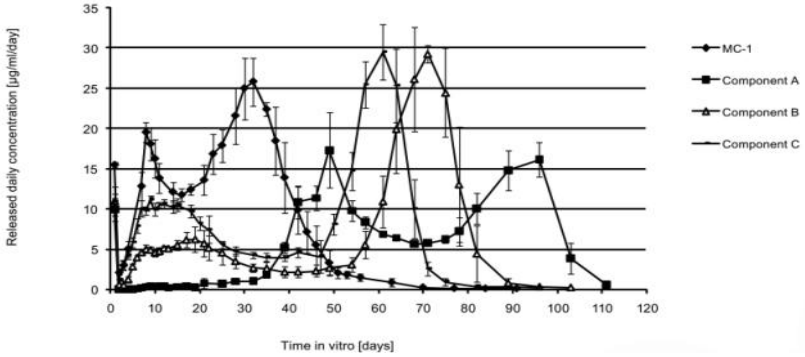

(a)

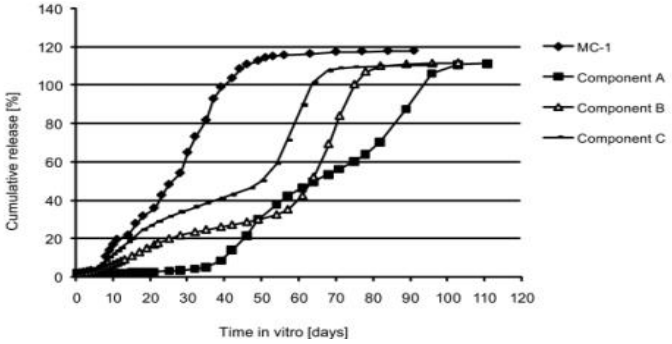

(b)

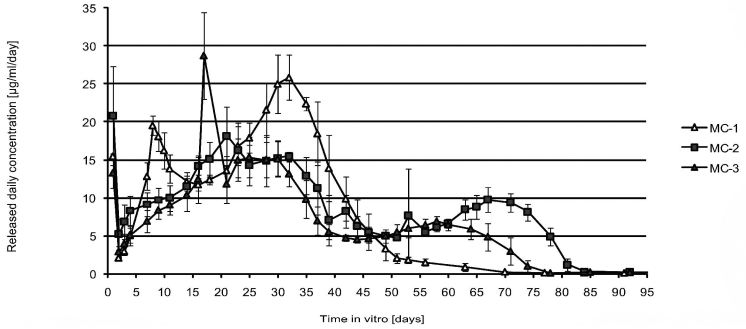

(c)

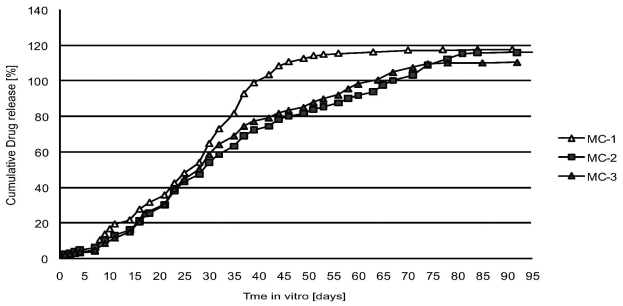

(d)

Figure 16. a) Daily released drug concentration curves of components A, B, and C and MC-1; b) cumulative drug release from components A, B , and C and MC-1; c) daily released concentrations of MC-1, MC-2, and MC-3; and d) cumulative drug release from MC-1, MC-2, and MC-3 (IV).

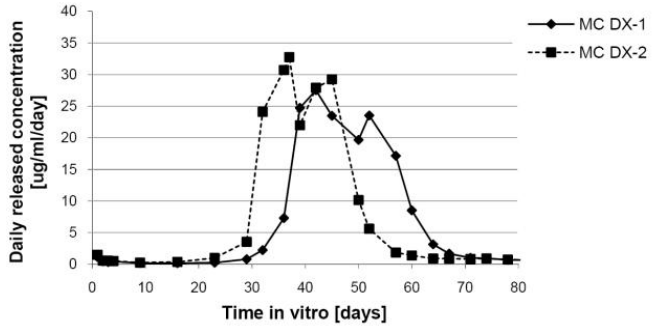

(a)

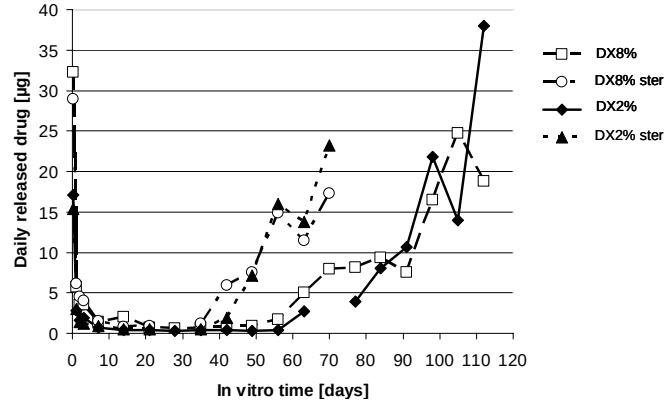

(b)

Figure 17. a) Daily released drug concentration of dexamethasone-loaded multicomponent rod (MC DX-1) and b) released drug concentration of the components (V).

The time points when 50 % of loaded drug and the rest of the drug was released from the components and rods are presented in Table 10.

Table 10. Table of time (days) points when 50 % of loaded drug and the rest of the drug was released from multicomponent rods and components of MC-1

Sample ID	Drug	50% [d]	End of release [d]	Pub. No/ref
Component A	diclofenac sodium	30	111	IV
Component B		64	96	
Component C		54	89	
MC-1		24	63	
MC-2		28	81	
MC-3		25	74	
MC-DX 1	dexamethasone	45	106	V
MC-DX 2		37	93	

5.2.3. Mechanical properties

The initial shear strength of the diclofenac sodium and dexamethasone-loaded multicomponent rods was 55 MPa and 135 MPa, respectively. After two weeks in hydrolysis, the shear strength of diclofenac sodium-loaded multicomponent decreased 40 MPa. The initial shear strength of diclofenac sodium-loaded components A, B and C

was 55 MPa, 88 MPa and 93 MPa, respectively. The shear strength of the dexamethasone-loaded multicomponent rod decreased 30 MPa in four weeks.

5.2.4. Thermal properties

The results of DSC analysis (melting temperatures, heat fusion and glass transition temperatures) of the diclofenac sodium-loaded components of MC-1 (no hydrolysis), multicomponent rod (MC-1) in hydrolysis (0-14 days), and dexamethasone-loaded multicomponent rod (MC-DX) (no hydrolysis) are presented in Table 11.

Table 11. DSC results of components of MC-1, MC-1 in hydrolysis, and dexamethasone loaded multicomponent rod

Sample type	T_m [C°]	ΔH [J/g]	Tg [C°]	Note	Publication
MC component A	58/159	6.8/4.3	53	2 x T_m	IV
MC component B	52/155	4.00/24.6	51	2 x T_m, crystallization at 92 °C	IV
MC component C	81/156	11.4/25.2	52	2 x T_m, crystallization at 91 °C	IV
MC-1 0d	61/157	0,3	53		IV
MC-1 3d	53/150	6,9	36	recrystallization after 95 °C	IV
MC-1 7d	60/155	1,6	47	recrystallization after 104 °C	IV
MC-1 14d	71/156	13,0	42	recrystallization after 103 °C	IV
MC-DX	61/151	24,3	53		* (V)

* unpublished data related to publication V

The T_m of components of the diclofenac sodium-loaded composite A, B, and C were 159 ºC, 155 ºC, and 156 ºC, respectively. All the components showed relaxation of orientation below 70 °C as negative heat flow. In component B (self-reinforced rod) some cold crystallization was observed between 80 °C and 110 ºC (Fig. 18a). Heat fusion (ΔH) of components A, B, and C were 4.3 J/g, 24.6 J/g, and 25.2 J/g, respectively. T_g of components A, B, and C was between 48- 55.5 ºC (Fig. 18b). Component B also showed cold crystallization between 110 °C and 150 °C, which melted at 154 °C. All the components showed some relaxation around 160 °C.

The initial heat of fusion of MC-1 was 13.3 J/g and the melting temperature was 157 ºC (Fig. 18c). During two weeks of hydrolysis of MC-1, the T_m did not change. In all samples (0, 3d, 7d, and 14d) some relaxation of the polymer fibers occurred between 42 °C and 59 °C. During two weeks of hydrolysis, T_m increased and cold crystallization phenomena increased during hydrolysis. The initial T_g of MC-1 was 53 ºC. Some relaxation of the polymer fibers can be observed at 158 °C. Some cold crystallization and melting can be observed between 100 ºC and 160 ºC (Fig. 18d).

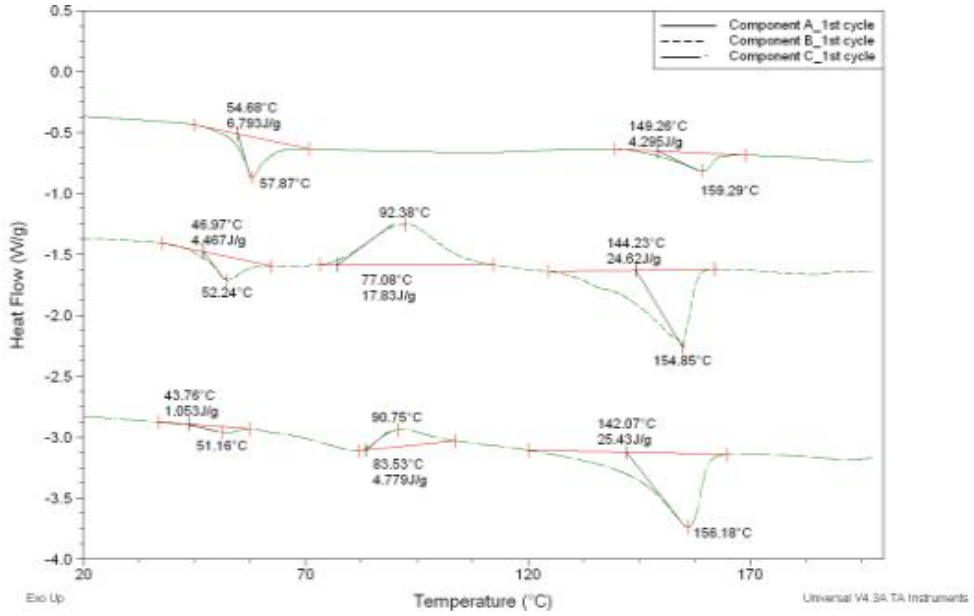
Component A_1st cycle
Component B_1st cycle
Component C_1st cycle
54.68°C
6.793J/g
57.87°C
149.26°C
4.295J/g
159.29°C
46.97°C
4.467J/g
52.24°C
92.38°C
77.08°C
17.83J/g
144.23°C
24.62J/g
154.85°C
43.76°C
1.053J/g
51.16°C
90.75°C
83.53°C
4.779J/g
142.07°C
25.43J/g
156.18°C
Heat Flow (W/g)
Temperature (°C)
Exo Up
Universal V4.3A TA Instruments

(a)

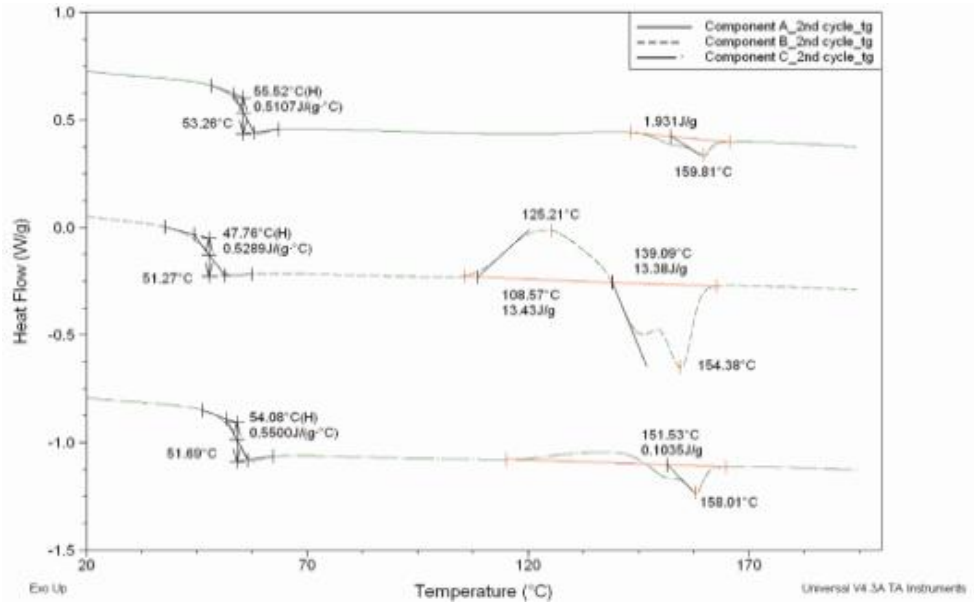
Component A_2nd cycle_tg
Component B_2nd cycle_tg
Component C_2nd cycle_tg
55.52°C(H)
0.5107J/g·°C)
53.26°C
1.931J/g
159.81°C
47.76°C(H)
0.5289J/g·°C)
51.27°C
126.21°C
139.09°C
13.38J/g
108.57°C
13.43J/g
154.38°C
54.08°C(H)
0.5500J/g·°C)
51.69°C
151.53°C
0.1035J/g
158.01°C
Heat Flow (W/g)
Temperature (°C)
Exo Up
Universal V4.3A TA Instruments

(b)

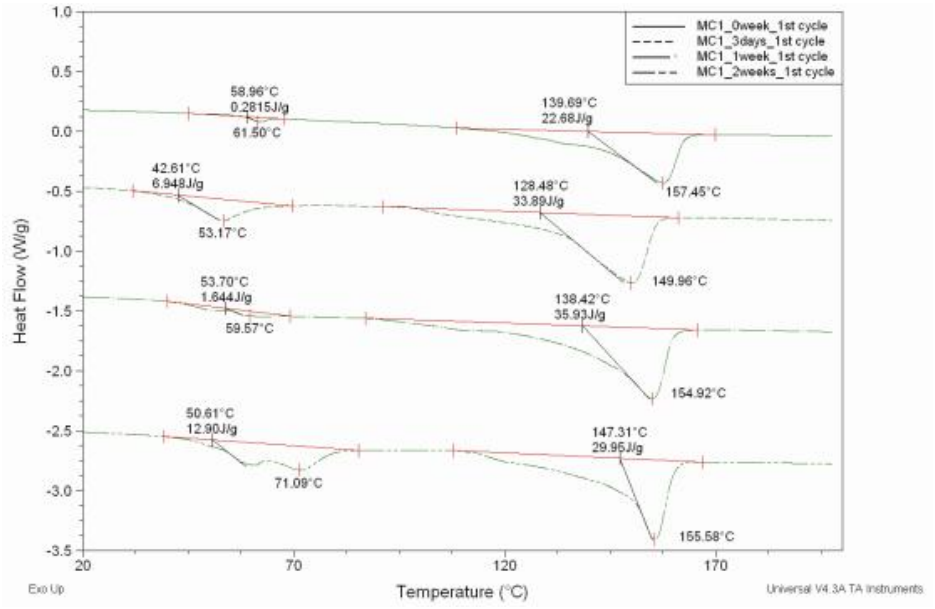

(c)

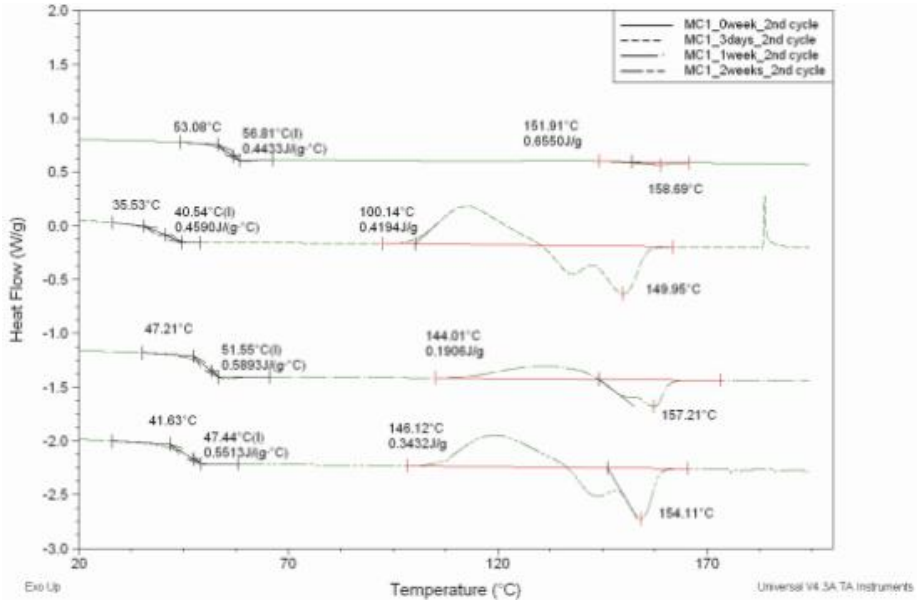

(d)

Figure 18. a) DSC curves of the first heating cycle and b) the second heating cycle of components A,B, and C of MC-1. c) DSC curves of the first heating cycle and d) the second heating cycle of MC-1 (IV).

MC-DX rods showed slight melting between 50-58 ºC in addition to the melting at 154 ºC (Fig. 19a). The T_g was around 54 ºC (Fig. 19b).

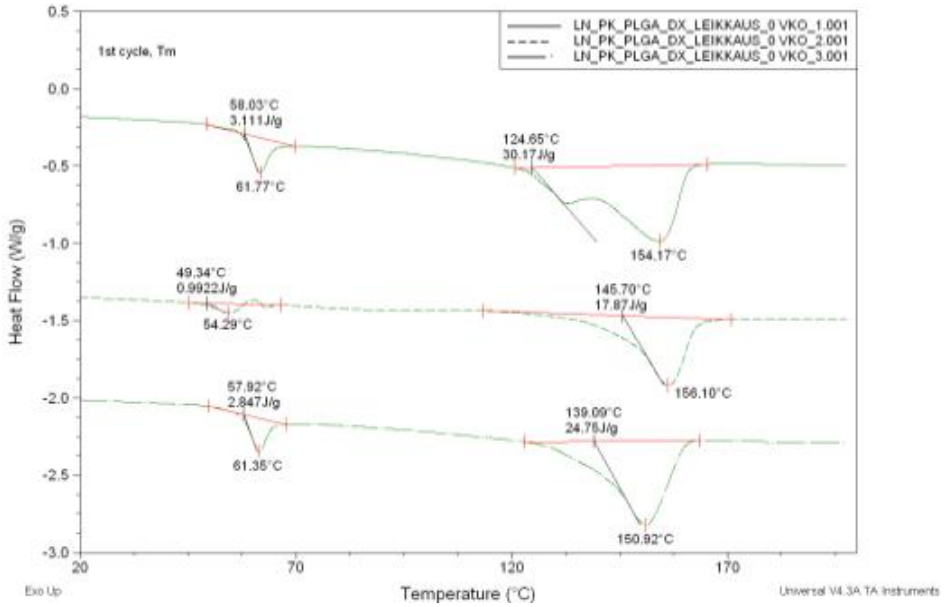

(a)

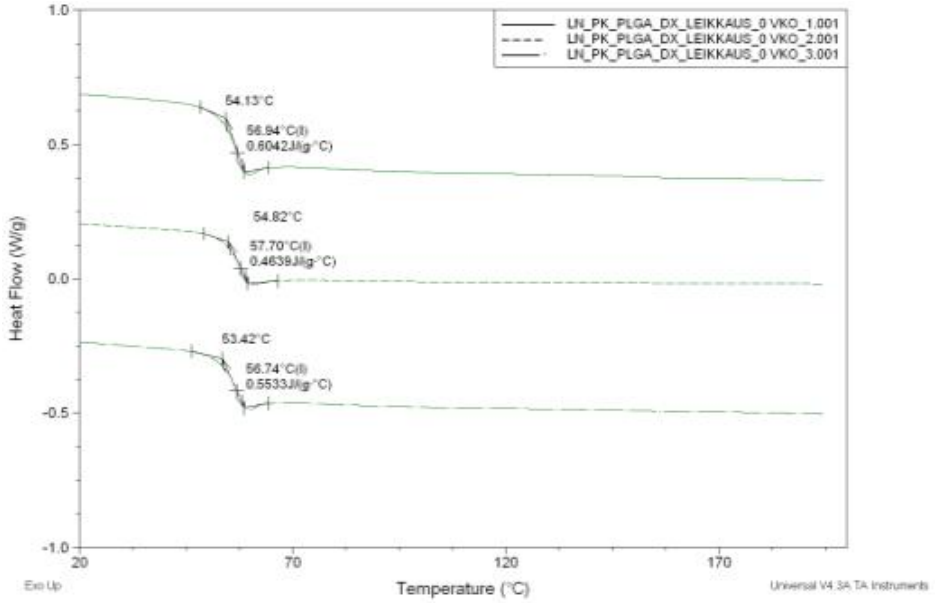

(b)

Figure 19. DSC curves of a) first heating cycle and b) second heating cycle of MC-DX rods (unpublished data).

5.3. Multidrug-loaded materials (VI, VII)

5.3.1. Structural properties

The macrostructure of the multilayer composite did not change substantially in buffer solution *in vitro*. Some fractures in the composite were observed but there was no evidence of dimensional changes. SEM analysis of the multilayer composite 1 (ML1) revealed that the nanofibrous part formed crater-like structures on the membrane (Fig. 20a). The nanofibers were oriented circularly near the rim of the craters. Orientation of the nanofibers was more random at the bottom of the crater (Fig. 20b). In addition, there

were fewer beads at the bottom of the craters, while near the rim there was a concentration of beads (Fig. 20c). Approximate crater diameter was 174 ± 62 µm and nanofiber and bead diameters were 143 ± 3.7 nm and 4.95 ± 2.67 µm, respectively. The thickness of the etidronate-carrying P(DLLCL 5/95 membrane was 300 µm (Fig. 20d). There was less nanofiber formation in the adjacent regions of the dexamethasone-containing P(DLLGA) 80/20 fiber net. The surface of the reverse side of the composite was quite smooth and only a few cracks were visible.

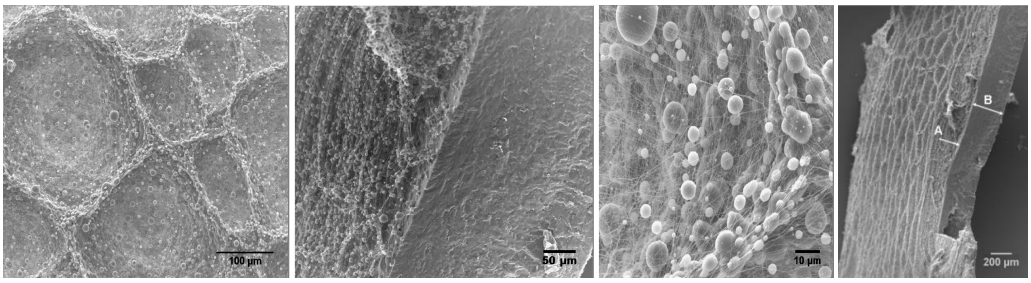

(a) (b) (c) (d)

Figure 20. SEM micrographs of multilayer implant 1 a) on the top of the implant, b) the oriented structure of nanofibers and beads in crater, c) the oriented fibrous structure in outer edge of crater, and d) cross section of multilayer implant 1. Arrow A shows the interface between diclofenac sodium-loaded nanofibers and etidronate-loaded solid membrane. Arrow B shows the cross section of solid membrane (VI).

5.3.2. Drug release

All multidrug releasing composites had high release rates of different drugs during the first day. The release curves of ML1 daily concentrations showed that after the first peak, the release of diclofenac sodium decreased to below a level of 1 µg/ml/day (Fig. 21). After about 40 days there was a small increase in the diclofenac sodium release rate, after which it decreased to zero at day 65. The release of dexamethasone was at a level of 2 µg/ml/day for 40 days, but increased to 4.5 µg/ml/day at day 43. It then decreased to zero within the next 30 days. After the first peak, the release of etidronate decreased to zero. At day 9, the release was at a level of 4 µg/ml/day but thereafter no release was observed for 10 days. After day 32 the release started to increase and rose to a level of 12 µg/ml/day at day 44. Then the release rate decreased slowly to zero within the next 16 days. The cumulative release curves showed that about 75 % of diclofenac sodium, 80 % of dexamethasone, and almost all etidronate were released during *in vitro* studies (80 days).

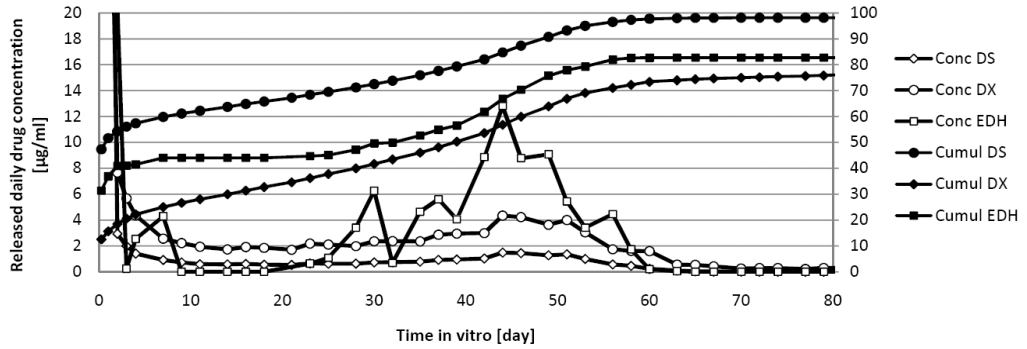

Figure 21. Cumulative release (%) and daily released concentrations of ML1 implant (VI).

The daily released concentration curves of ML2 showed that after the first peak the release of diclofenac sodium decreased to zero in 14 days (Fig. 22). Between days 23-27 and 55-70 the release increased slightly to a level of 0.5 µg/ml/day, otherwise it remained at zero. Release of etidronate decreased to almost zero within 11 days. The cumulative release curves of ML2 showed that about 90 % of diclofenac sodium and etidronate were released during *in vitro* studies (70 days).

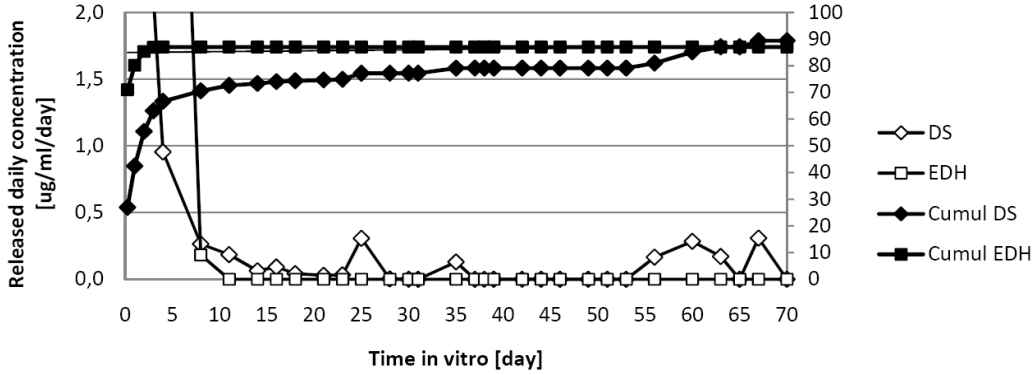

Figure 22. Cumulative release (%) and daily released drug concentration of ML2 implant (VI).

The daily release drug concentration curve of ML3 showed that after the first peak the release decreased to a level of 0.1 µg/ml/day in 10 days (Fig. 23). After 21 days *in vitro* the release started to increase and at day 29 it reached a level of 0.5 µg/ml/day. The cumulative release curve of ML3 showed that all diclofenac sodium was released during the period of *in vitro* studies (64 days).

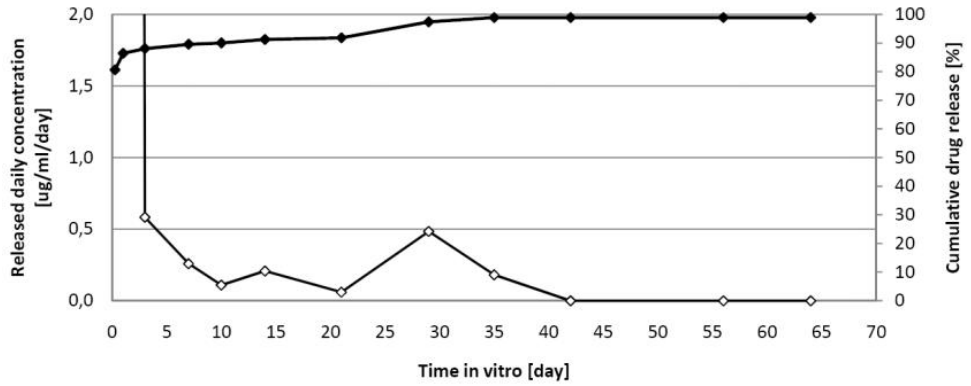

Figure 23. Cumulative release and daily released drug concentration of ML3 implant (VI).

The release of dexamethasone from ML 4 started after 70 days *in vitro* (Fig. 24). The daily released concentration increased to a level of 3 µg/ml/day at day 100 and stayed there for 20 days. After that the release rate increased to 19 µg/ml/day during the next 40 days and then decreased to zero during the next 35 days. About 75 % of the loaded drug was released during the total release period of 195 days.

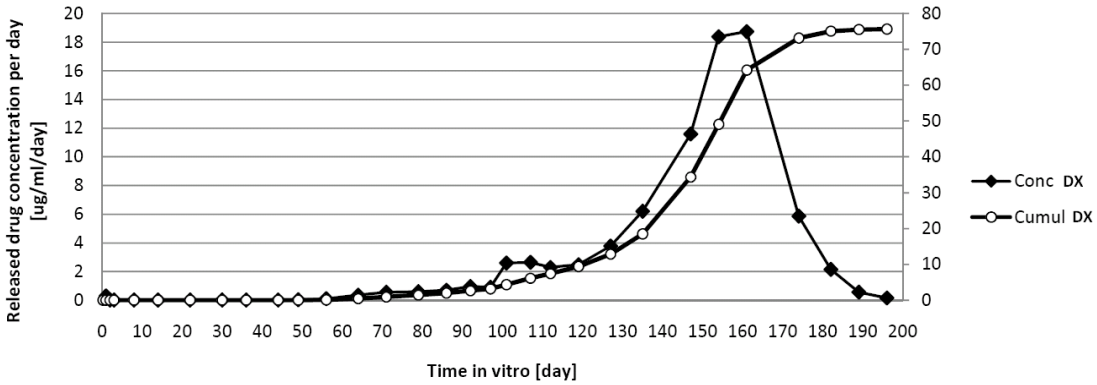

Figure 24. Cumulative release and daily released drug concentration of ML4 implant (unpublished).

Cumulative release curves for the multiphase fibers are presented in Figure 25. In general, the release of diclofenac sodium started earlier than dexamethasone when the same types of fiber compositions are compared.

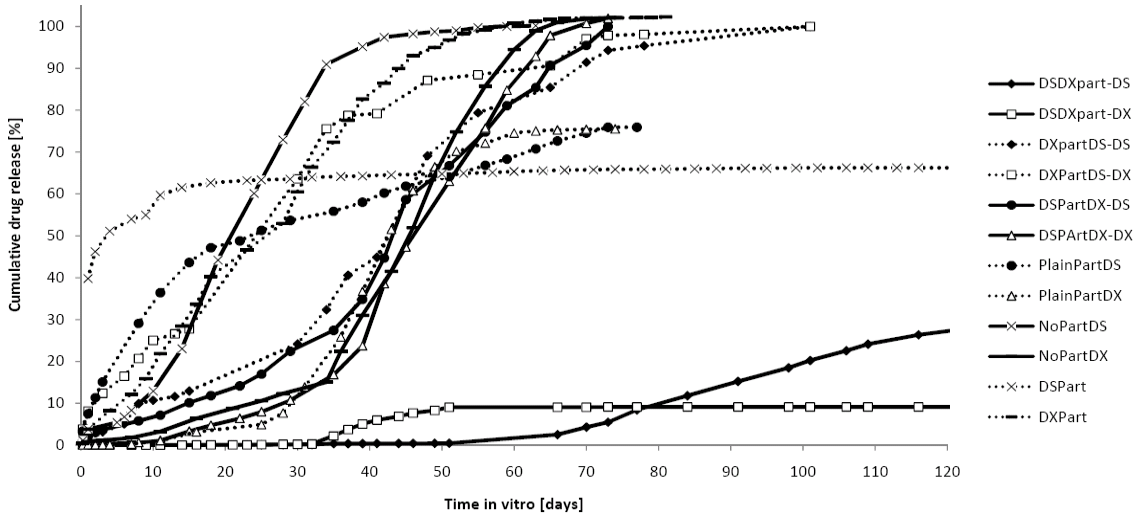

Figure 25. Cumulative drug release from multiphase fibers (VII).

The daily released concentration curves of diclofenac sodium and dexamethasone microparticle-loaded fibers (DSDXpart Fibers) showed that the release of diclofenac sodium started after 50 days of *in vitro* studies and lasted over 140 days (Fig. 26). The release concentration was mostly at a level of 0.6 µg/ml per day. The release of dexamethasone started after 30 days *in vitro* and lasted for 65 days. The concentration varied between 0.8 and 0.6 µg/ml per day.

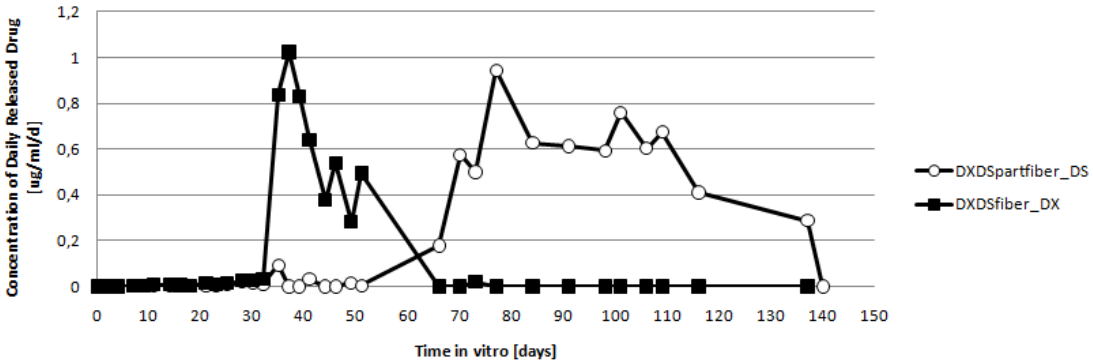

Figure 26. Daily released drug concentrations of DSDXpart fibers (VII).

The release of diclofenac sodium from the dexamethasone particle and diclofenac sodium-loaded fibers (DXpartDS fibers) started immediately and the rate was at level of 2.6 µg/ml per day for the following 40 days (Fig. 27). Release rate decreased to 1 µg/ml per day and stayed there for next 40 days. The release ended after 100 days *in vitro*. The release of dexamethasone also started immediately, though the release rate was below 1 µg/ml per day during the 75 days that it was released. From the diclofenac sodium particle- and dexamethasone-loaded fibers (DSpartDX fibers) the release of diclofenac sodium started after 10 days and lasted about 68 days (Fig. 27). The release rate of diclofenac sodium was between 1 and 5 µg/ml per day. The release of dexamethasone started after 10 days and lasted about 70 days. The highest release rate of dexamethasone (7-18 µg/ml per day) occurred between 40 and 65 days *in vitro*.

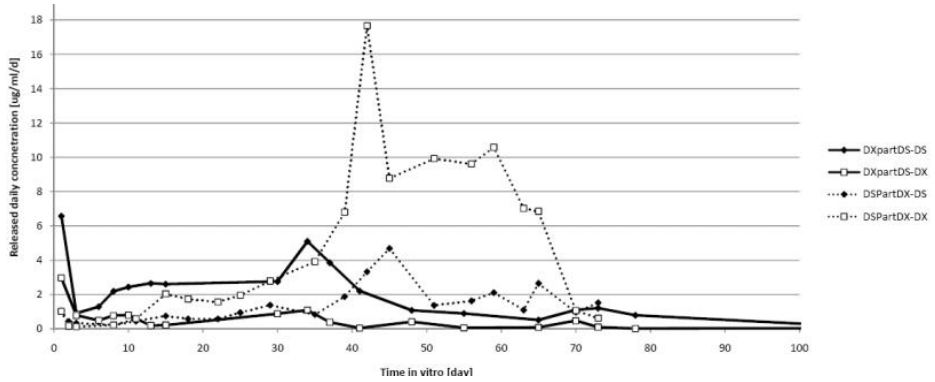

Figure 27. Daily released drug concentrations of DSpartDX and DXpartDS fibers (VII).

The release of diclofenac sodium started immediately and lasted 77 days from unloaded particle and diclofenac sodium-loaded composite fiber (PlainpartDS fibers) (Fig. 28). At the start, release was 4.5 µg/ml per day and during the next 22 days it decreased to a level of 0.6 µg/ml per day. The release of dexamethasone from unloaded particle and dexamethasone-loaded composite fiber (PlainpartDX fibers) started after 7 days *in vitro* and the rate was between 1 to 0.6 µg/ml per day for the next 17 days (Fig. 28). The release rate then increased to 9.5 µg/ml per day during the next 18 days, which was followed by a decrease to zero during the next 20 days. The total release period lasted about 55 days.

There was a high start peak in the release of diclofenac sodium from the diclofenac sodium-loaded fibers (NopartDS fibers), after which the release rate ranged between levels of 0.6 and 6 µg/ml per day for 15 days. For the next 20 days, the release rate was at 4 µg/ml per day. The release rate decreased to zero during the next 15 days (Fig. 28). The total release period lasted about 50 days. From the dexamethasone-loaded fibers (NopartDX fibers), the release started immediately and the rate increased slowly over 15 days from 0.7 to 2 µg/ml per day where it stayed for 20 days (Fig. 28). Then the rate increased rapidly to 8 µg/ml per day and remained between 8 and 14 µg/ml per day for 25 days. The release period lasted for 70 days.

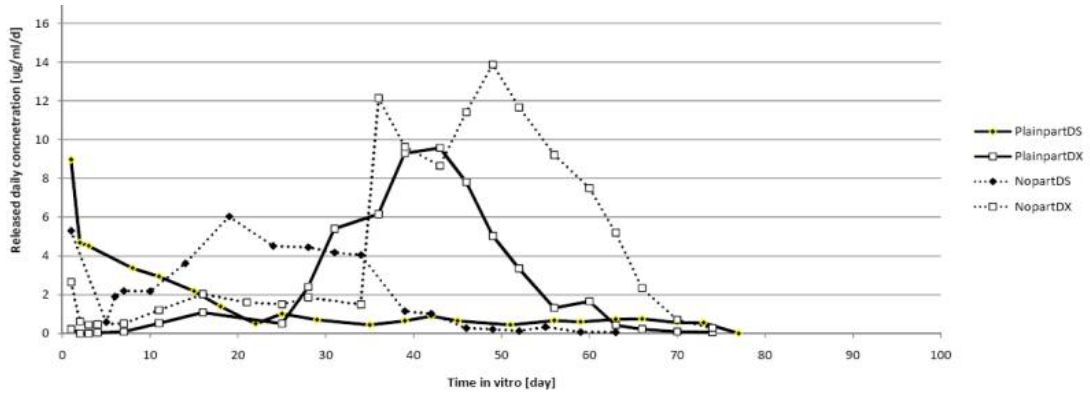

Figure 28. Daily released drug concentrations of PlainpartDS, PlainpartDX, NopartDS, and NopartDX fibers (VII).

There was a high start peak in the release of drug from the diclofenac sodium-loaded particles. The release rate decreased to 2 µg/ml per day during 9 days. At day 12, the release rate increased to a level of 10 µg/ml per day and decreased to zero during the next 8 days (Fig. 29). The total release period lasted 25 days. From dexamethasone-loaded microparticles, the drug release started immediately and after the high start peak the release rate was between 20 and 60 µg/ml per day for 30 days. The rate then decreased to zero during the next 20 days. The total release lasted about 55 days (Fig. 29).

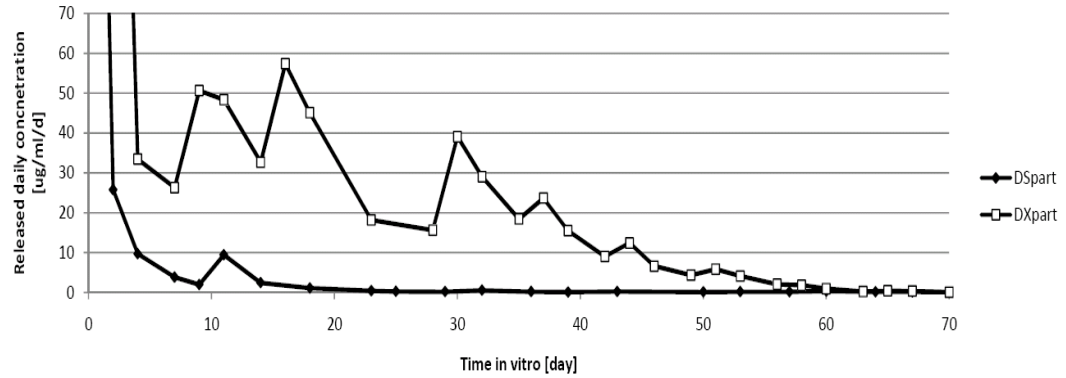

Figure 29. Daily released drug concentrations of diclofenac sodium and dexamethasone -loaded microparticles (VII).

The time points when 50 % and all drug was released from the multilayers, multiphase fibers and microparticles are presented in Table 12.

Table 12. Time points (days) of 50 % of loaded drug and the rest of the drugs from multidrug-loaded composites

Fiber types	50 % DS	50 % DX	50 % EDH	All DS	All DX	All EDH
ML1	1	39	32	65	142	58
ML2	2		<1	87		8
ML3	<1			35		
ML4		154			182	
DSDXpart fiber	90	39		137	51	
DXpartDS fiber	41	25		78	70	
DSpartDX fiber	42	46		73	73	
PlainpartDS fiber	29			70		
PlainpartDX fiber		43			66	
NopartDS fiber	20			46		
NopartDX fiber		46			66	
DSPart	7			39		
Dxpart		14			44	

5.3.3. Correlation of drug release rates

The results of the Pearson product-moment correlation coefficient analysis between multicomponent rods are presented in Table 13. There was a high correlation between the release rates of the multilayer implants. Exceptions to these correlations were the etidronate release rates between ML1 and ML2 and the dexamethasone release between ML1 and ML4, which were moderate and low, respectively. The results of the Pearson product-moment correlation coefficient analysis are presented in Table 14.

Table 13. Results of Pearson product-moment correlation coefficient analysis of multicomponent rods

Sample type		Sample type	Substance of interest	Coefficient	Correlation
MC1	vs	Component A	Diclofenac sodium	-0,56	moderate
MC1	vs	Component B	Diclofenac sodium	-0,37	low
MC1	vs	Component C	Diclofenac sodium	-0,15	neglible
MC2	vs	Component A	Diclofenac sodium	-0,41	moderate
MC2	vs	Component B	Diclofenac sodium	0,18	neglible
MC2	vs	Component C	Diclofenac sodium	0,16	neglible
MC3	vs	Component A	Diclofenac sodium	-0,41	moderate
MC3	vs	Component B	Diclofenac sodium	-0,26	low
MC3	vs	Component C	Diclofenac sodium	0,32	low
MC1	vs	MC2	Diclofenac sodium	0,39	low
MC1	vs	MC3	Diclofenac sodium	0,48	moderate
MC2	vs	MC3	Diclofenac sodium	0,65	high

Table 14. Results of Pearson product-moment correlation coefficient analysis of multilayer composites

Sample type		Sample type	Substance of interest	Coefficient	Correlation
ML1	vs	ML2	Diclofenac sodium	0,85	high
ML1	vs	ML2	Etidronate	0,41	moderate
ML2	vs	ML3	Diclofenac sodium	0,97	high
ML1	vs	ML3	Diclofenac sodium	0,89	high
ML1	vs	ML4	Dexamethasone	0,15	low

Generally, the correlation between the different multiphase fibers was low. The correlation of dexamethasone release was moderate between the DSDXpart and the DXpartDS fibers and between the PlainpartDX and the DX fibers. The correlation between the DXpartDS fibers and DS fibers was also moderate. The release correlations of the different multiphase fibers are presented in Table 15.

Table 15. Results of Pearson product-moment correlation coefficient analysis of multiphase fibers

Sample type		Sample type	Substance of interest	Coefficient	Correlation
DSDXpart	vs	DXpartDS	Dexamethasone	-0,44	moderate
DSDXpart	vs	DSpartDX	Diclofenac sodium	0,33	low
DSDXpart	vs	DX part	Dexamethasone	-0,34	low
DSDXpart	vs	DS part	Diclofenac sodium	-0,05	neglible
DXpartDS	vs	Plainpart DS	Diclofenac sodium	0,36	low
DXpartDS	vs	DS fiber	Diclofenac sodium	0,56	moderate
DSpartDX	vs	Plainpart DX	Dexamethasone	0,34	low
DSpartDX	vs	DX fiber	Dexamethasone	0,37	low
Plainpart DS	vs	DS fiber	Diclofenac sodium	0,19	neglible
Plainpart DS	vs	DX fiber	Dexamethasone	0,52	moderate

5.3.4. Thermogravimetric analysis

Analysis of the derivate weight curve of TGA showed that dexamethasone-containing fibers had two decomposition temperatures, the first at 300 °C and the second at 330-350 °C (Fig. 30a). Mass changes at 300 °C varied between 19-45 % while at 330-350 °C mass changes were higher, 45-55 %. Fibers that contained diclofenac sodium had only one peak on the derivate weight curve at 300 °C (Fig. 30b). Mass changes at 300 °C were 19-73 %. Dexamethasone had two decomposition temperatures, the first at 282 °C with mass change of 2 % and the second at 521 °C with mass change of 82 %. P(DLLCL) 80/20 polymer had a decomposition temperature of 302 °C with mass change of 11 %.

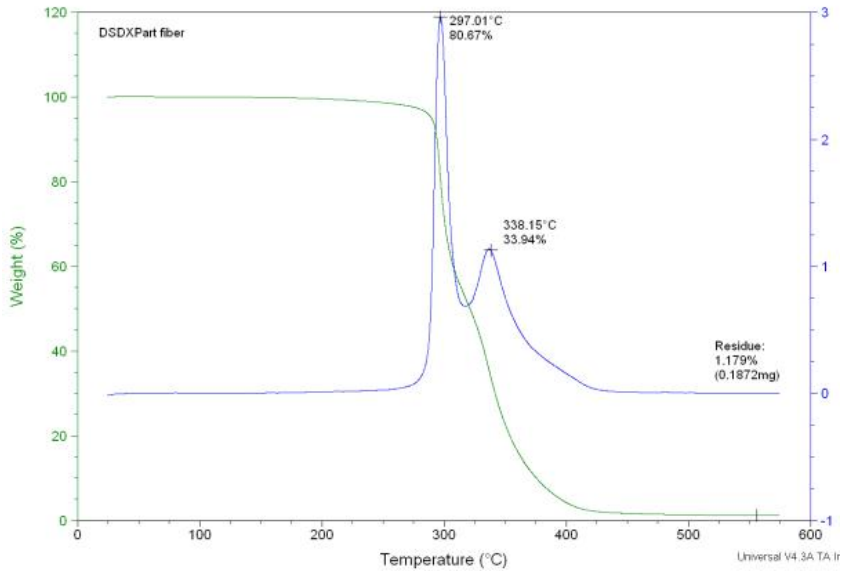

(a)

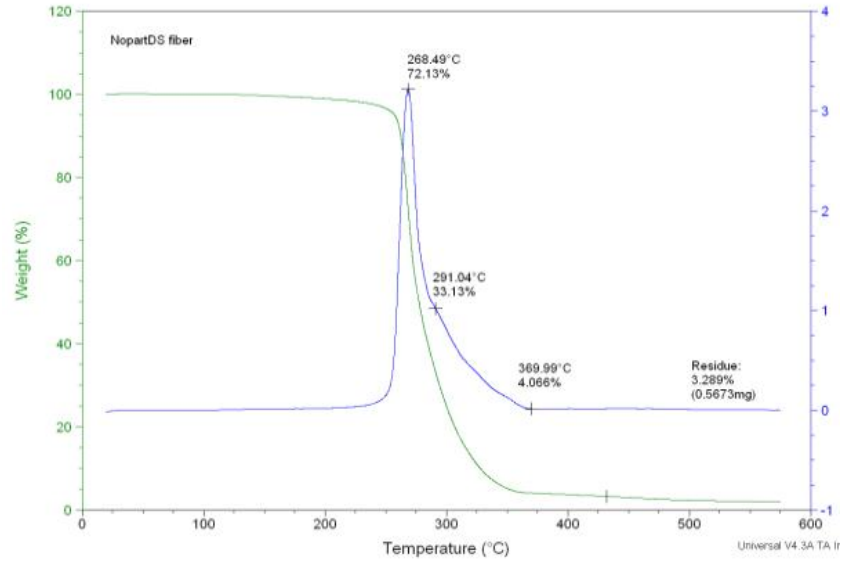

(b)

Figure 30. Examples of typical TGA thermograms of multiphase fibers containing a) dexamethasone and b) diclofenac sodium (VII).

Table 16 shows decomposition temperature and weight loss according to microparticle and free drug loading.

Table 16. Categorized TGA results of multiphase fibers by microparticles and free drug

DSPart	**Decomp.$_1$ [°C]**	**Weight loss 1 [%]**	**Decomp.$_2$ [°C]**	**Weight loss$_2$ [%]**
DSDXPart fiber	297	81	338	34
DSPart DX fiber	302	82	332	34
DSPart	320	66	no	no
DS free				
DXPartDS fiber	294	76	351	6
PlainpartDS fiber	294	77	315	34
DS fiber	268	72	no	no
DS	280-290*			
DXPart				
DSDXPart fiber	297	80	338	34
DXPartDS fiber	294	74	351	6
DXPart	308	56	no	no
DX free				
DSPartDX fiber	300	82	332	36
PlainpartDX fiber	297	81	332	35
DX fiber	300	87	334	35
DX	280-310			
P(DLLCL) 80/20 polymer	308	94	389	13
P(DLLCL) 80/20 fiber	302	90	391	14

6 DISCUSSION

Research into drug delivery has increased rapidly during the last three decades, resulting in the development of several commercially available implantable delivery devices. The obvious advantages of local drug delivery are the avoidance of systemic loading and the reduction in the total amount of drug required. Biodegradable synthetic polymers have been studied extensively for clinical applications and are thus the logical materials to be considered as matrixes for drug releasing devices. However, some problems with biocompatibility have been reported with ester-based synthetic polymer devices. They have been found to cause inflammatory reactions due to their acidic degradation products(Böstman and Pihlajamäki 2000, Böstman 1991), thus prompting interest in the addition of anti-inflammatory agents to these devices. Inflammatory reaction occurs immediately after injury, e.g. after incision. The early presence of active agents in the time scale can be critical and they can also adversely affect wound healing if the dosage is not controlled. The control of drug release has depended mainly on the chemistry and properties of the polymer, such as degradation by surface or bulk erosion. In this thesis, the series of studies have employed nanotechnology and several other polymer processing techniques to manufacture drug-releasing biodegradable polymer materials and also to prepare composites to introduce new approaches for controlled release applications.

6.1. Nanofibrous structures (I-III)

The objective of developing drug-releasing nanofiber scaffolds (I, III) was to prepare highly porous structures with a relatively long drug release period for use in tissue engineering. Electrospinning is a relatively new and versatile process for producing highly porous nanofibrous structures from biodegradable polymers (Subbiah *et al.*, 2005). The properties of polymer (subgroups and molecular weight of the polymer), solvent (dielectric constant, volatility) and thus, polymer solutions (concentration, conductivity) have an important effect on the stability of the process and the quality of nanofibers (McKee *et al.*, 2004). Too low viscosity of the solution causes breaking of the jet flow and results in nano- and micro-sized drops, which is called electrospraying. On the other hand, when the solution is too viscous the polymer solution dries in the needle and blocks the flow. Applied voltage and the distance between the needle tip and metal-made collector also affect the quality of the nanofibers; the longer the distance and the stronger the electrical force applied, the smaller the fiber diameters obtained (Ashammakhi *et al.*, 2007). Most ester-based biodegradable electrospun nanoscaffolds have been made of relatively low molecular weight (60 000-80 000 g/mol) polymers

(Kim *et al.*, 2004, Kumbar *et al.*, 2008, Zong *et al.*, 2005) since they are more suitable for the process. However, low molecular weight ester-based biodegradable polymers degrade and release agents relatively fast. Thus, to meet the objective of prolonged release, a slowly degrading polymer P(DLLCL) 5/95 (81 400 g/mol) and faster degrading P(DLLGA) 80/20 with high molecular weight (inherent viscosity 6.7 dl/g indicating high molecular weight) were used. With PAM14, the principal objective was to examine if it can be electrospun and also to explore the drug release kinetics.

PCL has been widely studied in drug releasing applications (Kwon and Furgeson 2007) and P(DLLCL 5/95 degrades slowly (Malin *et al.*, 1996), hence it was a good choice as a slow degrading biodegradable polymer. Even if the P(DLLGA) 80/20 degrades faster than P(DLLCL) 5/95, the high inherent viscosity of the P(DLGA) 80/20 polymer was thought to prolong the release period since the degradation is slower than with low M_w P(DLLGA). The basic problems in prolonged drug release from nanofibrous structures arise from the nanoscale and the properties of materials. For example, in nanofibers the distance for the drug molecule to diffuse to the surface is quite short and also there is a relatively large surface area that is prone to hydrolysis. PLGA degrades by bulk erosion and at a nanoscale level and degrading takes place almost simultaneously with release of the drug, leaving only a small amount of drug to be released by diffusion. Moreover, the high inherent viscosity caused problems in the electrospinning process because of the high viscosity of the polymer solution. In addition, the volatility of acetone is rather high and the polymer easily plugged the needle.

Conductivity of the polymer solution has a considerable effect on the electrospinning process. Ionic drugs can act as salts and the presence of these ions increases the charge density on the surface of the electrospun jet, which results in higher elongation forces when the electric field is applied (Fong *et al.*, 1999). Accordingly, the electrospinning process was enhanced substantially after adding the diclofenac sodium to the solution. Similar results of a salt effect were reported by Zong *et al.*, (2002) and Choi *et al.*, (2004). In addition, Choi *et al.*, (2004) reported a reduction in fiber diameter as was also the case with P(DLLCL) 5/95 (I) and PDLLA 80/20 (II). Unloaded P(DLLCL) 5/95 nanofibers (unpublished) were very difficult to prepare, mostly probably as a result of the low dielectric constant of glacial acetic acid (6.20 at 20 °C) when compared to the other solvents that were used with P(DLLGA) 80/20 and PAM14 (acetone 21, DMF 38.25, ethanol 25.3 at 20 °C) (Speight 2005). Acetone, acetic acid, and ethanol were selected for use as solvents since they are less toxic than others such as chloroform and they were able to dissolve the polymers. However, the conductivities of the polymer solutions were not measured in these studies and further analysis of the effect of conductivity on the electrospinning process and the resulting nanofibers is impossible. Very unusual results were found in the SEM studies of P(DLLGA) 80/20 nanofibers concerning beads. The scaffolds without drug were beadless (Fig. 12b) while the diclofenac the sodium-loaded scaffolds had beads in their structure (Fig. 11 and 12a).

This observation was in contrast to that reported by other authors, namely, that by adding salt to the polymer solution bead formation is decreased, (Ndreu *et al.,* 2008, Fong *et al.,* 1999) while formation of the Taylor cone enhanced (Hohman *et al.,* 2001). The surface tension of the solvent (acetic acid 28 dynes/cm, acetone 25.20 dynes/cm) may have had a positive effect on the bead formation since the surface tension of solvent changes in a polymer solution. High surface tension tends to lead to more beaded structures. Further, the decreased net charge of the polymer solution also leads to bead formation (Fong *et al.,* 1999). DMF has a high dielectric constant (38.3) compared to acetic acid (6.15), acetone (2.88), and ethanol (24.3). DMF was added to the unloaded P(DLLGA) 80/20 polymer solution to enhance the conductivity, which may explain the beadless structure of unloaded P(DLLGA) 80/20 nanofibers. In addition to the lower conductivity of the polymer solution, bead formation in diclofenac sodium-loaded nanofibers could be caused by the crystallization of the drug during the electrospinning process (Kim *et al.*, 2004, Verreck *et al.*, 2003). Crystallization of drug can change the conductivity of the solution. The drug localization of P(DLLGA) 80/20 non-UV-treated scaffold supports the idea that the drug is inside the beads. Diclofenac sodium is soluble in water, acidic media, and acetone in low concentrations. During the electrospinning process, evaporation of the solvent causes a decrease in the relative concentration of solvent and this might cause increased crystallization of the drug and thus bead formation. The resulting beads were of microscale size and much larger than the connecting nanofibers. This could be advantageous when different functions of cells are desired (Zong *et al.,* 2005, Curtis and Wilkinson 1997). A highly porous structure attracts cells, though the pore size (Von Recum *et al.,* 1996), fiber diameter (Tian *et al.,* 2008, Tuzlakoglu *et al.,* 2005), and polymer chemistry (Shin *et al.,* 2006) also affect cell attachment and proliferation.

The fastest release of diclofenac sodium was observed in PAM14. During the first 24 hours P(DLLCL) 5/95 , UV-treated, and non UV-treated P(DLLGA) 80/20 nanofibers released about 45/98 %, 25/40 %, and 58/93 % (percent of released drug/percent of loaded amount of drug) of loaded drug, respectively (Table 9). The fast release at the start of the tests suggested (Fig. 13) that more of the drug was located on the surface of the fiber than encapsulated within the polymer matrix. The negative effect of UV on diclofenac sodium release considerably decreased the total release (Fig. 13b). As a result, the sterilization method must be changed from UV-treatment to another type such as gamma irritation. The low solubility of diclofenac sodium to acetone and acids suggests that the drug is dissolved in the polymer phase in the electrospinning solution, since the solutions were clear. During electrospinning the rapid evaporation of solvent and the difference in hydrophobicity of the polymer and drug can cause drug migration to the surface during processing (He *et al.,* 2009, Kim *et al.,* 2004, Kenawy *et al.,* 2002). This can explain the fast releases during the first day from P(DLLCL) 5/95 and P(DLLGA) 80/20 nanofibers. The fast release from PAM14 was a consequence of a change in pH when the conformation of the polymer chains occurred, possibly releasing

the entrapped drug. The release period of P(DLLCL) 5/95 was longest and after the end of the release tests, the nanoscaffolds still retained their physical structure. P(DLLGA) 80/20 nanoscaffolds degraded during the test and only a few particles of the scaffolds remained in the test tube at the end of the release test. Thus, the release mechanisms differed according to the degradation properties. The drug was probably released mostly by diffusion from P(DLLCL) 5/95, while degradation was the predominant cause for the release from P(DLLGA) 80/20 nanoscaffolds. There is no data available on the effective therapeutic local concentration of diclofenac. The lowest reported therapeutic level in synovial fluid after 12 hours from oral administration of 75 mg diclofenac sodium was 0.12 μg/ml (Todd and Sorkin 1988). The release rates of diclofenac sodium from P(DLLCL) 5/95 and P(DLLGA) 80/20 nanofibers were above 0.12 μg/ml over 70 and 40 days, respectively. Thus, they could be used for controlling inflammatory reactions at the implant site over a month. Regarding the extended drug release from P(DLLGA) 80/20, the release of drug from the low molecular weight P(DLLGA) 80/20 (M_w 75 000 g/mol) nanoscaffold lasted only a few hours (Kim *et al.,* 2004), hence the extended release period was achieved with the higher molecular weight P(DLLGA) 80/20.

DSC analysis of P(DLLCL) 5/95 showed a small decrease in the melting temperature for diclofenac sodium-loaded scaffold (Fig. 14). This may be attributable to the decrease in the degree of crystallization of the polymer due to the added drug. The T_g did not change after processing. In the second heating cycle there was a double peak endothermic reaction, which might be due to the melting of cold crystallization that occurred during cooling at 4-25 °C.

6.2. Biodegradable drug-releasing polymer composites (IV-VII)

There were two types of biodegradable polymer composites used in this study. The first group, multicomponent rods, were manufactured by compression molding of either diclofenac sodium-loaded P(DLLGA) 80/20 billets or dexamethasone-loaded P(DLLGA) 80/20 fibers. Temporal control of drugs in pharmaceutical therapy is essential, hence in local drug delivery devices the release rate must be adjusted to the desired level to obtain maximum benefit at the implant site. Thus, the purpose of the development of multicomponent rods was to obtain a controlled drug release rate by a combination of components with known drug-releasing properties.

The second group comprised multidrug-releasing biodegradable polymer composites manufactured by a variety of processing methods. Tissue repair and regeneration is a multistep process involving several stages. Nevertheless, most of the drug delivery materials developed have carried just a single agent to control only those reactions covered by the agent (Weinberg *et al.,* 2008, Viitanen *et al.,* 2006, Huolman and Ashammakhi 2007, Veiranto *et al.,* 2004a, Wang *et al.,* 2002). In order to control the

different phases in the multistep process of tissue repair, the agents should be available in specific concentrations and at specific times. The aim in developing multidrug-releasing composites was to combine separate drug-releasing components into a single composite for the enhanced control of tissue reactions.

6.2.1. Multicomponent structures (IV, V)

Diclofenac sodium- and dexamethasone-loaded P(DLLGA) 80/20 multicomponents were manufactured by compression molding. The attachment between components was caused by adhesion due to a lower applied temperature (120 °C) than the melting temperature of P(DLLGA) 80/20 (160 °C) during compression. The components of the MC-DS and MC-DX rods disintegrated after two and four weeks in immersion, respectively, thus the adhesion lacked sufficient strength in hydrolytic conditions. The microstructure of the cross section of the MC-DS rod showed no clear boundaries between components (Fig. 15a). However, after compression it is likely that there were microchannels between the components, enabling water penetration between them. Another reason for early disintegration can be the relaxation of the self-reinforced components due to heating the system above the glass transition temperature of P(DLGA) (60 °C) during compression molding. Self-reinforcing by solid state technique produces holes around the added particles and probably increases the surface area available for hydrolysis (Niiranen and Törmälä 1999). Relaxation of polymer chains can cause some closing of the holes while still retaining a slightly porous structure, which can cause loosening as well as earlier drug release than from the self-reinforced components. In dexamethasone-loaded fibers, the orientation of polymer chains was good around the holes caused by the drug particles. The surface of the multicomponent rods contained some flaps and cuts (Fig. 15b), indicating possible routes for water penetration. The dexamethasone fibers had a thick skin on the fiber surface (unpublished), which can cause considerable delay in the release of fibers. However, when these fibers were compression molded to form a single piece, the release of dexamethasone from multicomponent rods started much earlier compared to the component fibers (Fig. 17b). This also leads to the assumption that the relaxation of the polymer chains forms microspores or micro channels in the polymer matrix. Dexamethasone and diclofenac sodium particles can cause osmotic pressure in the polymer matrix (Ravivaparu 2006) and the water penetration through the channels can be improved as a result of this osmotic pressure. Slight swelling was also observed during *in vitro* tests, indicating moderate water absorption. The possible adhesion between drug particle and polymer was destroyed in cavity formation during self-reinforcement, revealing an increased free area for particles to dissolve in water. The releases of diclofenac sodium-loaded multicomponents seemed to show a similar trend (Fig. 16c-d). The release from the diclofenac sodium-loaded multicomponent rods was faster than from the components (Table 10). The shape of the MC-1 curve followed the trend of the curve for non-self-reinforced component A, which had a short processing history (Fig. 16a). Pearson product-moment correlation coefficient analysis partly

supports the similarity between the releases of these two, since the correlation was moderate (Table 13). The release of MC-2 and MC-3 lasted longer than MC-1, which is probably attributable to a difference in size (Ø MC-1 1.5 mm, Ø MC-2 and MC-3 mm), in addition to the difference in the relative amount of components (Fig. 16c-d). In MC-1 the proportions of all components were equal (each 1/3) and it might be assumed that the correlation of releases between components would also have been quite similar. However, components B and C had only a low and negligible correlation, respectively with MC-1. This can be explained by the differences in processing history of the original components. The relative amount of components in MC-2 and MC-3 was A 56 %, B 27 %, and C 18 %. Correlation of component A between MC-2 and MC-3 was moderate and for components B and C it was negligible and low, respectively. Different processing histories, different proportions of components in MC-2 and MC-3, and the different diameters of MC-1 and MC-2 (and MC-3) can also explain the differences in the correlations. The effect of gamma sterilization by scission of the polymer chains (Loo *et al.*, 2005, Loo *et al.*, 2006) on the release rate can be observed from the release curves of the multicomponents loaded with diclofenac sodium (component C and MC-3) (Fig. 16) and dexamethasone (MC-DX 2) (Fig. 17). The release of drugs was accelerated, which is in accordance with the earlier findings of Soriano *et al.*, (2006).

Bone healing usually takes six weeks (Suuronen *et al.*, 1992, Manninen *et al.*, 1992a) depending on the anatomical area (Böstman and Pihlajamäki 2000, Ashammakhi *et al.*, 2001, Suuronen *et al.*, 1998), the age of the patient, micromotion (Viljanen *et al.*, 1995), and weight-bearing (Tonino *et al.*, 1976), etc.. During four weeks the shear strength of MC-DX 1 decreased considerably from 105 MPa to 30 MPa. According to Manninen *et al.*, (1992) after six weeks 8.8 MPa *in vivo* tests with PLLA screws is suitable for fixation of a sheep cortical bone (Manninen *et al.*, 1992b). The *in vitro* test of the PLLA screws showed shear strength of 62 MPa after six weeks incubation. The *in vivo* properties of the multicomponents are unknown, but according to the results of Manninen *et al.*, (1992b) strength retention is too high and so the rods are unsuitable for cortical bone fixation. However, the shear strength of cancellous bone is 65.3 MPa (Turner *et al.*, 2001) and for a potential application for cancellous bone fixation, MC-DX rods might have the required strength properties. The shear strength of MC-1 was 55 MPa, which was also the shear strength of component A (compounded billet), indicating that the strengthening effect of self-reinforcing was lost during compression molding. The shear strength of human cranial bone (cancellous bone) has been reported to be 21.4 MPa (McElhaney *et al.*, 1970), which is lower than the initial shear strength of the MC-1. However, the shear strength of MC-1 decreased to 15 MPa during two weeks in hydrolysis, which is not appropriate for fixation. In terms of the suitability of multicomponents for bone fixation, it was concluded that dexamethasone-loaded multicomponent rods might be useful in cranio-maxillofacial applications but a diclofenac sodium-loaded multicomponent does not yet possess the required strength

properties. Moreover, the disintegration of the components is clearly undesirable and thus their development needs further investigation.

Thermal analysis of the initial components A, B, C, and the multicomponent implant MC-1 revealed that heat treatment had only a minor effect on melting temperatures. The first cycle of DSC analysis of components and MC-1 revealed abnormal endothermal reactions between 42-59 ºC (Fig. 18a and 18 c) that may be the result of crystallization near the T_g of P(DLLGA) 80/20 (52 ºC) (Fig. 18b). Components B and C showed exothermal reactions near 90 ºC, which is close to the temperature used in self-reinforcement. The exothermic reaction can be caused by the relaxation of highly oriented polymer chains (Fig. 18a and 18c) releasing the energy trapped during self-reinforcement. The second heat cycle curve (Fig. 18b) showed a large cold crystallization phenomenon in component B, thus indicating that self-reinforcement releases more space in which polymer chains can move and release energy. The second heat treatment revealed a similar cold crystallization phenomenon in hydrolyzed MC-1 samples (Fig. 18d). This could be caused by component B and also by crystallization of oligomers that can be produced during hydrolysis. The DSC curve of component C showed a similar cold crystallization reaction to component B, though much smaller (Fig. 18b). Changes in thermal properties are quite complex, most likely because of the heterogeneity of the components in the composites. DSC analysis of the dexamethasone-loaded multicomponent rods showed an endothermal reaction at 50-58 ºC (Fig. 19a) similar to the diclofenac sodium-loaded multicomponent rods. The melting temperature of MC-DX 1 at 154 ºC was close to the melting temperature of MC-1 at 155-159 ºC (Table 11). However, there was no abnormal thermal reaction at 90 ºC unlike the MC-1, which supports the explanation that the phenomenon was caused by self-reinforcement. The T_g of MC-DX 1 was also similar to MC-1, indicating some crystallinity in the polymer (Fig. 19b).

6.2.2. Multidrug releasing biodegradable composites (VI,VII)

Multilayer composite

The effect of a combination of layers carrying different drugs on drug release rates was studied in a multilayer composite. The material can be called multifunctional since it can simultaneously guide tissue ingrowth and release therapeutic agents. The ingrowth of tissues can occur in a nanostructured scaffold (layer 3) while a smooth membrane on the reverse side (layer 2) can restrict the ingrowth of tissue to the structure. Layer 1 (dexamethasone-loaded P(DLLGA) 80/20 macro fibers) enhances the mechanical stability of the elastic composite and it can also control a late inflammatory tissue reaction. Layer 3 (diclofenac sodium P(DLLCL) 5/95 nanofibers) was selected on the basis of the previous studies of drug-releasing nanofibers (I-III) to meet the following requirements: over one month release to control early inflammatory reaction with a burst release, and over six weeks good mechanical stability of the scaffold for possible use in bone applications. Layer 2 (etidronate-loaded P(DLLCL) 5/95 membrane) was

intended for use as a tissue separating membrane loaded with bisphosphonate to inhibit bone resorption.

The manufacturing of the multilayer composite involved various polymer processing techniques (melt spinning, compression molding, solvent casting, and electrospinning), which naturally affect the properties of individual components. In SEM analysis, the microstructure of the multilayer composite (Fig.20a-c) revealed a nanofiber structure with spheres. This was similar to the diclofenac sodium-loaded P(DLLCL) 5/95 nanofiber scaffold (I) (Fig. 11). However, at low magnification, the nanofiber layer seemed to have a crater-like structure on the multilayer composite. This might be due to the instabilities of repulsive forces during electrospinning, together with the effect of a more insulating polymer sheet as a collector than the highly conductive aluminum foil, as in the publication I. The adhesion between nanofibers and the etidronate-loaded P(DLLCL) 5/95 membrane was not studied, though the SEM images did show good attachment (Fig. 20b and d).

Different combinations of layers (ML1-ML4) were manufactured to determine the effect of combining the layers. The release of diclofenac sodium from ML2 and ML3 followed a trend similar to that from ML1 (Fig. 21-23). Any differences might be the result of an uneven diclofenac sodium distribution during electrospinning, which can be caused by the insulating effect of the P(DLLCL) 5/95 membrane. There was high correlation between all the diclofenac sodium releases (Table 14). The released concentration from ML1 was above the therapeutic level (0.12 μg/ml). However, the released concentrations from ML2 and ML3 were lower and for one month they were outside the therapeutic range. The difference between the etidronate release rates and those from ML1 and ML2 (Fig. 21 and 22) (Table 12) could be due to the presence of the P(DLLGA) 80/20 grid in ML1, which can affect the evaporation rate of the solvent. A reduced evaporation rate can lead to phase separation and drug aggregation on the surface of dexamethasone-loaded P(DLLGA) 80/20 grid. Etidronate is sparingly soluble in water, thus P(DLLGA) 80/20 as a more hydrophilic material might have attracted the drug to its surface. Furthermore, the method of detection of etidronate was not entirely reliable. There were problems in the preparation of a standard curve for the UV-spectrophotometer. Pearson product-moment correlation coefficient analysis, however, showed a medium correlation between the etidronate releases from ML1 and ML2 (Table 14). The therapeutic concentration of etidronate in blood is approximately 2.4 μg/ml (Hillilä 2007). The local therapeutic concentration of etidronate in tissue was not available and thus, 2.4 μg/ml was thought to be the lower limit of the therapeutic concentration of etidronate. The concentration was calculated by multiplying the normal dose of etidronate (400 mg/day) by bioavailability (3 %) (Kettunen 2003) and the average blood volume of man weighing 70 kg (5000 ml). In ML-1, the therapeutic concentration of etidronate was achieved after 28 days *in vitro.* The concentration stayed above the lower limit for 28 days. This release profile could be useful in late

bone regeneration therapy. The therapeutic concentration of dexamethasone depends on the purpose of the treatment. As in the case of etidronate, no data are available for local tissue concentration. The lower limit of therapeutic concentration was calculated by multiplying the normal dexamethasone dose (1.5 – 10 mg/day) by bioavailability (78 %) (Kettunen 2003) and the average blood volume of man weighing of 70 kg (5000 ml), resulting in a concentration of 0.24 μg/ml. The released concentration of dexamethasone from ML-1 remained above the therapeutic level from the start and ended after 65 days *in vitro*. Comparison of the dexamethasone release rate from the compression-molded dexamethasone fibers (V) (Fig. 17) to the release of dexamethasone from ML1 (Fig. 21) showed that the end of the releases occurred around 65 days *in vitro*. The presence of a dexamethasone-loaded grid in ML1 might have caused micropores. These micropores could have allowed the dexamethasone to be released relatively quickly, even if dexamethasone-loaded grid was embedded in the P(DLLCL) 5/95 membrane. Dexamethasone release from ML4 commenced later (Fig. 24) than from ML1 and the correlation was low (Table 14). This might have been due to better embedding of the dexamethasone grid in the P(DLLCL) 5/95 solution in ML4.

The multilayer composite ML1with loaded agents could be used in bone applications as tissue growth guiding material. NSAIDs have been shown to inhibit osteoclast-like cell formation, which might help to reduce osteolysis (Soekanto 1994, Reuben and Ekman 2005). A few studies have shown that early and long administration of non-steroidal anti-inflammatory agents (NSAIDs) has some inhibitory effect on bone healing *in vivo* studies (Goodman *et al.*, 2005, Gerstenfeld *et al.*, 2003). However, the inhibitory effect on bone healing of NSAIDs is still largely unknown in clinical use (Seidenberg and An 2004). Goodman *et al.*, (2005) reported that the early administration (before six weeks) of NSAIDs does not interfere with normal bone healing. Thus, the six weeks release period of diclofenac sodium should not impair bone healing. In ML1, however, the diclofenac sodium was released for about 60 days, which might cause some inhibitory effect. The theoretical effect of dexamethasone on bone healing is unclear. The common view is that corticosteroids inhibit bone healing through many modes of action. However, certain studies show no adverse effects of dexamethasone on bone healing. It has been suggested that healing can be dependent on dosage and duration as well as on traumatic extent (Salerno and Hermann 2006, Pountos *et al.*, 2008). Hence, bisphosphonate released at later stages (from 20-60 days) can overcome the possible adverse effects on bone healing caused by the released anti-inflammatories.

Multiphase fibers

In the multiphase fiber studies, the aim was to explore the differences in release rates in terms of whether the drug was loaded inside the microparticles or in the matrix polymer in fibers. Multiphase fibers carried anti-inflammatory agents, diclodenac sodium and dexamethasone for potential use in the control of inflammatory tissue reactions.

In multiphase fibers, diclofenac sodium and dexamethasone were loaded by the w-o-w method in P(DLLGA)50/50/PVA microparticles. This method is simple and widely used in the preparation of microparticles (O'Donnell and McGinity 1997, Couvreur *et al.,* 1997). Micro- and nanoparticles usually have very sustained and fast release rates (Vega *et al.*, 2008, Varshosaz and Soheili 2008, Ubrich *et al.*, 2004) since their spherical shape offers the advantage of a large contact area with the surrounding liquid. In the current study, the drug release from the microparticles lasted 18-60 days, which was rather long (Fig. 29). The released amount of diclofenac sodium in the loaded particles was much smaller than the amount of dexamethasone, even if the total amount of loaded drug was the same. Diclofenac sodium is a more hydrophilic compound than dexamethasone and during microparticle formation (water-in oil-step) the hydrophilicity of diclofenac sodium might have pulled it out of the P(DLLGA) 50/50 matrix to the PVA/water phase.

The loading efficiency of the drugs varied (Fig. 25) between the various multiphase fibers. The fibers containing unloaded microparticles and free drug, released only 75 % of loaded drug, while the other fibers released almost all loaded drug. Loading of both drugs in separate microparticles and loading the microparticles in a biodegradable fiber matrix (DSDXPart fibers) delayed the release of diclofenac sodium for about 30 days (Fig. 27) and the release of dexamethasone for 50 days. From the DSDXPart fibers, where only particles were loaded in the fibers, the release occurred after exposure of the surface of the microparticles to buffer and further degradation of the microparticles. Drug release from the microparticles and the free drug-carrying fibers started earlier than from the DSDXPart fibers (Fig. 26). This might be due to the early release of free drug from the fiber matrix leading to pore formation and also because of a larger surface area for hydrolysis. In addition, during processing the particles had forced the polymer chains to orientate and align according to the pulling force on the surface of the particles, leading to the cavity formation described earlier (section 6.2.1). By increasing the surface area, the cavities enable more hydrolysis to occur. Thus, the particles themselves seemed to increase the release rate of the free drug from the fibers (Fig. 27 and 28). The release of diclofenac sodium, which was loaded directly to the fiber matrix (DXPartDS fibers and Plainpart DS fibers), was enhanced by the loaded particles. However, the results of Pearson product-moment correlation coefficient analysis showed only a low correlation between the release of diclofenac sodium in these fibers (Table 15). A similar observation was made for free dexamethasone release (Fig. 27 and 28). The correlation between the release rates from the unloaded particle- and dexamethasone-loaded fibers (PlainpartDX fibers) and the no-particle-loaded dexamethasone fibers (DX fibers) was moderate. The release of dexamethasone from the dexamethasone microparticles in the diclofenac sodium-loaded fibers (DXPartDS fibers) was very small, thus distorting the result at 50 % release shown in Table 12. In addition, the release rate from the no-particle-loaded diclofenac sodium fibers (DS fibers) might be inaccurate, since the decomposition temperature in TGA analysis was

much lower than that of the other fibers (Table 16). Half of the diclofenac sodium was released from the DS fibers during 20 days while 50 % of the diclofenac sodium was released from the unloaded microparticle-loaded diclofenac sodium fibers (PlainpartDS fibers) during 29 days. Hence, the correlation between these two releases was negligible. When dexamethasone release rates were compared with the PlainpartDX and DX fibers, 50 % of the release was delayed for one week, from 39 to 46 days, respectively (Table 12). However, the correlation between these releases was moderate. The different characteristics of the release rates of diclofenac sodium and dexamethasone are most likely due to the different properties of the drugs. The diffusion of the smaller molecule of diclofenac sodium (M_w 318,1g/mol) was faster than the diffusion of the larger and more hydrophopic dexamethasone molecules (M_w 516.41g/mol) from the P(DLLCL) 80/20 matrix. The release of dexamethasone was more attributable to the degradation of the polymer matrix than was the release of diclofenac sodium. Poly-ε-caprolactone is quite hydrophopic, however, the copolymer used with DL-lactide P(DLLCL) 80/20 is quite hydrophilic and amorphous thus promoting the faster release of diclofenac sodium by flexible polymer chain organization. All the prepared fibers, including the unloaded fibers, swelled during the *in vitro* tests, which implied easy water penetration into the matrix. The inherent viscosity of the P(DLLCL) 80/20 polymer was low (0.88 dl/g), indicating the presence of many hydrophilic acid ends in the polymer. The Pearson product-moment correlation coefficient analysis showed only low or negligible correlations between releases of drug from most of the fibers. This suggests that it is possible to control the release rates of diclofenac sodium and dexamethasone by loading them in microparticles and/or directly in the fiber polymer matrix.

TGA analysis revealed some common features (Table 16) between the various fiber categories. Since the decomposition temperatures of diclofenac sodium (near 300 °C, (Murakami *et al.,* 2004), dexamethasone (near 300 °C), and P(DLLCL)80/20 (300 °C) are close to each other, it was impossible to determine the amount of drug in the fibers. However, TGA analysis suggested that some complexation of dexamethasone and polymer occurred during the extrusion process, which can cause delay to the dexamethasone release rate. All the dexamethasone-containing fibers had two decomposition temperatures (Fig. 30a), the first at 300 °C and the second at 330 °C (Table 16). An exception was noticed in the case of the DXPartDS fibers, whose second decomposition temperature occurred at 351 °C. The TGA derivate curves of dexamethasone were biphasic, comprising a first decomposition at 270-310 °C and a second at 310-540 °C. It is likely that dexamethasone interacted with P(DLLCL) 80/20 (Gamisans *et al.,* 1999), causing the second decomposition at 330 °C. Particularly those fibers, in which dexamethasone was loaded directly in the polymer matrix (DSPartDX fibers, DX fibers, PlainpartDX fibers) had similarities in their curves (Table 16). Similarities between the TGA curves were also noticed with the fibers to which diclofenac sodium was loaded directly (DXPartDS fibers, PlainpartDS fibers) (Fig.

30.b). The weight loss of the free diclofenac sodium-containing fibers (DXPartDS and PlainPartDS fibers) was 77 % at 294 °C. An exception was noticed with the DS fibers, whose first decomposition temperature was 25 °C lower (269 °C) with weight loss of 72 %. The decomposition of the fibers loaded with microparticles carrying diclofenac sodium (DSDXPart fibers and DSPartDX fibers) showed similarities, having a first decomposition temperature around 300 °C with 82 % weight loss and a second around 335 °C with 35 % weight loss. The first decomposition temperatures of dexamethasone microparticle-loaded fibers (DSDXPart fibers, DXPartDS fibers) were almost the same, 294-297 °C, but the second decomposition temperatures bore no such similarities (338 °C for DSDXPart fibers and 351 °C for DXPartDS fibers). These results suggest that the thermal properties of the various fibers are more closely related to the loaded drug than to the loading of microparticles into the fibers.

7 SUMMARY AND CONCLUSIONS

Tissue regeneration is a complex process and with suitable therapeutic control the healing of tissues can be enhanced. Polymeric biodegradable local drug delivery devices offer a variety of ways to control these tissue reactions. The timing of the release of active agents is important, in addition to the adjustment of the therapeutic dose. Furthermore, in the case of tissue regeneration, a porous structure can enhance recovery by providing a scaffold on to which cells can attach and proliferate.

The purpose of this thesis was to develop biodegradable drug releasing polymer composites with controlled release. The main goals were threefold: 1) to develop and characterize drug-releasing nanofiber structures of scaffolds for cells, 2) to develop and characterize drug-releasing multicomponent rods comprising combination release of components, and 3) to develop and characterize multidrug-releasing composites with multifunctional properties and the controlled release of different agents.

The anti-inflammatory agent release from nanofibers can be prolonged by using slowly degradable P(DLLCL) 5/95 and high molecular weight P(DLGLA) 80/20 as matrix polymers. However, long-term mechanical support for cells can be achieved by P(DLLCL) 5/95 since the P(DLGLA) 80/20 degraded during the release test. This was due to a large surface which is prone to hydrolytic degradation in nanofibrous structures.

In multicomponent rods, the release of anti-inflammatory agents involved a combination of released components. By varying the amount of the various components, the release from the composite can be adjusted. Heat pressing as a manufacturing method and gamma sterilization seemed to accelerate the release from the composites. The mechanical strength of self-reinforced components was lost during manufacture, leading to moderate shear strengths. Thus, the appropriate use of multicomponent rods can be applied in low stress fixation applications. It may also be possible to modify the processing temperature by selecting different components which may retain the higher strength.

The release of different active agents from multilayer composites was found to be dependent on the type of layered structure. Drug release was rapid from the nanofibrous layer, while release from the other layers was more sustained. The multilayered structure comprising an anti-inflammatory agent-releasing nanofibrous layer and a

bone-forming bisphosphonate-releasing smooth membrane on the reverse side of the composite offers potential for use in bone guidance applications. Further, in multiphase fibers, the release of anti-inflammatory agents can be controlled by loading the agents in different phases of the fibers. The release rate is thus dependent on the properties of the drug.

The temporal and quantitative control of drug release from biodegradable polymers is challenging and offers a great deal of scope for research. In those cases where the drug release properties of devices carrying a single therapeutic agent in a polymer matrix are insufficient for the application, a combination of different drug-releasing parts and structures and different agents provides the possibility to adjust the release properties of the devices. Though the combination of different structures increases the complexity of the device, it nevertheless offers the advantage of adjusting the dose to achieve controlled release of the desired amount. However, the local therapeutic concentrations of single agents and the synergistic effect of multiple different agents in tissues are not full understood. Further studies are needed to evaluate the physiological and therapeutic function of the released drugs after processing, sterilization, storage and long-term periods *in vitro* and *in vivo*. Further study is also needed to understand the mechanisms of drug release from the developed drug-releasing materials in order to achieve reliable tailored controlled drug-releasing devices. Thus, the results of this thesis provide a starting point for further development of tailored single drug- and multidrug-releasing implantable delivery devices.

The use of approved materials, such as PLA, PLGA, and PCL, and drugs like those used in this study can reduce product launch time for clinical applications. However, new legislation will still be needed for the use of devices constructed from a combination of drugs and polymers. Though many of them are well-known and have been approved for other applications, this is likely to prolong market launch.

Acknowledgements

This thesis is based on work carried out at the Department of Biomedical Engineering, Tampere University of Technology during 2004-2009. The results reported here were obtained from different projects funded by the Finnish Technology and Development Centre (TEKES), the Academy of Finland, and the Department of Biomedical Engineering. The work was carried out within the scope of the EC-funded project EXPERTISSUES.

I first wish to express my gratitude to my supervisor, Professor Nureddin Ashammakhi, who suggested the topic of this thesis. I would also like to thank him for his valuable guidance and support and for providing me with the opportunity to deepen my knowledge of biomaterials science by undertaking this thesis at the Department of Biomedical Engineering. I also owe a great debt of gratitude to Professor Minna Kellomäki for her support and help in completing my thesis. I would also like to thank all my colleagues at the Department of Biomedical Engineering, especially Hanna Jukola, for their encouragement and useful discussions. I am also indebted to the laboratory staff for their support and help with the laboratory work.

Finally, I would like to express my heartfelt gratitude to my husband Petri and my children Eliel and Lumi for their love, support, and inexhaustible patience. I also wish to thank the rest of my family for all their help and encouragement.

References

Abidian, M.R., Kim, D. & Martin, D.C. 2006, "Conducting-polymer nanotubes for controlled drug release", *Advanced Materials,* vol. 18, no. 4, pp. 405-409.

Agarwal, S., Wendorff, J.H. & Greiner, A. 2008, "Use of electrospinning technique for biomedical applications", *Polymer,* vol. 49, no. 26, pp. 5603-5621.

Agrawal, C.M. 2002, "Biodegradable Polymers for Orthopaedic Applications" in *Polymer Based Systems on Tissue Engineering, Replacement and Regeneration*, eds. R.L. Reis & D. Cohn, Kluwer Academic publishers, Dordrecht, The Netherlands, pp. 25-422.

Ahmed, A.R., Dashevsky, A. & Bodmeier, R. 2008, "Reduction in burst release of PLGA microparticles by incorporation into cubic phase-forming systems", *European Journal of Pharmaceutics and Biopharmaceutics,* vol. 70, no. 3, pp. 765-769.

Ahola, N., Rich, J., Karjalainen, T. & Seppälä, J. 2003, "Release of ibuprofen from poly(ε-caprolactone-co-D,L-lactide) and simulation of the release", *Journal of Applied Polymer Science,* vol. 88, no. 5, pp. 1279-1288.

Alexis, F. 2005, "Factors affecting the degradation and drug-release mechanism of poly(lactic acid) and poly[(lactic acid)-co-(glycolic acid)]", *Polymer International,* vol. 54, no. 1, pp. 36-46.

Ashammakhi, N., Ndreu, A., Nikkola, L., Wimpenny, I. & Yang, Y. 2008, "Advancing tissue engineering by using electrospun nanofibers.", *Regenerative Medicine,* vol. 3, no. 4, pp. 547-574.

Ashammakhi, N., Ndreu, A., Piras, A.M., Nikkola, L., Sindelar, T., Ylikauppila, H., Harlin, A., Gomes, M.E., Neves, N.M., Chiellini, E., Chiellini, F., Hasirci, V., Redl, H. & Reis, R.L. 2007, "Biodegradable nanomats produced by electrospinning: Expanding multifunctionality and potential for tissue engineering", *Journal of Nanoscience and Nanotechnology,* vol. 7, no. 3, pp. 862-882.

Ashammakhi, N., Peltoniemi, H., Waris, E., Suuronen, R., Serlo, W., Kellomäki, M., Törmälä, P. & Waris, T. 2001, "Developments in craniomaxillofacial surgery: Use of self-reinforced bioabsorbable osteofixation devices", *Plastic and Reconstructive Surgery,* vol. 108, no. 1, pp. 167-180.

Babazadeh, M. 2006, "Synthesis and study of controlled release of ibuprofen from the new acrylic type polymers", *International Journal of Pharmaceutics,* vol. 316, no. 1-2, pp. 68-73.

Baker, R. 1987, *Controlled Release of Biologically Active Agents,* Wiley, New York, USA.

Barr, J., Woodburn, K.W., Ng, S.Y., Shen, H. & Heller, J. 2002, "Post surgical pain management with poly(ortho esters)", *Advanced Drug Delivery Reviews,* vol. 54, no. 7, pp. 1041-1048.

Berkland, C., King, M., Cox, A., Kim, K. & Pack, D.W. 2002, "Precise control of PLG microsphere size provides enhanced control of drug release rate", *Journal of Controlled Release,* vol. 82, no. 1, pp. 137-147.

Bölgen, N., Vargel, I., Korkusuz, P., Menceloğlu, Y.Z. & Pişkin, E. 2007, "In vivo performance of antibiotic embedded electrospun PCL membranes for prevention of abdominal adhesions", *Journal of Biomedical Materials Research - Part B Applied Biomaterials,* vol. 81, no. 2, pp. 530-543.

Böstman, O. & Pihlajamäki, H. 2000, "Clinical biocompatibility of biodegradable orthopaedic implants for internal fixation: A review", *Biomaterials,* vol. 21, no. 24, pp. 2615-2621.

Böstman, O.M. 1991, "Osteolytic changes accompanying degradation of absorbable fracture fixation implants", *Journal of Bone and Joint Surgery - Series B,* vol. 73, no. 4, pp. 679-682.

Böstman, O.M. & Pihlajamäki, H.K. 2000, "Adverse tissue reactions to bioabsorbable fixation devices", *Clinical Orthopaedics and Related Research,* no. 371, pp. 216-227.

Burke, M., Langer, R. & Brem, H. 1999, "Central Nervous System, Drug Delivery to Treat" in *Encyclopedia of Controlled Drug Delivery,* ed. E. Mathiowitz, Wiley & Sons, Inc., USA, pp. 184-1057.

Chan, G. & Mooney, D.J. 2008, "New materials for tissue engineering: towards greater control over the biological response", *Trends in Biotechnology,* vol. 26, no. 7, pp. 382-392.

Chanda, M. & Roy, S., K. 2008, *Plastics Fabrication and Recycling (Plastics Engineering),* 1st edn, CRC Press, Boca Raton, USA.

Chen, L., Xie, Z., Hu, J., Chen, X. & Jing, X. 2007, "Enantiomeric PLA-PEG block copolymers and their stereocomplex micelles used as rifampin delivery", *Journal of Nanoparticle Research,* vol. 9, no. 5, pp. 777-785.

Chew, S.Y., Wen, J., Yim, E.K.F. & Leong, K.W. 2005, "Sustained release of proteins from electrospun biodegradable fibers", *Biomacromolecules,* vol. 6, no. 4, pp. 2017-2024.

Chia, N.K., Venkatraman, S.S., Boey, F.Y.C., Cadart, S. & Loo, J.S.C. 2008, "Controlled degradation of multilayered poly(lactide-co-glycolide) films using electron beam irradiation", *Journal of Biomedical Materials Research - Part A*, vol. 84, no. 4, pp. 980-987.

Chiellini, E. & Solaro, R. 1995, "Multifunctional bioerodible biodegradable polymeric materials", *Macromolecular Symposia*, vol. 98, pp. 803-824.

Chiellini, E., Chiellini, E.E., Chiellini, F. & Solaro, R. 2001, "Targeted administration of proteic drugs. I. Preparation of Polymeric Nanoparticles", *Journal of Bioactive and Compatible Polymers*, vol. 16, no. 6, pp. 441-465.

Choi, J.S., Lee, S.W., Jeong, L., Bae, S., Min, B.C., Youk, J.H. & Park, W.H. 2004, "Effect of organosoluble salts on the nanofibrous structure of electrospun poly(3-hydroxybutyrate-co-3-hydroxyvalerate)", *International Journal of Biological Macromolecules*, vol. 34, no. 4, pp. 249-256.

Choi, J.S., Leong, K.W. & Yoo, H.S. 2008, "In vivo wound healing of diabetic ulcers using electrospun nanofibers immobilized with human epidermal growth factor (EGF)", *Biomaterials*, vol. 29, no. 5, pp. 587-596.

Chu, C. 2003, "Biodegradable Polymeric Biomaterials: An updated overview" in *Biomaterials: Principles and Applications*, eds. J.B. Park & J.D. Bronzino, CRC Press LLC, Florida, USA, pp. 95-115.

Chung, H.J. & Park, T.G. 2007, "Surface engineered and drug releasing pre-fabricated scaffolds for tissue engineering", *Advanced Drug Delivery Reviews*, vol. 59, no. 4-5, pp. 249-262.

Couvreur, P., Blanco-Prieto, M.J., Puisieux, F., Roques, B. & Fattal, E. 1997, "Multiple emulsion technology for the design of microspheres containing peptides and oligopeptides", *Advanced Drug Delivery Reviews*, vol. 28, no. 1, pp. 85-96.

Crank, J. 1975, *The Mathematics of Diffusion*, 2nd edn, Oxford University Press, London, UK.

Cui, W., Li, X., Zhu, X., Yu, G., Zhou, S. & Weng, J. 2006, "Investigation of drug release and matrix degradation of electrospun poly(dl-lactide) fibers with paracetanol inoculation", *Biomacromolecules*, vol. 7, no. 5, pp. 1623-1629.

Curtis, A. & Wilkinson, C. 1997, "Topographical control of cells", *Biomaterials*, vol. 18, no. 24, pp. 1573-1583.

Dalton, P.D., Klinkhammer, K., Salber, J., Klee, D. & Möller, M. 2006, "Direct in vitro electrospinning with polymer melts", *Biomacromolecules*, vol. 7, no. 3, pp. 686-690.

Dash, A.K. & Cudworth II, G.C. 1998, "Therapeutic applications of implantable drug delivery systems", *Journal of Pharmacological and Toxicological Methods*, vol. 40, no. 1, pp. 1-12.

Deasy, P.B. 1989, *Multi-component long-acting medicament formulation for implantation*, US Patent 4874612, 1989.

Deitzel, J.M., Kleinmeyer, J., Harris, D. & Beck Tan, N.C. 2001, "The effect of processing variables on the morphology of electrospun nanofibers and textiles", *Polymer*, vol. 42, no. 1, pp. 261-272.

Erisken, C., Kalyon, D.M. & Wang, H. 2008, "Functionally graded electrospun polycaprolactone and β-tricalcium phosphate nanocomposites for tissue engineering applications", *Biomaterials*, vol. 29, no. 30, pp. 4065-4073.

Fong, H., Chun, I. & Reneker, D.H. 1999, "Beaded nanofibers formed during electrospinning", *Polymer*, vol. 40, no. 16, pp. 4585-4592.

Frank, A., Rath, S.K. & Venkatraman, S.S. 2005, "Controlled release from bioerodible polymers: Effect of drug type and polymer composition", *Journal of Controlled Release*, vol. 102, no. 2, pp. 333-344.

Freitas, S., Merkle, H.P. & Gander, B. 2005, "Microencapsulation by solvent extraction/evaporation: Reviewing the state of the art of microsphere preparation process technology", *Journal of Controlled Release*, vol. 102, no. 2, pp. 313-332.

Fu, Y., Nie, H., Ho, M., Wang, C. & Wang, C. 2008, "Optimized bone regeneration based on sustained release from three-dimensional fibrous PLGA/HAp composite scaffolds loaded with BMP-2", *Biotechnology and Bioengineering*, vol. 99, no. 4, pp. 996-1006.

Fung, L.K. & Saltzman, W.M. 1997, "Polymeric implants for cancer chemotherapy", *Advanced Drug Delivery Reviews*, vol. 26, no. 2-3, pp. 209-230.

Gamisans, F., Lacoulonche, F., Chauvet, A., Espina, M., García, M.L. & Egea, M.A. 1999, "Flurbiprofen-loaded nanospheres: Analysis of the matrix structure by thermal methods", *International Journal of Pharmaceutics*, vol. 179, no. 1, pp. 37-48.

Gard, P.R. 2000, *Human Pharmacology*, CRC Press LLC, New York, USA.

Gerstenfeld, L.C., Thiede, M., Siebert, K., Mielke, C., Phippard, D., Svagr, B., Cullinane, D. & Einhorn, T.A. 2003, "Differential inhibition of fracture healing by non-selective and cyclooxygenase-2 selective non-steroidal anti-inflammatory drugs", *Journal of Orthopaedic Research*, vol. 21, no. 4, pp. 670-675.

Giunchedi, P., Conti, B., Scalia, S. & Conte, U. 1998, "In vitro degradation study of polyester microspheres by a new HPLC method for monomer release determination", *Journal of Controlled Release*, vol. 56, no. 1-3, pp. 53-62.

Goodman, S.B., Ma, T., Mitsunaga, L., Miyanishi, K., Genovese, M.C. & Smith, R.L. 2005, "Temporal effects of a COX-2-selective NSAID on bone ingrowth", *Journal of Biomedical Materials Research - Part A*, vol. 72, no. 3, pp. 279-287.

Göpferich, A. 1999, "Biodegradable polymers: Polyanhydrides" in *Encyclopedia of Controlled Drug Delivery*, ed. E. Mathiowitz, Wiley & Sons, Inc., USA, pp. 60-71.

Gürsel, I., Korkusuz, F., Türesin, F., Gürdal Alaeddinoğlu, N. & Hasirci, V. 2001, "In vivo application of biodegradable controlled antibiotic release systems for the treatment of implant-related osteomyelitis", *Biomaterials,* vol. 22, no. 1, pp. 73-80.

Hagan, S.A., Dunn, S.E., Garnett, M.C., Davies, M.C., Illum, L. & Davis, S.S. 1995, "PLA-PEG micelles - A novel drug delivery system", *Proceedings of Controlled Release Society,* no. 22, pp. 194-195.

Harrison, K. 2007, "Introduction to polymeric drug delivery systems" in *Biomedical polymers*, ed. M. Jenkins, CRC Press LLC, Boca Raton, Florida, USA, pp. 33-56.

Hatefi, A. & Amsden, B. 2002, "Biodegradable injectable in situ forming drug delivery systems", *Journal of Controlled Release,* vol. 80, no. 1-3, pp. 9-28.

He, C., Huang, Z. & Han, X. 2009, "Fabrication of drug-loaded electrospun aligned fibrous threads for suture applications", *Journal of Biomedical Materials Research - Part A,* vol. 89, no. 1, pp. 80-95.

Heller, J. 1996, "Drug delivery systems" in *Biomaterials Science: An Introduction to Materials in Medicine,* eds. B.D. Ratner, A.S. Hoffman, F.J. Shoen & J. Lemons, Academic Press, San Diego, USA, pp. 346-356.

Heller, J. 2005, "Ocular delivery using poly(ortho esters)", *Advanced Drug Delivery Reviews,* vol. 57, no. 14 SPEC. ISS., pp. 2053-2062.

Heller, J., Barr, J., Ng, S.Y., Abdellauoi, K.S. & Gurny, R. 2002, "Poly(ortho esters): Synthesis, characterization, properties and uses", *Advanced Drug Delivery Reviews,* vol. 54, no. 7, pp. 1015-1039.

Henton, D.E., Gruber, P., Lunt, J. & Randall, J. 2005, " Polylactic Acid Technology" in *Natural Fibers, Biopolymers,and Biocomposites,* eds. A.K. Mohanty, M. Misra & L.T. Drzal, CRC Press, Taylor & Francis Group, LLC, Boca Raton, Florida, USA.

Higuchi, T. 1961, "Rate of release of medicaments from ointment bases containing drugs in suspension", *Journal in Pharmaceutical Sciences,* vol. 50, no. 10, pp. 874-875.

Hillilä, M. 2007, "Osteoporoosin lääkehoito" in *Farmakologia ja toksikologia*, eds. M. Koulu & J. Tuomisto, Medicina, pp. 479-1121, available at http://www.medicina.fi/index.php?option=com_content&view=article&id=48&Itemid=56.

Hohman, M.M., Shin, M., Rutledge, G. & Brenner, M.P. 2001, "Electrospinning and electrically forced jets. I. Stability theory", *Physics of Fluids,* vol. 13, no. 8, pp. 2201-2220.

Holland, T.A. & Mikos, A.G. 2006, "Biodegradable polymeric scaffolds. Improvements in bone tissue engineering through controlled drug delivery", *Advances in Biochemical Engineering/Biotechnology*, vol. 102, pp. 161-85.

Holland, T.A., Tabata, Y. & Mikos, A.G. 2005, "Dual growth factor delivery from degradable oligo(poly(ethylene glycol) fumarate) hydrogel scaffolds for cartilage tissue engineering", *Journal of Controlled Release*, vol. 101, no. 1-3 SPEC. ISS., pp. 111-125.

Hollinger, J.O. 2005, "Bone Dynamics: Morphogenesis, growth modeling, and remodeling" in *Bone Regeneration and Repair, Biology and Clinical Applications*, eds. J.R. Lieberman & G.E. Friedlaender, Humana Press, Totowa, New Jersey, USA, pp. 1-398.

Hong, Y., Fujimoto, K., Hashizume, R., Guan, J., Stankus, J.J., Tobita, K. & Wagner, W.R. 2008, "Generating elastic, biodegradable polyurethane/poly(lactide-co-glycolide) fibrous sheets with controlled antibiotic release via two-stream electrospinning", *Biomacromolecules*, vol. 9, no. 4, pp. 1200-1207.

Hoshino, A. & Isono, Y. 2002, "Degradation of aliphatic polyester films by commercially available lipases with special reference to rapid and complete degradation of poly(L-lactide) film by lipase PL derived from Alcaligenes sp.", *Biodegradation*, vol. 13, no. 2, pp. 141-147.

Huang, Z. & Ramakrishna, S. 2004, "Composites in biomedical applications" in *Engineering Materials for Biomedical Applications*, eds. S.H. Teoh, M. Agrawal, J.D. de Bruijn & Y. Tabata, World Scientific publishing Company, Inc., Singapore, pp. 260-350.

Huang, Z., He, C., Yang, A., Zhang, Y., Han, X., Yin, J. & Wu, Q. 2006, "Encapsulating drugs in biodegradable ultrafine fibers through co-axial electrospinning", *Journal of Biomedical Materials Research - Part A*, vol. 77, no. 1, pp. 169-179.

Hull, D. & Clyne, T.W. 1996, *An Introduction to Composite Materials*, 2nd edn, Cambridge University Press, Cambridge, UK.

Huolman, R. & Ashammakhi, N. 2007, "New multifunctional anti-osteolytic releasing bioabsorbable implant", *Journal of Craniofacial Surgery*, vol. 18, no. 2, pp. 295-301.

Hurrell, S. & Cameron, R.E. 2002, "The effect of initial polymer morphology on the degradation and drug release from polyglycolide", *Biomaterials*, vol. 23, no. 11, pp. 2401-2409.

Jain, J.P., Modi, S., Domb, A.J. & Kumar, N. 2005, "Role of polyanhydrides as localized drug carriers", *Journal of Controlled Release*, vol. 103, no. 3, pp. 541-563.

Jain, R.A. 2000, "The manufacturing techniques of various drug loaded biodegradable poly(lactide-co-glycolide) (PLGA) devices", *Biomaterials,* vol. 21, no. 23, pp. 2475-2490.

Janssen, L. 2005, *Reactive Extrusion System,* 1st edn, Marcel Dekker Inc., New York, USA

Jiang, H., Fang, D., Hsiao, B., Chu, B. & Chen, W. 2004, "Preparation and characterization of ibuprofen-loaded poly(lactide-co-glycolide)/poly(ethylene glycol)-g-chitosan electrospun membranes", *Journal of Biomaterials Science, Polymer Edition,* vol. 15, no. 3, pp. 279-296.

Jones, D. 2004, "Pharmaceutical Applications of Polymers for Drug Delivery", in *Rapra Review Reports,* vol 15, no. 6, Smithers Rapra, Shropshire, UK.

Jukola, H., Nikkola, L., Gomes, M.E., Chiellini, F., Tukiainen, M., Kellomäki, M., Chiellini, E., Reis, R.L. & Ashammakhi, N. 2008, "Development of a bioactive glass fiber reinforced starch-polycaprolactone composite", *Journal of Biomedical Materials Research - Part B Applied Biomaterials,* vol. 87, no. 1, pp. 197-203.

Katti, D.S., Robinson, K.W., Ko, F.K. & Laurencin, C.T. 2004, "Bioresorbable nanofiber-based systems for wound healing and drug delivery: Optimization of fabrication parameters", *Journal of Biomedical Materials Research - Part B Applied Biomaterials,* vol. 70, no. 2, pp. 286-296.

Kellomäki, M., Heller, J. & Törmälä, P. 2000, "Processing and properties of two different poly (ortho esters)", *Journal of Materials Science: Materials in Medicine,* vol. 11, no. 6, pp. 345-355.

Kempen, D.H.R., Lu, L., Kim, C., Zhu, X., Dhert, W.J.A., Currier, B.L. & Yaszemski, M.J. 2006, "Controlled drug release from a novel injectable biodegradable microsphere/scaffold composite based on poly(propylene fumarate)", *Journal of Biomedical Materials Research -Part A,* vol. 77, no. 1, pp. 103-111.

Kenawy, E., Abdel-Hay, F.I., El-Newehy, M.H. & Wnek, G.E. 2007, "Controlled release of ketoprofen from electrospun poly(vinyl alcohol) nanofibers", *Materials Science and Engineering A,* vol. 459, no. 1-2, pp. 390-396.

Kenawy, E., Bowlin, G.L., Mansfield, K., Layman, J., Simpson, D.G., Sanders, E.H. & Wnek, G.E. 2002, "Release of tetracycline hydrochloride from electrospun poly(ethylene-co-vinylacetate), poly(lactic acid), and a blend", *Journal of Controlled Release,* vol. 81, no. 1-2, pp. 57-64.

Kettunen, K. 2003, *Pharmaca Fennica 2004 II,* Lääketietokeskus Oy, Loviisa.

Kim, K., Luu, Y.K., Chang, C., Fang, D., Hsiao, B.S., Chu, B. & Hadjiargyrou, M. 2004, "Incorporation and controlled release of a hydrophilic antibiotic using poly(lactide-co-glycolide)-based electrospun nanofibrous scaffolds", *Journal of Controlled Release,* vol. 98, no. 1, pp. 47-56.

Kim, K., Yu, M., Zong, X., Chiu, J., Fang, D., Seo, Y., Hsiao, B.S., Chu, B. & Hadjiargyrou, M. 2003, "Control of degradation rate and hydrophilicity in electrospun non-woven poly(D,L-lactide) nanofiber scaffolds for biomedical applications", *Biomaterials*, vol. 24, no. 27, pp. 4977-4985.

Ko, J., Park, K., Kim, Y., Kim, M.S., Han, J.K., Kim, K., Park, R., Kim, I., Song, H.K., Lee, D.S. & Kwon, I.C. 2007, "Tumoral acidic extracellular pH targeting of pH-responsive MPEG-poly(β-amino ester) block copolymer micelles for cancer therapy", *Journal of Controlled Release*, vol. 123, no. 2, pp. 109-115.

Kohn, J. & Langer, R. 1996, "Bioresorbable and bioerodible material" in *Biomaterials Science: An Introduction to Materials in Medicine*, eds. B.D. Ratner, A.S. Hoffman, F.J. Schoen & J.E. Lemons, Academic Press Inc., San Diego, California, USA, pp. 64-74.

Koort, J.K., Mäkinen, T.J., Suokas, E., Veiranto, M., Jalava, J., Knuuti, J., Törmälä, P. & Aro, H.T. 2005, "Efficacy of ciprofloxacin-releasing bioabsorbable osteoconductive bone defect filler for treatment of experimental osteomyelitis due to Staphylococcus aureus", *Antimicrobial Agents and Chemotherapy*, vol. 49, no. 4, pp. 1502-1508.

Koort, J.K., Suokas, E., Veiranto, M., Mäkinen, T.J., Jalava, J., Törmälä, P. & Aro, H.T. 2006, "In vitro and in vivo testing of bioabsorbable antibiotic containing bone filler for osteomyelitis treatment", *Journal of Biomedical Materials Research - Part A*, vol. 78, no. 3, pp. 532-540.

Kryczka, T., Marciniec, B., Popielarz-Brzezinska, M., Bero, M., Kasperczyk, J., Dobrzyński, P., Kazimierczuk, Z. & Grieb, P. 2003, "Effect of gamma-irradiation on cladribine and cladribine-containing biodegradable copolymers", *Journal of Controlled Release*, vol. 89, no. 3, pp. 447-456.

Kulkarni, A., Reiche, J., Hartmann, J., Kratz, K. & Lendlein, A. 2008, "Selective enzymatic degradation of poly(ε-caprolactone) containing multiblock copolymers", *European Journal of Pharmaceutics and Biopharmaceutics*, vol. 68, no. 1, pp. 46-56.

Kulkarni, A., Reiche, J., Kratz, K., Kamusewitz, H., Sokolov, I.M. & Lendlein, A. 2007, "Enzymatic chain-scission kinetics of poly(ε-caprolactone) monolayers", *Langmuir*, vol. 23, no. 24, pp. 12202-12207.

Kumbar, S.G., Nukavarapu, S.P., James, R., Nair, L.S. & Laurencin, C.T. 2008, "Electrospun poly(lactic acid-co-glycolic acid) scaffolds for skin tissue engineering", *Biomaterials*, vol. 29, no. 30, pp. 4100-4107.

Kwon, G.S. & Furgeson, D.Y. 2007, "Biodegradable polymers for drug delivery systems" in *Biomedical Polymers*, ed. M. Jenkins, Woodhead Publishing Limited, Cambridge, England, pp. 83-28.

Lee, J.S., Bae, J.W., Joung, Y.K., Lee, S.J., Han, D.K. & Park, K.D. 2008, "Controlled dual release of basic fibroblast growth factor and indomethacin from heparin-

conjugated polymeric micelle", *International Journal of Pharmaceutics,* vol. 346, no. 1-2, pp. 57-63.

Lee, S. & Shin, H. 2007, "Matrices and scaffolds for delivery of bioactive molecules in bone and cartilage tissue engineering", *Advanced Drug Delivery Reviews,* vol. 59, no. 4-5, pp. 339-359.

Lee, T.H., Wang, J. & Wang, C. 2002, "Double-walled microspheres for the sustained release of a highly water soluble drug: Characterization and irradiation studies", *Journal of Controlled Release,* vol. 83, no. 3, pp. 437-452.

Lemmouchi, Y. & Schacht, E. 1997, "Preparation and in vitro evaluation of biodegradable poly(ε-caprolactone-co-D,L lactide)(X-Y) devices containing trypanocidal drugs", *Journal of Controlled Release,* vol. 45, no. 3, pp. 227-233.

Lemmouchi, Y., Schacht, E., Kageruka, P., De Deken, R., Diarra, B., Diall, O. & Geerts, S. 1998, "Biodegradable polyesters for controlled release of trypanocidal drugs: In vitro and in vivo studies", *Biomaterials,* vol. 19, no. 20, pp. 1827-1837.

Li, J., Jiang, G. & Ding, F. 2008, "The effect of pH on the polymer degradation and drug release from PLGA-mPEG microparticles", *Journal of Applied Polymer Science,* vol. 109, no. 1, pp. 475-482.

Li, S., Garreau, H. & Vert, M. 1990, "Structure-property relationships in the case of the degradation of massive poly(α-hydroxy acids) in aqueous media - Part 3 Influence of the morphology of poly(l-lactic acid)", *Journal of Materials Science: Materials in Medicine,* vol. 1, no. 4, pp. 198-206.

Li, S., Girod-Holland, S. & Vert, M. 1996, "Hydrolytic degradation of poly(DL-lactic acid) in the presence of caffeine base", *Journal of Controlled Release,* vol. 40, no. 1-2, pp. 41-53.

Li, S.M., Garreau, H. & Vert, M. 1990, "Structure-property relationships in the case of the degradation of massive aliphatic poly-(α-hydroxy acids) in aqueous media - Part 1: Poly(dl-lactic acid)", *Journal of Materials Science: Materials in Medicine,* vol. 1, no. 3, pp. 123-130.

Liao, I.C., Chew, S.Y. & Leong, K.W. 2006, "Aligned core-shell nanofibers delivering bioactive proteins.", *Nanomedicine (London, England),* vol. 1, no. 4, pp. 465-471.

Liu, X., Shanmugasundaram, S. & Arinzeh, T.L. 2006, "Polymeric materials" in *Encyclopedia of Medical Devices and Instrumentation*, ed. J.G. Webster, 2nd edn, John Wiley & Sons Inc., pp. 387-3666.

Loo, J.S.C., Ooi, C.P. & Boey, F.Y.C. 2005, "Degradation of poly(lactide-co-glycolide) (PLGA) and poly(L-lactide) (PLLA) by electron beam radiation", *Biomaterials,* vol. 26, no. 12, pp. 1359-1367.

Loo, S.C.J., Tan, H.T., Ooi, C.P. & Boey, Y.C.F. 2006, "Hydrolytic degradation of electron beam irradiated high molecular weight and non-irradiated moderate molecular weight PLLA", *Acta Biomaterialia,* vol. 2, no. 3, pp. 287-296.

Luong-Van, E., Grøndahl, L., Chua, K.N., Leong, K.W., Nurcombe, V. & Cool, S.M. 2006, "Controlled release of heparin from poly(ε-caprolactone) electrospun fibers", *Biomaterials,* vol. 27, no. 9, pp. 2042-2050.

Luu, Y.K., Kim, K., Hsiao, B.S., Chu, B. & Hadjiargyrou, M. 2003, "Development of a nanostructured DNA delivery scaffold via electrospinning of PLGA and PLA-PEG block copolymers", *Journal of Controlled Release,* vol. 89, no. 2, pp. 341-353.

Mak, M., Fung, L., Strasser, J.E. & Saltzman, W.M. 1995, "Distribution of drugs following controlled delivery to the brain interstitium", *Journal of Neuro-Oncology,* vol. 26, no. 2, pp. 91-102.

Malin, M., Hiljanen-Vainio, M., Karjalainen, T. & Seppälä, J. 1996, "Biodegradable lactone copolymers. II. Hydrolytic study of ε-caprolactone and lactide copolymers", *Journal of Applied Polymer Science,* vol. 59, no. 8, pp. 1289-1298.

Manninen, M.J., Päivärinta, U., Pätiälä, H., Rokkanen, P., Taurio, R., Tamminmäki, M. & Törmälä, P. 1992a, "Shear strength of cancellous bone after osteotomy fixed with absorbable self-reinforced polyglycolic acid and poly-L-lactic acid rods", *Journal of Materials Science: Materials in Medicine,* vol. 3, no. 4, pp. 245-251.

Manninen, M.J., Paivarinta, U., Taurio, R., Törmälä, P., Suuronen, R., Raiha, J., Rokkanen, P. & Patiala, H. 1992b, "Polylactide screws in the fixation of olecranon osteotomies. A mechanical study in sheep", *Acta Orthopaedica Scandinavica,* vol. 63, no. 4, pp. 437-442.

Mano, J.F. 2008, "Stimuli-responsive polymeric systems for biomedical applications", *Advanced Engineering Materials,* vol. 10, no. 6, pp. 515-527.

Martins, A., Reis, R.L. & Neves, N.M. 2008, "Electrospinning: Processing technique for tissue engineering scaffolding", *International Materials Reviews,* vol. 53, no. 5, pp. 257-274.

McElhaney, J.H., Fogle, J.L., Melvin, J.W., Haynes, R.R., Roberts, V.L. & Alem, N.M. 1970, "Mechanical properties of cranial bone", *Journal of Biomechanics,* vol. 3, no. 5, pp. 495-511.

McKee, M.G., Wilkes, G.L., Colby, R.H. & Long, T.E. 2004, "Correlations of solution rheology with electrospun fiber formation of linear and branched polyesters", *Macromolecules,* vol. 37, no. 5, pp. 1760-1767.

Megelski, S., Stephens, J.S., Bruce Chase, D. & Rabolt, J.F. 2002, "Micro- and nanostructured surface morphology on electrospun polymer fibers", *Macromolecules,* vol. 35, no. 22, pp. 8456-8466.

Merkli, A., Heller, J., Tabatabay, C. & Gurny, R. 1996, "Purity and stability assessment of a semi-solid poly(ortho ester) used in drug delivery systems", *Biomaterials*, vol. 17, no. 9, pp. 897-902.

Middleton, J.C. & Tipton, A.J. 2000, "Synthetic biodegradable polymers as orthopedic devices", *Biomaterials*, vol. 21, no. 23, pp. 2335-2346.

Mit-Uppatham, C., Nithitanakul, M. & Supaphol, P. 2004, "Effects of solution concentration, emitting electrode polarity, solvent type, and salt addition on electrospun polyamide-6 fibers: A preliminary report", *Macromolecular Symposia*, vol. 216, no. 1, pp. 293-300.

Miyajima, M., Koshika, A., Okada, J. & Ikeda, M. 1999, "Mechanism of drug release from poly(L-lactic acid) matrix containing acidic or neutral drugs", *Journal of Controlled Release*, vol. 60, no. 2-3, pp. 199-209.

Miyajima, M., Koshika, A., Okada, J., Kusai, A. & Ikeda, M. 1998, "The effects of drug physico-chemical properties on release from copoly (lactic/glycolic acid) matrix", *International Journal of Pharmaceutics*, vol. 169, no. 2, pp. 255-263.

Moroni, L., Licht, R., de Boer, J., de Wijn, J.R. & van Blitterswijk, C.A. 2006, "Fiber diameter and texture of electrospun PEOT/PBT scaffolds influence human mesenchymal stem cell proliferation and morphology, and the release of incorporated compounds", *Biomaterials*, vol. 27, no. 28, pp. 4911-4922.

Murakami, T., Ajima, K., Miyawaki, J., Yudasaka, M., Iijima, S. & Shiba, K. 2004, "Drug-loaded carbon nanohorns: adsorption and release of dexamethasone in vitro.", *Molecular Pharmacology*, vol. 1, no. 6, pp. 399-405.

Nair, L.S. & Laurencin, C.T. 2007, "Biodegradable polymers as biomaterials", *Progress in Polymer Science (Oxford)*, vol. 32, no. 8-9, pp. 762-798.

Naraharisetti, P.K., Ning Lew, M.D., Fu, Y., Lee, D. & Wang, C. 2005, "Gentamicin-loaded discs and microspheres and their modifications: Characterization and in vitro release", *Journal of Controlled Release*, vol. 102, no. 2, pp. 345-359.

Ndreu, A., Nikkola, L., Ylikauppilar, H., Ashammakhi, N. & Hasirci, V. 2008, "Electrospun biodegradable nanofibrous mats for tissue engineering", *Nanomedicine*, vol. 3, no. 1, pp. 45-60.

Nelson, K.D., Romero-Sanches, A.A., Smith, G.M., Alikacem, N., Radulescu, D., Waggoner, P. & Hu, Z. *Drug releasing biodegradable fiber implant*, World Patent 0110421, 2003

Neut, D., Van De Belt, H., Van Horn, J.R., Van Der Mei, H.C. & Busscher, H.J. 2003, "The effect of mixing on gentamicin release from polymethylmethacrylate bone cements", *Acta Orthopaedica Scandinavica*, vol. 74, no. 6, pp. 670-676.

Nie, H. & Wang, C. 2007, "Fabrication and characterization of PLGA/HAp composite scaffolds for delivery of BMP-2 plasmid DNA", *Journal of Controlled Release,* vol. 120, no. 1-2, pp. 111-121.

Niiranen, H. & Törmälä, P. 1999, "Self-reinforced bioactive glass-bioabsorbable polymer composites", *Materials Research Society Symposium - Proceedings,* vol. 550, pp. 267-272.

O'Donnell, P.B. & McGinity, J.W. 1997, "Preparation of microspheres by the solvent evaporation technique", *Advanced Drug Delivery Reviews,* vol. 28, no. 1, pp. 25-42.

Okada, H. 1997, "One- and three-month release injectable microspheres of the LH-RH superagonist leuprorelin acetate", *Advanced Drug Delivery Reviews,* vol. 28, no. 1, pp. 43-70.

Ostovic, D., Stelmach, C. & Hulshizer, B. 1993, "Formation of a chromophoric complex between aldendronate and copper(II) ions", *Pharmaceutical Research,* vol. 10, no. 3, pp. 470-474.

Panyam, J. & Labhasetwar, V. 2004, "Sustained cytoplasmic delivery of drugs with intracellular receptors using biodegradable nanoparticles.", *Molecular Pharmacology,* vol. 1, no. 1, pp. 77-84.

Panyam, J., William, D., Dash, A., Leslie-Pelecky, D. & Labhasetwar, V. 2004, "Solid-state solubility influences encapsulation and release of hydrophobic drugs from PLGA/PLA nanoparticles", *Journal of Pharmaceutical Sciences,* vol. 93, no. 7, pp. 1804-1814.

Papapoulos, S.E. 2008, "Bisphosphonates: how do they work?", *Best Practice and Research: Clinical Endocrinology and Metabolism,* vol. 22, no. 5, pp. 831-847.

Patel, P., Mundargi, R.C., Babu, V.R., Jain, D., Rangaswamy, V. & Aminabhavi, T.M. 2008, "Microencapsulation of doxycycline into poly(lactide-co-glycolide) by spray drying technique: Effect of polymer molecular weight on process parameters", *Journal of Applied Polymer Science,* vol. 108, no. 6, pp. 4038-4046.

Pountos, I., Georgouli, T., Blokhuis, T.J., Pape, H.C. & Giannoudis, P.V. 2008, "Pharmacological agents and impairment of fracture healing: What is the evidence?", *Injury,* vol. 39, no. 4, pp. 384-394.

Ravi Kumar, M.N. 2000, "Nano and microparticles as controlled drug delivery devices.", *Journal of pharmacy & pharmaceutical sciences [electronic resource] : a publication of the Canadian Society for Pharmaceutical Sciences, Societe canadienne des sciences pharmaceutiques,* vol. 3, no. 2, pp. 234-258.

Ravivaparu, H. 2006, "Biodegradable polymeric delivery systems" in *Design of Controlled Release Drug Delivery Systems*, eds. X. Li & B. Jasti R, The McGraw-Hill Companies, Inc., USA, pp. 280.

Reneker, D.H. & Chun, I. 1996, "Nanometre diameter fibres of polymer, produced by electrospinning", *Nanotechnology*, vol. 7, no. 3, pp. 216-223.

Reneker, D.H. & Yarin, A.L. 2008, "Electrospinning jets and polymer nanofibers", *Polymer*, vol. 49, no. 10, pp. 2387-2425.

Reuben, S.S. & Ekman, E.F. 2005, "The effect of cyclooxygenase-2 inhibition on analgesia and spinal fusion", *Journal of Bone and Joint Surgery - Series A*, vol. 87, no. 3, pp. 536-542.

Rokkanen, P.U., Böstman, O., Hirvensalo, E., Mäkelä, E.A., Partio, E.K., Pätiälä, H., Vainionpää, S., Kimmo Vihtonen & Törmälä, P. 2000, "Bioabsorbable fixation in orthopaedic surgery and traumatology", *Biomaterials*, vol. 21, no. 24, pp. 2607-2613.

Rothen-Weinhold, A., Besseghir, K., Vuaridel, E., Sublet, E., Oudry, N., Kubel, F. & Gurny, R. 1999, "Injection-molding versus extrusion as manufacturing technique for the preparation of biodegradable implants", *European Journal of Pharmaceutics and Biopharmaceutics*, vol. 48, no. 2, pp. 113-121.

Rothon, R.N. 2002, "Particulate Fillers for Polymers", in *Rapra Review Report*, vol. 12, no. 9, Smithers Rapra, Shropshire, UK.

Ryu, W.H., Vyakarnam, M., Greco, R.S., Prinz, F.B. & Fasching, R.J. 2007, "Fabrication of multi-layered biodegradable drug delivery device based on micro-structuring of PLGA polymers", *Biomedical Microdevices*, vol. 9, no. 6, pp. 845-853.

Salerno, A. & Hermann, R. 2006, "Efficacy and safety of steroid use for postoperative pain relief: Update and review of the medical literature", *Journal of Bone and Joint Surgery - Series A*, vol. 88, no. 6, pp. 1361-1372.

Saxena, V., Sadoqi, M. & Shao, J. 2004, "Indocyanine green-loaded biodegradable nanoparticles: Preparation, physicochemical characterization and in vitro release", *International Journal of Pharmaceutics*, vol. 278, no. 2, pp. 293-301.

Schally, A.V. & Maria Comaru-Schally, A. 1997, "Rational use of agonists and antagonists of luteinizing hormone- releasing hormone (LH-RH) in the treatment of hormone-sensitive neoplasms and gynaecologic conditions", *Advanced Drug Delivery Reviews*, vol. 28, no. 1, pp. 157-169.

Schmaljohann, D. 2006, "Thermo- and pH-responsive polymers in drug delivery", *Advanced Drug Delivery Reviews*, vol. 58, no. 15, pp. 1655-1670.

Schmitt, E. & Bailey, W. *Polyglycolic acid in solutions*, US Patent 3737440, 1973.

Seidenberg, A.B. & An, Y.H. 2004, "Is there an inhibitory effect of COX-2 inhibitors on bone healing?", *Pharmacological Research*, vol. 50, no. 2, pp. 151-156.

Shantha, K.L. & Harding, D.R.K. 2003, "Synthesis, characterisation and evaluation of poly[lactose acrylate- N -vinyl-2-pyrrolidinone] hydrogels for drug delivery", *European Polymer Journal,* vol. 39, no. 1, pp. 63-68.

Shenoy, S.L., Bates, W.D., Frisch, H.L. & Wnek, G.E. 2005, "Role of chain entanglements on fiber formation during electrospinning of polymer solutions: Good solvent, non-specific polymer-polymer interaction limit", *Polymer,* vol. 46, no. 10, pp. 3372-3384.

Shin, H.J., Lee, C.H., Cho, I.H., Kim, Y., Lee, Y., Kim, I.A., Park, K., Yui, N. & Shin, J. 2006, "Electrospun PLGA nanofiber scaffolds for articular cartilage reconstruction: Mechanical stability, degradation and cellular responses under mechanical stimulation in vitro", *Journal of Biomaterials Science, Polymer Edition,* vol. 17, no. 1, pp. 103-119.

Siepmann, J. & Siepmann, F. 2006, "*Microparticles used as drug delivery systems"* in Smart Colloidal Materials in book series Progress in Colloid and Polymer Science, vol. 133, pp. 15-21.

Singer F.R. & Minoofar P. 2000, "Bisphosphonate therapy of Osteoporosis" in *The Osteoporosis Primer,* eds. J.E. Henderson & Goldzman D., The Cambridge University Press, Cambridge, UK.

Södergård, A. & Stolt, M. 2002, "Properties of lactic acid based polymers and their correlation with composition", *Progress in Polymer Science (Oxford),* vol. 27, no. 6, pp. 1123-1163.

Soekanto, A. 1994, "Inhibition of osteoclast-like cell formation by sodium salicylate and indomethacin in mouse bone marrow culture", *Japanese Journal of Pharmacology,* vol. 65, no. 1, pp. 27-34.

Soriano, I., Martín, A.Y., Évora, C. & Sánchez, E. 2006, "Biodegradable implantable fluconazole delivery rods designed for the treatment of fungal osteomyelitis: Influence of gamma sterilization", *Journal of Biomedical Materials Research - Part A,* vol. 77, no. 3, pp. 632-638.

Speight, J. 2005, *Lange's Handbook of Chemistry,* 16th edn, McGraw-Hill, USA.

Subbiah, T., Bhat, G.S., Tock, R.W., Parameswaran, S. & Ramkumar, S.S. 2005, "Electrospinning of nanofibers", *Journal of Applied Polymer Science,* vol. 96, no. 2, pp. 557-569.

Sun, Z., Zussman, E., Yarin, A.L., Wendorff, J.H. & Greiner, A. 2003, "Compound core-shell polymer nanofibers by co-electrospinning", *Advanced Materials,* vol. 15, no. 22, pp. 1929-1932.

Sung, K.C., Han, R., Hu, O.Y.P. & Hsu, L. 1998, "Controlled release of nalbuphine prodrugs from biodegradable polymeric matrices: influence of prodrug hydrophilicity and polymer composition", *International Journal of Pharmaceutics,* vol. 172, no. 1-2, pp. 17-25.

Suuronen, R., Laine, P., Sarkiala, E., Pohjonen, T. & Lindqvist, C. 1992, "Sagittal split osteotomy fixed with biodegradable, self-reinforced poly-L-lactide screws. A pilot study in sheep", *Enternational Journal of Oral and Maxillofacial Surgery,* vol. 21, no. 5, pp. 303-308.

Suuronen, R., Pohjonen, T., Hietanen, J. & Lindqvist, C. 1998, "A 5-year in vitro and in vivo study of the biodegradation of polylactide plates", *Journal of Oral and Maxillofacial Surgery,* vol. 56, no. 5, pp. 604-614.

Tian, F., Hosseinkhani, H., Hosseinkhani, M., Khademhosseini, A., Yokoyama, Y., Estrada, G.G. & Kobayashi, H. 2008, "Quantitative analysis of cell adhesion on aligned micro- and nanofibers", *Journal of Biomedical Materials Research - Part A,* vol. 84, no. 2, pp. 291-299.

Todd, P.A. & Sorkin, E.M. 1988, "Diclofenac sodium. A reappraisal of its pharmacodynamic and pharmacokinetic properties, and therapeutic efficacy.", *Drugs,* vol. 35, no. 3, pp. 244-285.

Tonino, A.J., Davidson, C.L., Klopper, P.J. & Linclau, L.A. 1976, "Protection from stress in bone and its effects. Experiments with stainless steel and plastic plates in dogs", *Journal of Bone and Joint Surgery - Series B,* vol. 58, no. 1, pp. 107-113.

Topp, E.M. 2000, "Principles of mass transport" in *Transport Processes in Pharmaceutical Systems,* eds. G.L. Amidon, P.I. Lee & E.M. Topp, Marcel Dekker, Inc., New York, USA, pp. 1-22.

Törmälä, P. 1992, "Biodegradable self-reinforced composite materials: Manufacturing structure and mechanical properties", *Clinical Materials,* vol. 10, no. 1-2, pp. 29-34.

Törmälä, P., Pohjonen, T. & Rokkanen, P. 1998, "Bioabsorbable polymers: Materials technology and surgical applications", *Proceedings of the Institution of Mechanical Engineers, Part H: Journal of Engineering in Medicine,* vol. 212, no. 2, pp. 101-111.

Törmälä, P., Pohjonen, T. & Rokkanen, P. 1998, "Bioabsorbable polymers: Materials technology and surgical applications", *Proceedings of the Institution of Mechanical Engineers, Part H: Journal of Engineering in Medicine,* vol. 212, no. 2, pp. 101-111.

Tsuji, H., Horikawa, G. & Itsuno, S. 2007, "Melt-processed biodegradable polyester blends of poly(L-lactic acid) and poly(ε-caprolactone): Effects of processing conditions on biodegradation", *Journal of Applied Polymer Science,* vol. 104, no. 2, pp. 831-841.

Tsuji, H., Kidokoro, Y. & Mochizuki, M. 2006, "Enzymatic degradation of biodegradable polyester composites of poly(L-lactic acid) and poly(ε-caprolactone)", *Macromolecular Materials and Engineering,* vol. 291, no. 10, pp. 1245-1254.

Turner, C.H., Wang, T. & Burr, D.B. 2001, "Shear strength and fatigue properties of human cortical bone determined from pure shear tests", *Calcified Tissue International,* vol. 69, no. 6, pp. 373-378.

Tuzlakoglu, K., Bolgen, N., Salgado, A.J., Gomes, M.E., Piskin, E. & Reis, R.L. 2005, "Nano- and micro-fiber combined scaffolds: A new architecture for bone tissue engineering", *Journal of Materials Science: Materials in Medicine,* vol. 16, no. 12, pp. 1099-1104.

Ubrich, N., Bouillot, P., Pellerin, C., Hoffman, M. & Maincent, P. 2004, "Preparation and characterization of propranolol hydrochloride nanoparticles: a comparative study", *Journal of Controlled Release,* vol. 97, no. 2, pp. 291-300.

Varshosaz, J. & Soheili, M. 2008, "Production and in vitro characterization of lisinopril-loaded nanoparticles for the treatment of restenosis in stented coronary arteries", *Journal of Microencapsulation,* vol. 25, no. 7, pp. 478-486.

Vega, E., Gamisans, F., García, M.L., Chauvet, A., Lacoulonche, F. & Egea, M.A. 2008, "PLGA nanospheres for the ocular delivery of flurbiprofen: Drug release and interactions", *Journal of Pharmaceutical Sciences,* vol. 97, no. 12, pp. 5306-5317.

Veiranto, M., Suokas, E., Ashammakhi, N. & Törmälä, P. 2004a, "Novel bioabsorbable antibiotic releasing bone fracture fixation implants", *Advances in Experimental Medicine and Biology,* vol. 553, pp. 197-208.

Veiranto, M., Tiainen, J., Niemelä, S., Suokas, E., Ikäheimo, I., Koskela, M., Syrjälä, H., Ashammakhi, N. & Törmälä, P. 2004b, "Novel ciprofloxacin releasing SR-PLGA miniscrews", *Transactions - 7th World Biomaterials Congress,* pp. 173.

Veiranto, M., Törmälä, P. & Suokas, E. 2002, "In vitro mechanical and drug release properties of bioabsorbable ciprofloxacin containing and neat self-reinforced P(L/DL)LA 70/30 fixation screws", *Journal of Materials Science: Materials in Medicine,* vol. 13, no. 12, pp. 1259-1263.

Verreck, G., Chun, I., Rosenblatt, J., Peeters, J., Van Dijck, A., Mensch, J., Noppe, M. & Brewster, M.E. 2003, "Incorporation of drugs in an amorphous state into electrospun nanofibers composed of a water-insoluble, nonbiodegradable polymer", *Journal of Controlled Release,* vol. 92, no. 3, pp. 349-360.

Viitanen, P., Suokas, E., Törmälä, P. & Ashammakhi, N. 2006, "Release of diclofenac sodium from polylactide-co-glycolide 80/20 rods", *Journal of Materials Science: Materials in Medicine,* vol. 17, no. 12, pp. 1267-1274.

Viljanen, J., Kinnunen, J., Bondestam, S., Majola, A., Rokkanen, P. & Törmälä, P. 1995, "Bone changes after experimental osteotomies fixed with absorbable self-reinforced poly-L-lactide screws or metallic screws studied by plain radiographs, quantitative computed tomography and magnetic resonance imaging", *Biomaterials,* vol. 16, no. 17, pp. 1353-1358.

Villiers, C., Braud, C., Vert, M. & Chiellini, E. 1979, "Optically active polyelectrolytes with variable hydrophobicity. 3. Effects of pH-induced chromophore and conformation changes on chiroptical properties of alternating copolymers of maleic acid and optically active 1-methylalkyl vinyl ethers", *Macromolecules*, vol. 12, no. 1, pp. 103-107.

Von Recum, A.F., Shannon, C.E., Cannon, C.E., Long, K.J., Van Kooten, T.G. & Meyle, J. 1996, "Surface roughness, porosity, and texture as modifiers of cellular adhesion", *Tissue Engineering*, vol. 2, no. 4, pp. 241-253.

Walenkamp, G.H.I.M. 2001, "Gentamicin PMMA beads and other local antibiotic carriers in two-stage revision of total knee infection: A review", *Journal of Chemotherapy*, vol. 13, no. SPEC. ISS. 1, pp. 66-72.

Wang, F., Lee, T. & Wang, C. 2002, "PEG modulated release of etanidazole from implantable PLGA/PDLA discs", *Biomaterials*, vol. 23, no. 17, pp. 3555-3566.

Wei, L., Cai, C., Lin, J. & Chen, T. 2009, "Dual-drug delivery system based on hydrogel/micelle composites", *Biomaterials*, vol. 30, no. 13, pp. 2606-2613.

Weiler, A., Helling, H., Kirch, U., Zirbes, T.K. & Rehm, K.E. 1996, "Foreign-body reaction and the course of osteolysis after polyglycolide implants for fracture fixation: Experimental study in sheep", *Journal of Bone and Joint Surgery - Series B*, vol. 78, no. 3, pp. 369-376.

Weinberg, B.D., Blanco, E. & Gao, J. 2008, "Polymer implants for intratumoral drug delivery and cancer therapy", *Journal of Pharmaceutical Sciences*, vol. 97, no. 5, pp. 1681-1702.

Williams, D.F. 1999, *The Williams Dictionary of Biomaterials*, Liverpool University Press, Liverpool, UK.

Wischke, C. & Schwendeman, S.P. 2008, "Principles of encapsulating hydrophobic drugs in PLA/PLGA microparticles", *International Journal of Pharmaceutics*, vol. 364, no. 2, pp. 298-327.

Xie, J., Ruo, S.T. & Wang, C. 2008, "Biodegradable microparticles and fiber fabrics for sustained delivery of cisplatin to treat C6 glioma in vitro", *Journal of Biomedical Materials Research - Part A*, vol. 85, no. 4, pp. 897-908.

Xie, J. & Wang, C. 2006, "Electrospun micro- and nanofibers for sustained delivery of paclitaxel to treat C6 glioma in vitro", *Pharmaceutical Research*, vol. 23, no. 8, pp. 1817-1826.

Xu, X., Chen, X., Ma, P., Wang, X. & Jing, X. 2008, "The release behavior of doxorubicin hydrochloride from medicated fibers prepared by emulsion-electrospinning", *European Journal of Pharmaceutics and Biopharmaceutics*, vol. 70, no. 1, pp. 165-170.

Xu, X., Yang, L., Xu, X., Wang, X., Chen, X., Liang, Q., Zeng, J. & Jing, X. 2005, "Ultrafine medicated fibers electrospun from W/O emulsions", *Journal of Controlled Release*, vol. 108, no. 1, pp. 33-42.

Ye, W. & Chien, Y.W. 1996, "Dual-controlled drug delivery across biodegradable copolymer. II. Delivery kinetics of levonorgestrel and estradiol from (matrix/matrix) laminate drug delivery system", *Journal of Controlled Release*, vol. 41, no. 3, pp. 259-269.

Yoo, J.Y., Shin, J.H., Khang, G., Shin, H.S., Yuk, S.H., Kim, Y.S., Kim, M.S., Rhee, J.M. & Lee, H.B. 2007, "Effect of glycolide monomer on release behavior of gentamicin sulfate-loaded PLGA microparticles", *Journal of Applied Polymer Science*, vol. 104, no. 2, pp. 1019-1025.

Zalfen, A.M., Nizet, D., Jérôme, C., Jérôme, R., Frankenne, F., Foidart, J.M., Maquet, V., Lecomte, F., Hubert, P. & Evrard, B. 2008, "Controlled release of drugs from multi-component biomaterials", *Acta Biomaterialia*, vol. 4, no. 6, pp. 1788-1796.

Zeng, J., Xu, X., Chen, X., Liang, Q., Bian, X., Yang, L. & Jing, X. 2003, "Biodegradable electrospun fibers for drug delivery", *Journal of Controlled Release*, vol. 92, no. 3, pp. 227-231.

Zeng, J., Yang, L., Liang, Q., Zhang, X., Guan, H., Xu, X., Chen, X. & Jing, X. 2005, "Influence of the drug compatibility with polymer solution on the release kinetics of electrospun fiber formulation", *Journal of Controlled Release*, vol. 105, no. 1-2, pp. 43-51.

Zhang, Y.Z., Wang, X., Feng, Y., Li, J., Lim, C.T. & Ramakrishna, S. 2006, "Coaxial electrospinning of (fluorescein isothiocyanate-conjugated bovine serum albumin)-encapsulated poly(ε-caprolactone) nanofibers for sustained release", *Biomacromolecules*, vol. 7, no. 4, pp. 1049-1057.

Zong, X., Bien, H., Chung, C., Yin, L., Fang, D., Hsiao, B.S., Chu, B. & Entcheva, E. 2005, "Electrospun fine-textured scaffolds for heart tissue constructs", *Biomaterials*, vol. 26, no. 26, pp. 5330-5338.

Zong, X., Kim, K., Fang, D., Ran, S., Hsiao, B.S. & Chu, B. 2002, "Structure and process relationship of electrospun bioabsorbable nanofiber membranes", *Polymer*, vol. 43, no. 16, pp. 4403-4412.

Zong, X., Li, S., Chen, E., Garlick, B., Kim, K., Fang, D., Chiu, J., Zimmerman, T., Brathwaite, C., Hsiao, B.S. & Chu, B. 2004, "Prevention of postsurgery-induced abdominal adhesions by electrospun bioabsorbable nanofibrous poly(lactide-co-glycolide)-based membranes", *Annals of Surgery*, vol. 240, no. 5, pp. 910-915.